DURBAN UNIVERSITY OF TECHNOLOGY
INYUVESI YASETHEKWINI YEZOBUCHWEPHESHE

EXPERIMENTAL AND COMPUTATIONAL EXPLORATION OF ADVANCED BIODIESEL FUELS AND HYBRIDISATION PROCESS EVALUATION OF FEEDSTOCKS AND THEIR CHEMICAL COMBINATIONS

By

Anietie Okon Etim

BEng, MEng (Chemical Engineering)

Thesis submitted in fulfilment of the academic requirements for the award of the degree of

DOCTOR OF ENGINEERING (DEng)

Department of Chemical Engineering,

Faculty of Engineering and the Built Environment,

Durban University of Technology, South Africa

Supervisor

Prof. Paul Musonge

Co-Supervisor

Prof. Andrew C. Eloka-Eboka

March 2022

DECLARATION

I, Anietie Etim, hereby declare that the content presented in this thesis entitled "***Experimental and Computational Exploration of Advanced Biodiesel Fuels and Hybridisation Process Evaluation of Feedstocks and their Chemical Combinations"*** is my own research work and to the best of my knowledge, contains no material previously published or written by another person nor material to which substantial extent has been accepted for the award of any other degree at DUT or at any other educational institution. Moreover, I declare that the content presented in this thesis does not violate any copyright as all the work of others has been indicated accordingly by means of in-text referencing and a comprehensive list of references has been listed at the end of this thesis.

Author : Anietie Okon Etim

Signature: ___ Date: __05/09/2022_____

Co-Supervisor: Prof Andrew C. Eloka-Eboka

Signature: _ _____ Date: __05/09/2022_____

Supervisor: Prof Paul Musonge

Signature: __ _____ Date: _ 05/09/2022_____

ACKNOWLEDGEMENT

I would like to thank the Almighty God for His grace throughout my academic journey to this extent, and for the successful completion of this doctoral study.

I would like to acknowledge and specially thank my supervisor, Prof Paul Musonge for his invaluable support, encouragement and guidance at every stage of this work. His effort in the provision of equipment and materials, sponsoring of analysis, organising of meetings and workshops to give directions, present at every progress and presentation meeting, detailed review of manuscript and valuable contributions is much appreciated.

I gratefully acknowledge and thank my co-supervisor, Prof Andrew Eloka-Eboka, whom through his assistance has made this doctoral study to be accomplished at DUT. I also thank him for his support and encouragement through the scrupulous review of every manuscript and constructive contributions at every progress stage of this study.

I wish to also express my special thanks to:

Prof Francis Shode in Food Science and Technology Department, for his assistance in carrying out the oil extraction process in his laboratory.

Staff in Chemical Engineering Department especially Prof. Yusuf Isa and Prof. Rathilal Suddesh for their interventions and provision of basic equipment in the laboratory.

The technicians in Chemical Engineering laboratory, especially Mr. Jaafar Mohammed, for his assistance in requisition processing and procurement of all the equipment and materials used in this study.

The National Research Foundation in collaboration with the World Academy of Sciences (NRF-TWAS) South Africa, for the doctoral financial support throughout this research work

The Durban University of Technology research office, particularly Prof. Bloodless Dzwairo and Mr Tshabalala for the thorough screening of my documents to ensure timely release of funds.

Ms Avenal Finlayson and Ms Sara Mitha in Library department DUT, for their frequent research workshop on MS words document and endnote referencing guide, which has gone a long way in facilitating the compilation of this thesis.

My colleagues in postgraduate office, Chemical Engineering Department for their assistance, emotional support, co-operation, friendship, occasional humour and social interactions, which enable me to stay focused on this study.

Finally, sincere thanks to my family for their kind support. To my lovely husband Mr. Uwem Ikitde for his continuous support and encouragement throughout this PhD journey thanks for believing in me. To my dear father, late Chief Okon Etim (gone but not forgotten), your love and support for my education has made me go this far in life. To my beloved mother, Mrs Mbak-Abasi Etim for her kind support and encouragement in all my academic endeavours. To all my siblings, for their moral support and encouragement throughout this journey. I say a big thank you to you all.

DEDICATION

This work is dedicated to my beloved mother, Mrs Mbak-Abasi Etim and to the honour of my late father, Chief Okon Etim.

PUBLICATIONS

The following are the research outputs emanated from this thesis: They have been published or under review in ISI/Scopus/DoHET accredited journals:

1. **Etim, A.O.,** Musonge, P., Eloka-Eboka, A.C (2022) A novel green bio-composite heterogeneous catalyst synthesis for the optimized transesterification of linseed-marula oil blend methyl ester production. *Results in Engineering*, 16:100-646.

2. **Etim, A.O.,** Eloka-Eboka, A.C., Musonge, P. (2022). Optimization of flaxseed oil methyl ester synthesis using bio-alkaline catalyst. *Scientific African*, 16: e01275

3. **Etim, A.O.,** Musonge, P., Eloka-Eboka, A.C. (2022). Evaluation of in-situ and ex-situ hybridization study in the optimised transesterification of waste and pure vegetable oils. *Biofuels, Bioproducts & Biorefining*, 16(7), 1-13.

4. **Etim, A. O.,** Musonge, P., & Eloka-Eboka, A. C. (2021). An effective green and renewable heterogeneous catalyst derived from the fusion of bi-component biowaste materials for the optimized transesterification of linseed oil methyl ester. *Biofuels, Bioproducts and Biorefining*, *15*(5), 1461-1472.

5. **Etim, A.O.,** Musonge, P., Eloka-Eboka, A.C. (2021). Transesterification via Parametric Modelling and Optimization of Marula (*Sclerocarya birrea*) Seed Oil Methyl Ester Synthesis. *J. Oleo Sci*. 93:77–93.

6. **Etim, A.O**., Eloka-Eboka, A.C., Musonge, P. (2021). Potential of *Carica papaya* peels as effective biocatalyst in the optimized parametric transesterification of used vegetable oil. *Environ. Eng. Res*. 26: 200–299.

7. **Etim, A. O.,** Musonge, P., & Eloka-Eboka, A. C. (2020). Effectiveness of biogenic waste-derived heterogeneous catalysts and feedstock hybridization techniques in biodiesel production. *Biofuels, Bioproducts and Biorefining*, *14*(3), 620-649.

8. **Etim, A.O.,** Musonge, P., Eloka-Eboka, A.C. (2022). Potential of bi-hybridization of used frying/marula seed oils for biodiesel production via optimized transesterification process. (*Submitted*)

9. **Etim, A.O.,** Musonge, P., Eloka-Eboka, A.C. (2022). A novel biodiesel synthesis from baobab seed oil using organic wastes heterogeneous catalyst. (*Submitted*)

Accredited Conferences

1. **Etim, A.O.,** Eloka-Eboka, A.C., Musonge, P. Optimization of flaxseed oil methyl ester synthesis using bio-alkaline catalyst. Conference proceedings, 18th International Conference on Science, Engineering (SETWM-2020), Technology and waste Management, Vol. 1, ISBN: 978-86878-46-5, Nov. 16-17, 2020, Johannesburg, South Africa, *(Oral Presentation*)

2. **Anietie O. Etim**, P. Musonge and Andrew C. Eloka-Eboka. Potential of green heterogeneous catalyst derived from the fusion of eggshells and pawpaw peels in the optimised transesterification of linseed oil methyl ester. Conference Proceedings, International Conference on Green Technologies for Sustainable Development (GTSD-2021), 9-11 March 2021, India. (*Oral presentation*)

3. **Anietie O. Etim**, Paul Musonge, Andrew C. Eloka-Eboka. Potential of bi-hybridization of used frying/marula seed oils for biodiesel production via optimized transesterification process. 13th International Conference on Applied Energy (ICAE), 29 Nov – 5th Dec 2021, Thailand. (*Oral presentation*)

4. **Etim, Anietie O**., Musonge, P., Eloka-Eboka, A.C Evaluation of in-situ and ex-situ hybridization study in the optimised transesterification of waste and pure vegetable oils. 1st Sustainable Bioenergy and Processes (SBP), 13 – 15th Dec. 2021, Cape Town, South Africa. (*Oral presentation*)

5. **Anietie Okon Etim**, Musonge P., Eloka-Eboka, A.C. A novel green bio-composite heterogeneous catalyst synthesis for the optimized transesterification of linseed-marula oil blend methyl ester production. 33rd JOHANNESBURG International Conference on "Chemical, Biological and Environmental Engineering" (JCBEE-22), March 17 – 18th 2022, Johannesburg, South Africa. (*Oral presentation*)

The candidate is the main author for all the publications. Prof P. Musonge and Prof. AC Eloka-Eboka are the supervisor and co-supervisor respectively.

ABSTRACT

To address the alarming crisis of global energy demand, environmental degradation and climate change, biomass derived diesel fuel is one of the superior renewable fuel options, considered as suitable alternative to petroleum fuel. Important fuel characteristics of biomass derived diesel fuel ranges from being recyclable available local fuel to auspicious performance in combustion emission reduction. In this study, waste oil and other indigenous tropical seed oils, which include; used sunflower oil (USO), linseed oil (LSO), marula seed oil (MSO), baobab seed oil (BSO) and *Trichilia emetica* kernel oil (TEKO) were investigated for biodiesel production and further scrutinised for the hybridization process for effective applications. The process of hybridization applied was a two-pathway approach via *in-situ* and *ex-situ* transesterification reactions. Biological wastes mineral-rich materials such as eggshells, banana peels and pawpaw peels were used to produce the bio-alkaline catalysts. The waste materials were washed with distilled water, dried in the oven and further subjected to high temperature of calcination in the furnace. Eggshells were calcined at 900 ^{o}C for 3 h while pawpaw and banana peel were calcined for 3 h at 700 ^{o}C respectively. The calcined ash of eggshells and banana peel, eggshells and pawpaw peels were bonded respectively via wet impregnation method and further activated at high temperatures to obtain hybridized bio-alkaline catalysts. The synthesized samples of all catalyst were characterized using Fourier transforms infrared (FT-IR), X-ray diffraction (XRD), and scanning electron microscopy (SEM). The catalysts produced were applied in the production of biodiesel from waste and underutilized oils such as used sunflower oil (USO), linseed oil (LSO), marula seed oil (MSO), baobab seed oil (BSO) and *Trichilia emetica* kernel oil (TEKO) under an optimized transesterification reaction process. The operating parameters considered viz methanol-to-oil ratio, catalyst loading, and reaction time temperature were investigated and optimized using Response surface methodology (RSM) to obtain the best operation condition for the maximum yields. The optimized condition established from the biodiesel fuel produced was used as a standard for the transesterification reaction condition for the single and hybrid oils. The two pathways hybrid process; *In-situ* (co-mingling of oils prior transesterification) and *Ex-situ* (comingling of the single biodiesel fuels after transesterification) was used to evaluate and compare the differences between the two processes and how effective they can be deployed commercially. The four crude oils considered for the study (USO, LSO, MSO and BSO) were analysed while fractions of them were individually converted via transesterification to obtain single biodiesel fuels (SOBFs): used sunflower oil methyl ester (USOME), linseed oil methyl ester (LOME), marula oil methyl ester (MOME) and baobab oil methyl ester (BOME). Then the remaining fractions were pre-treated and co-mingled

in 27 various combinations to form new oils (of bi-and poly-hybrids) called the hybridized oils (HOs). These different combinations were then trans-esterified to obtain hybridized oil methyl esters (HOMEs) - *In-situ hybridization*. Thereafter, the SOBFs - (USOME, LSOME, MSOME and BSOME) were hybridized in the same pattern following the same ratios to form new products termed hybridized methyl ester (HMEs) - *Ex-situ hybridization*. All the produced biodiesel fuels: USOME, TEKOME, LOME, MOME, BOME and HOMEs were individually blended with petrol-diesel and their chemo-physical properties were analysed and compared with the international (ASTM and EN) and South African (SANS) standards. The impact of the chemical combinations on the physico-chemical properties of all the biodiesel produced was investigated and computed using artificial neural networks (ANN). Their influence on the important thermophysical fuel properties such as cetane number and calorific values were also evaluated.

The characterization results revealed that eggshell is an excellent source of natural CaO while the banana and pawpaw peels are rich in potassium compounds such as: KCl, K_2SO_4, K_2CO_3, K_2O which are efficient catalyst compounds for biodiesel production. The hybridized catalysts were found to be effective and of high basicity and active in oil conversion to biodiesel. The process of *in-situ* and *ex-situ* hybridization and their blends with petro-diesel were found to be a very effective approach to be adopted in the biodiesel production process. High conversion of biodiesel yields was obtained via the process of *in-situ transesterification*, indicating that the transesterification process is not affected by the number of mixing ratios of oils. The two process pathways offered improved properties that are much more conformable to standards than most of the single biodiesel produced fuels. Some properties such as density, acid value, viscosity, calorific value and cetane number were found a bit lower in *ex-situ* than in *in-situ* hybrids under the same hybrid conditions. The predicted properties obtained from the two protocols by ANN show good alignment with the experimental values with high regression coefficients close to unity (1). The improved fuel properties obtained following these protocols were within the international and South African standard specifications. The general principles and model predictions of the subsequent properties of biodiesel presented in this study will serve as a database and template for effective development for the overall biofuels application.

TABLE OF CONTENTS

LIST OF TABLES

LIST OF FIGURES

GLOSSARY AND ACRONYMS

ANOVA	Analysis of variance
ATOR	Alcohol to oil ratio
ASTM	American society for testing and material
AV	Acid value
EN	European Nation
BDF	Biomass diesel fuel
BBD	Box Behnken design
BO	Baobab oil
BOME	Baobab oil methyl ester
CBP	calcine banana peels
CPP	Calcine pawpaw peels
CE-CaO	Calcined eggshells –calcium oxide
CIE	Compression ignition engine
CN	Cetane number
CCD	Central composite design
CFPP	Cold filter plugging point
CT	Calcination temperature
Ct	Calcination time
CV	Calorific value
FAME	Fatty acid methyl ester
FFA	Free fatty acid

FAAE	Fatty acid alkyl ester
FCC	Face centred cubic
HOMEs	Hybrid oil methyl esters
HMEs	Hybrid methyl esters
$KOCH_3$	Potassium methoxide
K_2O	Potassium oxide
KOH	Potassium hydroxide
LO	Linseed oil
LOME	Linseed oil methyl ester
LOB	Linseed oil biodiesel
LTFT	Low temperature flow test
MO	Marula oil
MOME	Marula oil methyl ester
MTOR	Methanol to oil ratio
MSE	Mean square error
NaOH	Sodium hydroxide
NPs	Nano particles
NMR	Nuclear magnetic resonance
NIRS	Near-infrared spectroscopy
OPEC	Organization of petroleum exporting countries
OFAT	One factor at a time
PAH	Polycyclic aromatics hydrocarbons

PDF	Petroleum derived fuel
SOFs	Single oil fuels
SDGs	Sustainability development goals
HOME	Hybrid oil methyl ester
HME	Hybrid methyl ester
HV	Heating value
HCl	Hydrochloric acid
IEA	International energy agency
RSM	Response surface methodology
USO	Used sunflower oil
USOB	Used sunflower oil biodiesel
USOME	Used sunflower methyl ester
δ	Density

CHAPTER ONE

1.1 Introduction

Energy generated from fossil fuel sources are non-renewable and are linked with the constant release of pollutant gases during usage. Thus, this increases the greenhouse gases that leads to climate change. Air and water pollution emanating from plants powered by fossil fuel sources such as coal and natural gas have negative impact on health, causing neurological damage, heart attack, breathlessness, cancer and lots more. Renewable energies are the cleanest and inexhaustible fuel source derived from natural and biological resources such as wind, water, sunlight and organic materials of plants. They offer viable solutions to prevent environmental degradation and greenhouse gases escalation in the atmosphere because they generate no pollutant gases. As an indigenous source of energy, it reduces energy dependence and improve local economies. Fossil fuel dependence leads to energy insecurity, political and economic instability. Adaptation of energy system based on renewable technologies appears the convenient approach for improving the world economy and development. It enhances improved power quality supply and reliability. Additionally, diversification of energy sources can reduce fuel importation, boost job creations and improve green economy. Renewable energies are sustainable, abundant and possess potentials to be used in any area of the world without restrictions.

1.2 Background of study

High rate of energy consumption, insecurity and environmental deterioration associated with the fossil fuel energy has advanced the interest of alternative fuel resources. Fossil fuel constitutes about 80% of the world's primary energy and it is depleting in source daily due to increase in the world population growth, urbanization and industrialization. According to recent report, the world population is expected to increase by 8.8 billion in 2035, and fossil fuel will still be accounted for more than three quarters of global energy. Figure1.1 shows the forecast of the primary energy consumption for the next twenty years (Mohd Noor *et al*., 2018). However, the consumption of renewable energy is likely to increase from 439 million tonne oil (Mtoe) in 2015 to 1715 Mtoe by 2035. Among other fossil derived products, diesel is the most demanded due to high thermodynamic and fuel conservation efficiency of the diesel engine (Aghbashlo *et al.*, 2021). The current statistical data released by OPEC indicates that the global demand for diesel and gasoline is expected to increase from 1660 billion litres in 2017 to 1834 billion litres in 2040 (Figure 1.2). With this alarming increase, the excessive dependence on

fossil fuel consumption will confront the human society with lots of challenges such as acute health problems, environmental degradation, climate change and ozone layer depletion. This is linked to the constant release of the detrimental gas pollutants during refining, exploitation and utilization of fossil fuels.

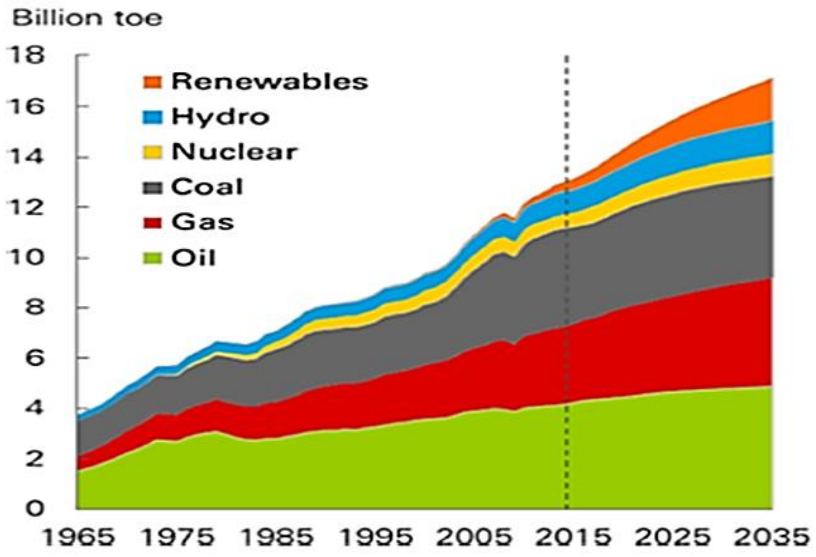

Figure 1.1: Forecast of the global energy consumption growth for 2015 – 2035

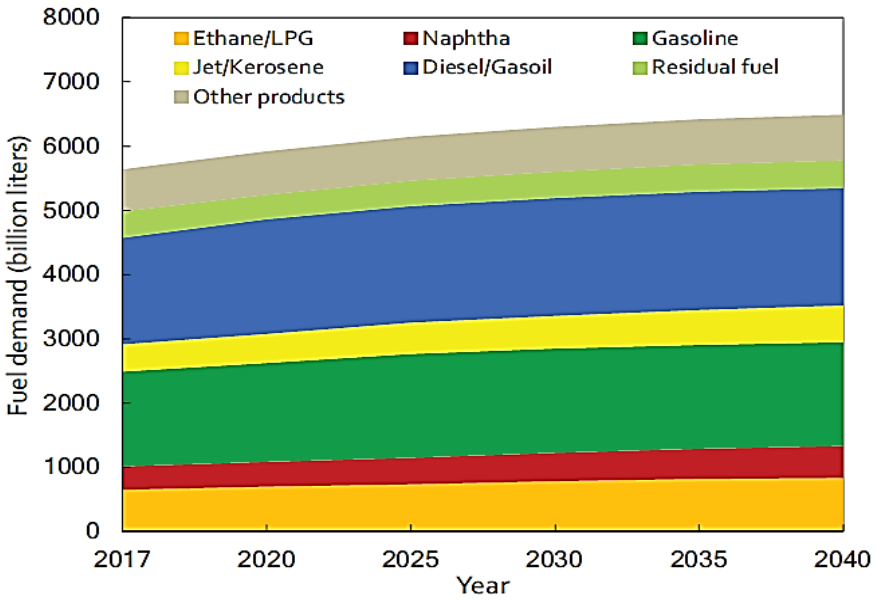

Figure 1.2: The demand for the global refined product from 2017 to 2040

Among biofuel sources, biodiesel is superior and the most suitable alternative fuel option to replace liquid petroleum fuel due to their similarities in physicochemical properties. Biodiesel is an indigenous liquid fuel that can be sourced and produced locally, which is an added

advantage to countries that are solely dependent on importation of energy and most rural areas that are off the energy grid. The current reflection in the amount of biofuel traded globally according to the International Energy Agency (IEA), biodiesel is expected to meet the demand of 27% of the total transport fuel by 2050 and save up to 2.1×10^9 gigatons CO_2 emission which would have been generated by fossil fuel (Atabani *et al*., 2014). In line with section 7 of the South Africa's sustainable development goals (SDGs), access to sustainable and affordable energy is a pre-requisite to meet up with 2030 target of achieving a sustainable environment, which involve environmental risk reduction and climate change. Biofuel usage has a potential impact on greenhouse emission reduction due to its carbon neutral nature. However, to ensure biodiesel sustainability, the overall production process should be economically viable and environmentally friendly. The major problem of biodiesel production is in the nature of the feedstock of production. Biodiesel feedstock are region specific and unsustainable manner of sourcing can result in a negative impact on environment and the secular economy at large. The process of feedstock sourcing and selection offers a significant opportunity to improve biofuel performance and simultaneously plays a fundamental role in cost reduction. The traditional input feedstock for biodiesel are mostly edible oils and they are costly in price. Aside cost, they are not sustainable due to the conflicting competition between food and energy supply, as both are contending for the same resources. Therefore, they cannot be considered a sustainable source for a long-term usage. Attention has shifted to the non-edible oils as the potential sources for biodiesel production such as jatrohpa, karanja, yellow oleander and so on. They contain high amount of lipid content and possess quality fuel properties, but their major drawback is the presence of high free fatty acids, which requires additional pre-treatment for their proper conversion. However, this can be addressed by the application of modern intensified equipment and process modelling in order to make non-edible oil sources sustainable for a long term usage (Manaf *et al*., 2019a).

There are other underutilized oil sources abundantly available in Southern Africa and around the tropics. Seed oils such as *Trichilia emetica* seed with 60-68 % oil content has been studied and applied in cosmetics and soap production but has not extensively been reported for its use in biodiesel production. The report shows that the seed oil is rich in saturated fatty acids (43-53 % of palmitic acid) and monounsaturated fatty acid (51 % of oleic acid), and with acid value of 8.13 wt% (Adinew, 2014). Marula seed oil has been reported to have been used in soap making and other cosmeceutical products but not for biodiesel production. It is highly a monounsaturated oil with high percent of oleic acid ranging from 70-78 % (Vermaak *et al*., 2011). Baobab seed oil has also been reported to contain high percent of oleic (30-42 %) and

linoleic acids (20-35 %) respectively. It has also been applied majorly for soap and other cosmetic production but not for biodiesel production. For biodiesel to be meet the global fuel demand as an alternative fuel option, its feedstock of production must be abundantly accessible and of acceptable quality. Feedstock for biodiesel could be found in various locations and differs in compositions due to their origin (soil), harvesting and storage methods, geographical and climatic conditions. These can also affect the chemo-physical properties of the oil when deployed for biodiesel production. The fuel properties are directly linked to the composition of the oil, most times, biodiesel produced from single oil feedstock are deficient in some properties and therefore, not conformable to standards. However, the application of a new technological strategy of feedstock hybridization process to optimise the oil composition and content of the input materials could make the biodiesel production a sustainable and viable process. This process leads to creation of new oil sources with similar but more improved properties than the parent oils (Fadhil *et al*., 2015). Biodiesel is produced via a simple chemical process called transesterification. This can be achieved through a reaction of alcohol (mostly short chains) with acids, base or bi-functional catalyst or enzymes.

Alcohol is an important raw material that is required in every step of the oil conversion process. It is used either as a solvent or as reactant and it brings about the alkylation of esters during the transesterification process, which yields the final alkyl ester called the biodiesel. It is required in excess to facilitate the conversion process to favor ester formation. In terms of the stoichiometry, three moles of alcohol is needed for one mole of triglyceride. However, the mole ratio can increase in practical situations depending on the applied process, oil quality, composition, and the catalyst type. Several alcohols can be used but the most preferred ones are the short chains such as the methanol and ethanol because of fast conversion in limited time, easy separation, availability, low cost, and physicochemical advantage (Etim *et al*., 2020). Biodiesel produced via transesterification reaction are widely performed with inorganic acids and base catalysts. Due to the inherent characteristic inorganic catalyst, organic catalysts from biomass resources are considered viable alternative and have been widely studied for this purpose.

Biodiesel is a mixture that is made up of a complex chemical system, its composition is influenced by many factors such as oil sources, geographical conditions, method of seed harvesting, storage method of the seed oil, extraction and production methods (Aghbashlo *et al*., 2021). Transesterification is the most acceptable route for biodiesel production, and it involve many factors that can in turn influence the final product. These are methanol to oil ratio, process reaction time, catalyst concentration, temperature, stirring speed and so on. Effective

statistical modelling tools like response surface methodology (RSM) can be utilised to visualise the effect these factors have on the biodiesel yield(s). RSM tool helps in designing less number of experiments in order to get an optimum result. It saves time, costs and materials unlike the traditional modelling methods such as one factor at a time (OFAT). Artificial neural network (ANNs) system is another effective tool in modelling and predicting the biodiesel production and its properties. It is a data processing technique motivated by the biological neural system. It has widely been applied in biodiesel production and in prediction of the performance, combustion and emission characteristics of the diesel engines (Domínguez-Sáez *et al*., 2018; Meng *et al*., 2014; Tosun *et al*., 2016). The comparison of its modelling efficacy with RSM in biodiesel production has also been investigated and reported to be more effective and superior than RSM (Betiku *et al*., 2016b; Stamenković *et al*., 2013).

Biodiesel is a promising renewable substitute to petrol diesel due their proximity in physiochemical properties. However, biodiesel contains 10-11 % oxygen by weight, which improved combustion than hydrocarbon-based diesel fuels. Biodiesel has many advantages over conventional diesel fuel. These include reproducibility, biodegradability, non-toxicity, better lubricity, lower flammability, sulphur, and benzene free nature. Nevertheless, there are some technical challenges associated with its use, these include high viscosity, low energy content, high cold flow properties, higher copper strip corrosion and low oxidative stability. These challenges are attributed to the fatty acid profile of the feedstocks used in biodiesel production (Papargyriou *et al*., 2019). However, application of the new evolving technology of oil hybridization can compensate for these problems and improve their fuel properties. Since its properties are directly related to the fatty acid profile of the oil, altering the fatty acid profile of the input oil used for the production will reduce the percentage of fatty acids responsible for these problems in a particular oil, resulting in improved properties as well as optimization of the oil content for production (Hegde *et al*., 2015).

Biodiesel is a clean burning fuel with less pollutant emission unlike petrol-diesel. The usage as transport fuel enhances improve environmental air quality, increase energy security and provides safety benefits. Diesel fuel engines exhaust emissions with fossil fuel sources have the potential to cause a range of health problems. Biodiesel reduces carbon dioxide (CO_2), carbon monoxide (CO), polycyclic aromatics hydrocarbons (PAH), nitrated PAHs emissions, which have been identified as potential cancer-causing compounds. The use of biodiesel decreases the solid carbon fraction of PM and reduces the sulphate fraction (Demirbas, 2007).

Biodiesel blends with diesel-fuel have excellent lubricity, which have the ability to reduce wear and tear on the diesel engine parts and prolong the engine life span (Knothe and Razon, 2017). However, some of the drawback of biofuel includes production costs, poorer cold flow, low temperature properties and higher emissions of oxides of nitrogen. Moreover, NOx emission formation is determined by the differences in chemical structure of biofuel. It is also reported that short chain length and more saturated biodiesel are preferable to reduce NOx emission (Jahirul *et al*., 2013)

The global economic advantage of biodiesel is driven by many factors which include: the support of renewable energy, the support for cleaner and environmentally friendly energy sources to limit global warming, upliftment of the agricultural sector through utilization of surplus and under-develop agricultural lands, promotion of sustainable development, exertion of reduction of pressure on global oil prices and the need to improve energy security, provision of new labour and market opportunities for domestic crops. Biofuel production is also supported by the government through implementation of various policy measures; the use of variety of economic incentives, including grants, price subsidy of fuel blended with bio-component, tax exemption, tax credits subsidies and loans to promote biofuel research and development (Manaf *et al.*, 2019a).

1.3 Research context and motivation

The place of renewable energy in the emerging world cannot be overemphasized. The global concern on economic and environmental degradation associated with fossil fuel usage and depletion coupled with the need to secure energy supply, reduce overdependence on fossil fuels and lower the greenhouse gases emissions have fostered the exploration of renewable alternative and sustainable energy resources. Biomass based diesel (biodiesel) fuels are receiving great attention as indigenous liquid fuels capable of replacing petro-diesel fuels from fossil sources due to obvious availability, recyclability, sustainability and eco-friendly characteristics. However, its development and standardization in South Africa and other developing countries are not encouraging. The general challenge faced by the biodiesel industries in South Africa and around the world is the scarcity and quality of feedstock. The feedstock accounts for about 85 % of the overall cost of biodiesel production. The limited feedstock supply therefore prevents large-scale production and commercialization. The non-availability of feedstock arises because varieties of feedstock can be found in different regions with varying property profiles or compositions. Most times, single feedstock sources are insufficient in quantity and quality due to some factors such as soil and climate conditions, post

agricultural and storage process which can affect the biodiesel quality. Hence, to offset this inconvenience, investigation into feedstock hybridization process as a recent evolving technological strategy to optimise and improve the chemical composition of feedstock for effective biodiesel production is a step in the right direction. This research work investigates hybridization of oil and catalyst feedstocks from renewable resources with a view towards developing a sustainable path for effective biodiesel production and standardization. Some awareness has already been escalated through conferences and published articles of this work.

1.4 Research aim

The aim of this study is the experimental and computational exploration of advanced biodiesel fuels and hybridisation process evaluation of feedstocks and their chemical combinations

1.5 The specific study objectives

To achieve the above aim, the objectives include the following:

i. Preparation of single and hybrid bio-alkaline heterogeneous catalysts from available biogenic waste materials; banana peels, pawpaw peels and eggshells.

ii. Production of advanced biodiesel fuels from used sunflower oil (USO), Linseed oil (LO), Marula seed oil (MSO), Baobab seed oil (BSO) and *Trichilia emetica* kernel oil (TEKO) via optimised transesterification process using the prepared catalyst.

iii. To carry out *in-situ* and *ex-situ* hybridization studies on the advanced biodiesel fuels produced for effective applications.

iv. To evaluate and compute the fuel properties of the single and hybrid fuels based on chemical combinations.

v. To investigate the physical and chemical properties of the single and hybrid biodiesel fuels with petro-diesel blends.

1.6 Contribution of the study

There is dearth information on biodiesel industrial development and usage in South Africa and other developing countries since they are mainly reliant on fossil diesel consumption and importations. Biodiesel industries are still under the developmental stage in South Africa and

African continent as a whole. Therefore, the contributions from this study will serve in the following ways:

1. The study will proliferate the biodiesel research and development
2. It will enhance feedstock availability and technological framework of conversion in South Africa and beyond.
3. This will form a basis for the development of a database for advance and sustainable biodiesel from hybrid feedstock.
4. It will be relevant to the biodiesel industries as new and improve method of production
5. It will stimulate more research on waste biomass utilization for biodiesel production.
6. It will escalate the research information on advanced biodiesel production.
7. It will instigate further research activities on advanced/fourth generation biodiesel feedstock.
8. It will create awareness.
9. It will improve rural economy and create jobs

1.7 Thesis outlines

The layout of this thesis is presented in Table 1.1

Table 1.1: Thesis outline

Chapter	Outline
1: Introduction	This chapter contains the background information of biodiesel, sources and methods of production, research context and motivation, research aim and objectives and contributions of the study
2: Literature review	This chapter present the extensive literature review of other research works on biodiesel production processes, particularly the method of production, feedstock types, catalyst types, transesterification, modelling, process intensification, analytical and

	quantification methods, biodiesel properties and characterization
3: Bio-alkaline synthesis from biogenic waste materials and their hybrids	In this chapter, bio-alkaline catalysts synthesis from biogenic waste materials were presented. Specific waste materials used and their availability, preparation of single and hybrid catalyst, characterization and catalysts reusability were discussed.
4: Advanced biodiesel synthesis via application of single and hybrid waste-based bio-alkaline catalysts in the optimised transesterification of used sunflower oil and other tropical plant oils	This chapter indicates the syntheses of advanced biodiesel through application of the produced catalysts in biodiesel production. Sources of oil feedstock, oil extraction and characterization, procedure of the transesterification and experimental design were presented
5: *In-situ* and *Ex-situ* techniques for biodiesel production	This chapter present the evaluation of *in-situ* and *ex-situ* hybridization technology. The preparation of oil and FAME hybrids, transesterification of *in-situ* hybrids and their property characterizations
6: Application of machine learning technology in modelling and computing biodiesel properties	In this chapter, application of machine learning technology in predicting the fuel properties of the *in-situ* and *ex-situ* hybrids were discussed. ANN modelling and evaluation of the two pathway hybrid processes were presented
7: Biodiesel fuel blend with petro-diesel and characterization	This chapter present the single and hybrid biodiesel fuel blends with petro-diesel. Preparation of biodiesel – diesel fuel blending and their characterization were discussed

8: General conclusions	General conclusions from the study, covering all the objectives studied are documented under this section.
9: Recommendation	Recommendations for further study to interested researchers in this research field are outlined in this section
References	This contains the bibliography of all referenced materials in the in-text citation.
Appendix	Result tables from the experimental analysis are documented in this section.

2 CHAPTER TWO: Literature Review

2.1 General Introduction

Biodiesel is considered an attractive fuel due to its salient characteristics in emission and performance. The key source of global energy supply, which is the non-renewable conventional petroleum fuel, is dwindling in sources due to over exploitation. This leads to increase in price of petroleum fuel and the degradation of the environment. However, a sustainable alternative fuel must be available and renewable, non-competitive with other resources and should have little or no impact on pollution. The petroleum fuel causes environmental pollution due to emission of toxic compounds during combustion. Biodiesel as a renewable and non-pollutant fuel is found suitable and addresses these issues. Most countries such as Brazil, Japan, Europe, USA, Germany, Malaysia, and India have adopted biodiesel to be used even in the transportation sector. Biodiesel can be derived from biomass sources such as oil-bearing plants, animal fats and wastes. These plants and animal sources are very vital and of great potential for sustainable biodiesel production. Biodiesel has the capacity to provide energy security as it can be produced locally depending on the type of feedstock available in the region. Unlike petroleum fuel, biodiesel is renewable, nontoxic, and biodegradable and contributes less to the greenhouse gas accumulation. The high oxygenated nature makes it environmentally friendly, as it allows for complete combustion in engine thereby reducing the exhaust emission of hydrocarbons, particulate matter and gases such as sulphur oxide, carbon dioxide and carbon monoxide (Perdomo *et al*., 2014). High flash point makes it safer for transport and storage. The ability to be used in neat form and blends with the petroleum-based fuel makes it an attractive and viable option. Biodiesel can be used in an already existing diesel engine with minimal or no modifications and can be executed using the same mechanism and infrastructure for the petroleum fuel. For effective application of biodiesel, the properties and quality have to comply with certain standards such as American society for testing and materials (ASTM D6751), European Norms (EN D14214) and South African (SANS 833) standards.

Biodiesel is chemically composed of mono-alkyl ester of long chain fatty acid derived from natural lipids which are components of plant oils and animal fats (Corro *et al*., 2017). Transesterification is the major process route for biodiesel production. Transesterification involves a chemical reaction process whereby the triglyceride reacts with light alcohol in the presence of a base, acid, enzyme catalyst to yield mono-alkyl esters and glycerol. Transesterification can be hindered by some factors, which may possibly lead to low yield of

biodiesel produced. These are free fatty acid content, catalyst type and concentration, purity of the reactants, reaction temperature, reaction time, and alcohol-to-oil molar ratio. Researchers are currently investigating on the advances in transesterification process especially the technological and catalytic methods, parametric optimization approaches, feedstock quality and sustainability, improvement on biodiesel quality, to make transesterification a viable and cost-effective process.

2.2 Method of biodiesel production

There are several methods of biodiesel production. This includes blending, micro-emulsion, pyrolysis, and transesterification

2.2.1 Dilution of crude vegetable oil with diesel

Although plant oils and animal fats are potential renewable alternative to petro-diesel, the higher viscosity hinders their widespread application in the compression ignition (CI) engines. To this effect, vegetable oils are blended with petro-diesel in order to reduce their viscosity. This approach has been reported to be effective and blending of biodiesel up to 30 % can sustain the engine power without any modification (Yesilyurt *et al*., 2020). However, this process has some adverse effects on the engine since it can lead to emulsion formation, incomplete combustion, injector plugging, high exhaust emission, atomization difficulties and high engine wear (Tabatabaei *et al.*, 2019)

2.2.2 Micro-emulsification

This method involves the dispersion of a colloidal-stable optically isotropic fluid microstructures with the general droplet dimension size ranging from 1-150 nm, produced spontaneously from the two normally immiscible liquids with one or more ionic and non-ionic amphiphilic molecules. The micro-emulsion process can offer a stable spray property during injection into the engine nozzles. The use of micro-emulsion fuels in diesel engine is also linked with various practical problems such as heavy deposit of carbon residue, irregular injector needle sticking, lubricating thickening, and low combustion. Micro-emulsion with short chain alcohol such as methanol, ethanol and 1-butanol can reduce the viscosity of vegetable oil as well as improving the spray characteristics of the of the fuel but resulted in the reduction of cetane number and heating value due to the presence of alcohol in the fuel (Yesilyurt *et al*., 2020).

2.2.3 Pyrolysis

Pyrolysis is a non-oxygenated thermal process in which organic materials are converted to fuel. The heat application in this process results in the cleavage of the biomass bond molecules, leading to the mixture of hydrocarbons formation with properties similar to petroleum fuel. It is a dicarboxylic reaction performed at elevated temperatures (above 350 ^{o}C) in the presence or absence of a catalyst (Avhad and Marchetti, 2015). Fast pyrolysis process can be achieved between 400 ^{o}C and 600 ^{o}C in a short residence time without the use of a catalyst. However, catalytic pyrolysis is effective in terms of producing quality products such as bio-oil that requires lesser processing steps than non-catalytic pyrolysis. This process is expensive and requires complicated equipment. The process also produces deoxygenated short-chain molecules similar to petro-diesel (Bora *et al*., 2016). The final product of this approach contains sulphur, which influences the final exhaust composition.

2.2.4 Transesterification for biodiesel production

Transesterification is the most established and widely used method for the conversion of oil to biodiesel due to simple operating process and quality biodiesel properties obtained, which are close to those of petro-diesel. It involves the chemical reactions between triglycerides and alcohol in the presence of a catalyst to produce esters and glycerol. The process consists of three sequential reversible reactions; the conversion of triglycerides to di-glyceride, and di-glycerides to mono-glyceride and mono-glyceride to esters and glycerol at each step (Etim *et al*., 2020). The theoretical stoichiometric reaction involves one mole of TAGs reacting with three molecules of alcohol to produce three molecules of fatty acid alkyl ester (FAAE) and one molecule of glycerol. This method is preferable due to the production of the by-product (glycerol), which can serve as a source of raw material in manufacturing of several other value-added products. The general and sequential transesterification reaction process are depicted in Figure 2.1 and Figure 2.2 (Avhad and Marchetti, 2015). Due to the reversible nature of the reaction, excess alcohol is needed to shift the reaction equilibrium towards the product formation. Alcohols used for the transesterification reactions include short chain, long chains and cyclic. However, the short chains (methanol and ethanol) are mostly used due to the inherent availability, low costing, polarity and fast reactivity (Avhad and Marchetti, 2015). Transesterification is a slow process, as a result of the immiscibility of oil and methanol. Therefore, different heating techniques such as microwaves, ultrasonic-irradiation and supercritical method are employed to improve the miscibility process. Catalysts used in the transesterification process can be an acid, a base or bi-functional (acid-base) and enzymes.

However, this is reliant on the feedstock composition used for the biodiesel production. Operative reaction parameters such as alcohol type, alcohol to oil molar ratio, catalyst type, catalyst amount, reaction time, reaction temperature, stirring intensity, co-solvent and catalyst reusability are the major deciding factors on the rate of reaction, final yield of the biodiesel and the overall cost of production.

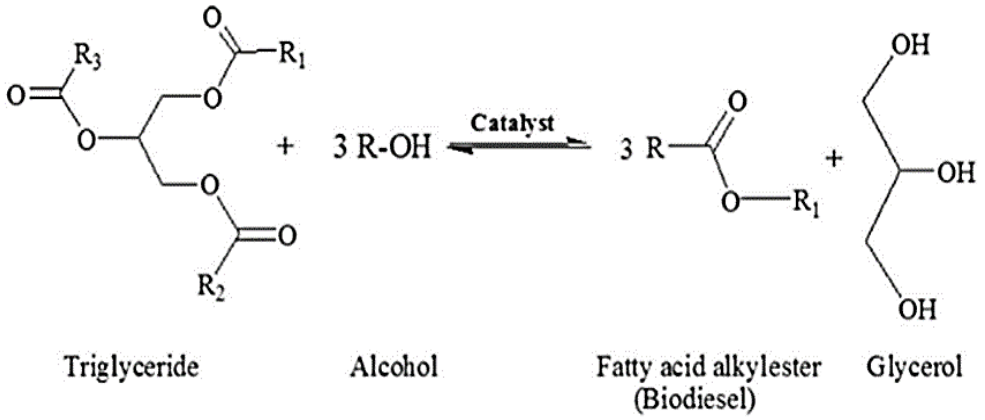

Figure 2.1: General transesterification reaction of vegetable oil (Avhad and Marchetti, 2015)

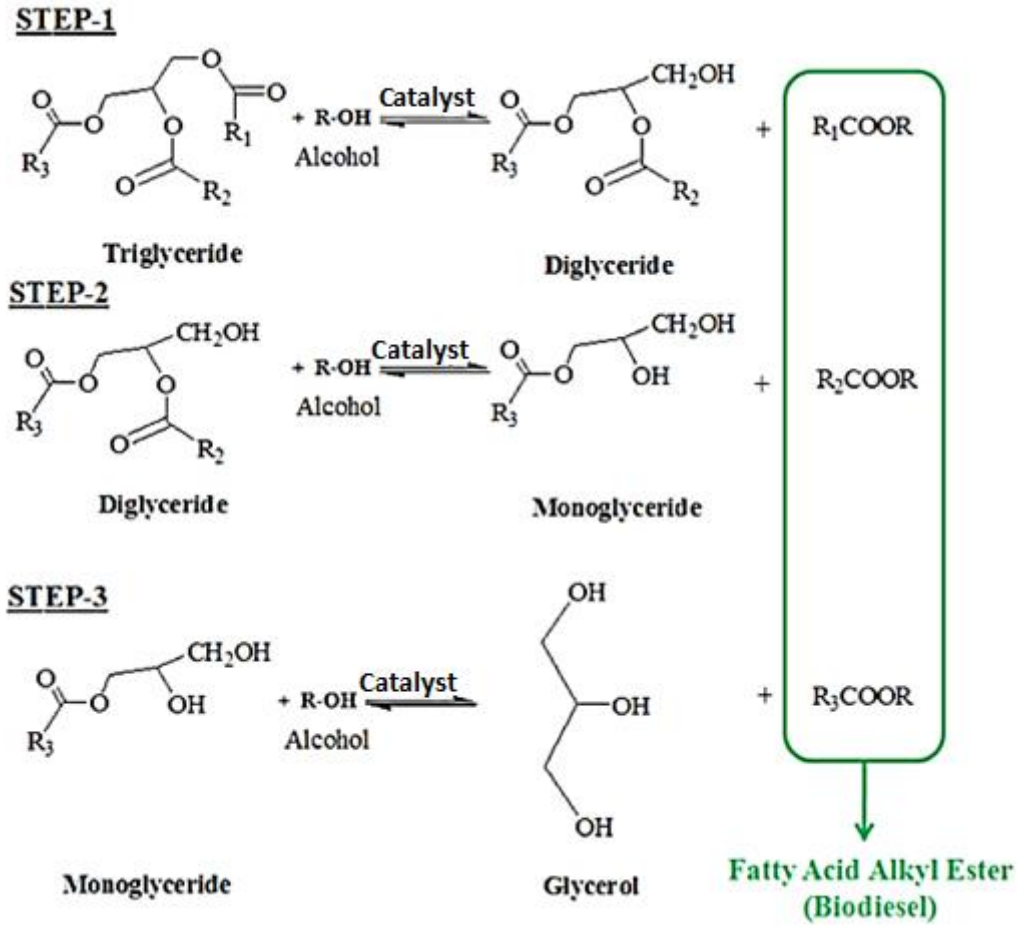

Figure 2.2: Stepwise transesterification reaction (Avhad and Marchetti, 2015)

2.3 Feedstock for biodiesel production

The widespread adoption of biodiesel is facing a number of challenges among which the biggest of them all is the feedstock of production. Feedstock is the chief factor that influences other important factors such as the cost, yield, composition and the quality of the biodiesel properties. Thus, plant oils and other oil sources need to be significantly improved and increased in order to meet the major portion of the global fuel needs in the present and in the future. Biodiesel feedstock come from various sources and are different in their composition and properties. Variations in biodiesel feedstocks originates from the climatic conditions, geographical locations, method of cultivation, harvesting season, genetic differences and breeding conditions of source materials (Aghbashlo *et al.*, 2021). The important criteria for the selection of feedstocks are based on the oil composition, percentage oil content/yield and availability (Verma and Sharma, 2016). To ensure economic and quality biodiesel production, selection process is inevitable and vital to its feasibility. The selection process can be done based on the sources and availability of the oil type in the region; for instance, rapeseed oil are used in Canada, soybeans oil in US, sunflower oil in Europe, palm oil in Malaysia, coconut oil in Philippines and so on. Other factors such as the oil content, the physical properties and chemical composition, and quality compliance to the required fuel specification are also considered vital for effective selection process (Ambat *et al*., 2018). A wide spectrum of feedstock has been investigated for biodiesel production and these can be classified into first, second, third and fourth generations.

2.3.1 First generation (Edible oils)

First generation biodiesel comprises of sources from edible vegetable oils such as soybeans, sunflower, rapeseed, canola, palm, safflower, peanuts, coconut, mustard seed, corn and olive. They are the most predominantly employed feedstock for biodiesel production and about 95% of biodiesel from the biofuel market comes from this source (Mofijur *et al*., 2014). However, the use of edible oils has been criticised as this has resulted in significant increase in seed prices. Consequently, the existing conflict between food supply and energy production has also queried their sustainability potentials for a long-term use. According to the current biofuel report update, the proposal of the European Commission towards 2030 renewable energy target achievement has been revised to completely phase-out edible-crop biodiesel production. Hence, first-generation feedstocks are not sustainable and cannot be considered as a long-term choice.

2.3.2 Second generation (non-edible oils)

Second generation biodiesel are mainly non-edible vegetable oils, waste/recycled oil and animal fats. They are another potential feedstock with high oil content and low costing. They do not pose a food versus fuel problem as barren and arid regions, which are not suitable for agriculture can be used for their cultivation. They can grow well in harsh conditions without fertilizer, thus reduces the cost involvement in their cultivation. Some of the commonly investigated potential oils in this category are camelina, pongamia, pennycress, *Jatropha curcas* (ratanjyot), *Pongamia pinnata* (karanj), *Ricinus communis* (castor), *Cerbera odollam* (sea mango), *Hevea brasiliensis* (rubber tree), *Calophyllum inophyllum* (polanga), *S. chinensis* (jojoba), *Madhuca indica* (mahua), *Thevettia peruviana* (yellow oleander), *Azadirachta indica* (neem), rice bran seed (*Oryza sativa*), caper spurge oil (*Euphorbia lathyrism L.*), *Pistacia chinensis* (bunge seed), Euphorbia tirucalli (milk bush), *Sapindus mukorossi* (soapnut), *Nicotiana tabacum* (tobacco), cottonseed oil and so on (Changmai et al., 2020; Mofijur *et al*., 2013). Waste or recycled oils include; brown grease, yellow grease, and vegetable oil soap stock and pomace oil. Animal fats include; tallow, lard, chicken fat, by-product of fish oil. Oils derived from animal sources are high in saturated fatty acid, which have some negative shortcomings on cold flow properties, but beneficial in terms of high cetane number and oxidation stability.

2.3.3 Third generation (Micro algal oil)

The third-generation feedstock are obtained from microalgae. These are considered as the most promising feedstock for the industrial-scale synthesis of biodiesel. Algal oil is highly sustainable for biodiesel production because several strains of microalgae can double in size within short period of time (Changmai *et al*., 2020). They have the tendency of creating a huge quantity of biodiesel per hectare yearly. They can be cultivated in degraded and non-agricultural lands, which prevents interference with high-valued lands and crop producing areas. It can also utilize salt and waste water sources which significantly reduces fresh water usage *(*Hegde *et al*., 2015). Other advantages include short growth cycle, small footprint, non-interference with food supply (Alam *et al*., 2015). It is reported that an acre of microalgae can generate up to 5000 gallons of biodiesel a year compared to soybeans planted in an equivalent area of land (Alam *et al*., 2015; Joshi *et al*., 2017). Algae biomass can be grown on different carbon sources environment to convert directly the carbon emission into usable fuel with no carbon-dioxide emission (Girdhar *et al*., 2017). However, the technical challenge in the cultivation and development remains a major hurdles towards large scale commercialization (Ma *et al*., 2018).

2.3.4 Fourth generation (genetically engineered /hybridized oils)

Fourth generation feedstocks are obtained via advanced genetic engineering approach to induce lipid production in vegetable oil tissue of cellulosic crops (Singh *et al*., 2021). Owing to several limitations associated with the traditional and non-traditional feedstock such as availability, insufficient oil content and composition, biofuel research has developed into another field of interest where genetic engineering technology can be applied to improve the biodiesel feedstock from plant and microbial sources. The fuel properties of biodiesel are closely related to the fatty acid composition. Inexpensive and better quality biodiesel can therefore be produced by altering the fatty acid composition of the oil used for production (Hegde *et al*., 2015). However, appropriate blend of various fatty acids containing higher amount of unsaturated fatty acids such as oleate and lesser amount of saturated and polyunsaturated fatty acids would yield better-quality biodiesel (Durrett *et al*., 2008). Application of biosynthesis process strategy in improving the biodiesel fuel properties such as cold temperature flow characteristics, oxidative stability and NOx emission was also reported feasible by altering the fatty acid profile of the raw oil used in biodiesel production (Durrett *et al*., 2008; Hegde *et al.*, 2015). Long chain saturated fatty acid esters significantly increase CP and PP whereas unsaturated esters have little effect on them. Therefore, by reducing saturated fatty acid content of the plant oil, the cold flow properties of the biodiesel produced can be improved. Genetic engineering approach to biodiesel production from various sources of plant, algae and yeast is the latest attractive technology in creating an alternative technically feasible, sustainable and cost-effective biodiesel.

Following this protocol, several research works are on-going on the hybridization of feedstock for biodiesel production in order to standardize this concept for industrial applications. Co-mingling of oils to ensure sufficiency and quality improvement is therefore a sustainable approach, since different oils have different compositional profile based on their sourced geographical location(s) and climate(s) (Aghbashlo *et al*., 2021). Biodiesel synthesis from a mixture of oils has been exploited via the combination of edible, non-edible and waste cooking oils, with yields ranging from 86 – 98 % *(*Almeida *et al. 2015;* Dharma *et al. 2016;* Falowo *et al*. 2020; Freire *et al*. 2012; Milano *et al*. 2018; Serqueira *et al*. 2014). However, this has been investigated using a one-pathway process to study the improved properties.

2.4 Catalysts for transesterification reaction

Transesterification can be both non-catalytic and catalytic. The non-catalytic transesterification process is sometimes referred to as supercritical alcohol transesterification. It is a catalyst-free technique employed for the conversion of triglycerides using alcohol at a high temperature (between 350 – 400 ºC) and pressure (10 – 25 MPa). Alcohol plays a dual function in this process both as a reactant and as a catalyst. Thus, the operating conditions enhance the solubility and mass transfer of the reactant. The reaction completion is also achieved at a shorter time due to the high rate of reaction. Transesterification is a slow process due to the immiscible nature of the reactant (oil and methanol). Catalyst is therefore introduced to the system to speed up the rate of the conversion process. The classes of catalysts use to accomplish both esterification and transesterification processes is shown in Figure 2.3. Catalysts employed in the biodiesel production process can be liquid or solid (acid, base or bi-functional) and are majorly grouped into three: they are either homogeneous, heterogeneous or enzymatic (Changmai *et al.*, 2020).

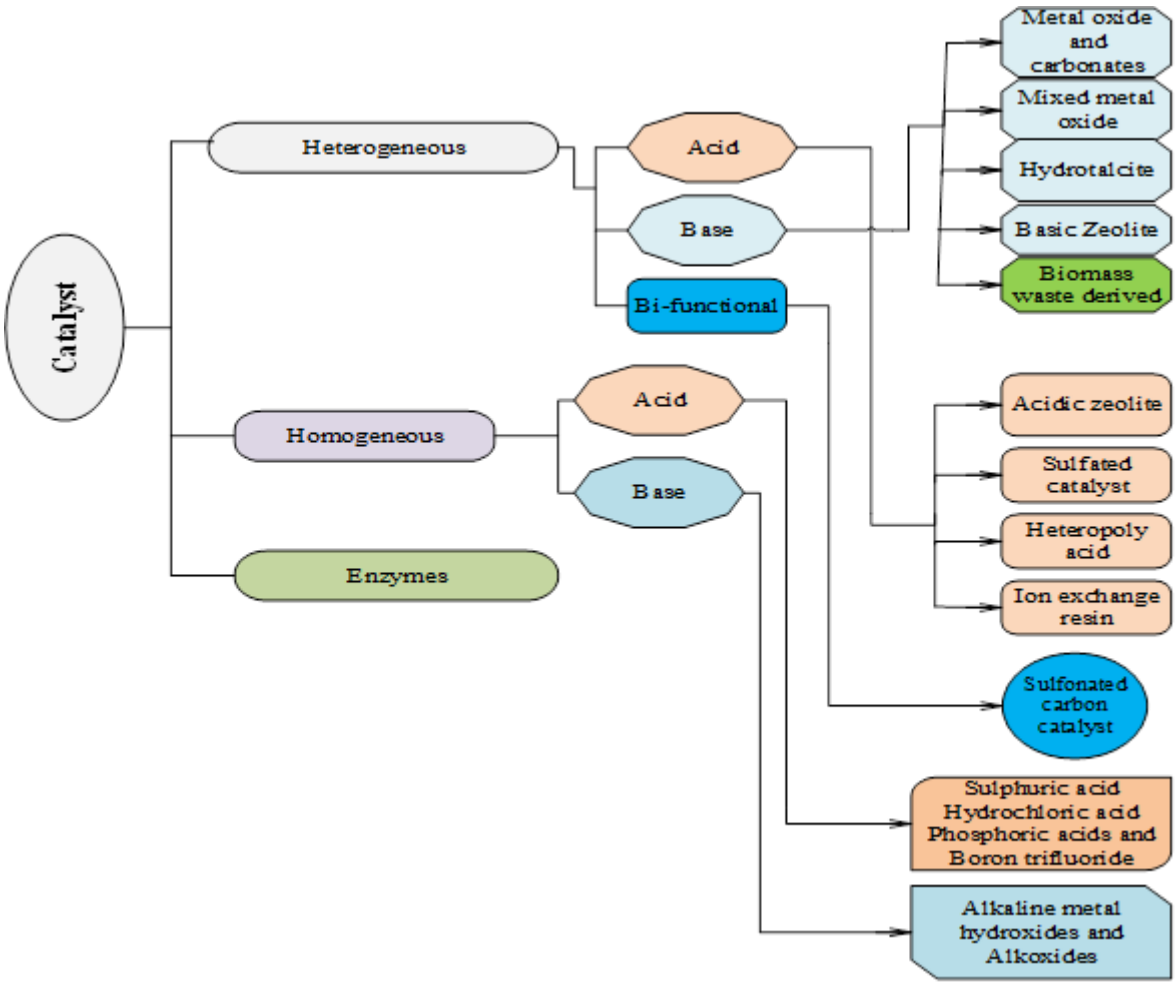

Figure 2.3: Catalysts used for the transesterification reaction process

2.4.1 Homogenous catalyst

Homogenous catalysts used in transesterification comprises of strong acids and base catalysts. Strong liquid acid catalysts such as sulphuric acid (H_2SO_4), phosphoric acid (P_3PO_4) and hydrochloric acid (HCl) are used and considered suitable for feedstock with high FFA content such as waste frying oil, non-edible vegetable oils and animal fats. The significant advantage of these catalysts are the insensitivity to the presence of FFA and water, capability to catalyse both esterification and transesterification reactions and the formation of no soap as by-product (Hanis *et al*., 2017). However the wide spread application is hindered by some other issues such as longer reaction time (usually up to 4000 times slower than the base counterparts), acidic and corrosive nature, complicated purification steps, large amount of spent water generation, difficulty in the recovery process and high operational cost (Ullah *et al*., 2018).

Homogenous base catalysts include sodium hydroxide (NaOH), potassium hydroxide (KOH) and other alkoxides such as potassium methoxide ($KOCH_3$), and sodium ethoxide ($NaOCH_2CH_3$) (Rahman *et al*., 2019). These offer several advantages such as high catalytic activities, modest condition operations, shorter reaction time and availability. However, they are highly sensitive to high FFA and water in oil, which leads to soap formation as a result of the side reaction of neutralization and saponification. Soap formation reduces the final biodiesel yield(s) because it eventually gets dissolved in the ester-glycerol emulsion which creates complexity in the separation and purification process, leading to the generation of voluminous waste water and high cost of additional operation which makes for environmental unfriendliness and overall expensiveness (Avhad and Marchetti, 2015).

2.4.2 Heterogeneous catalysts

This is a combination of solid base and acid catalysts. The solid nature gives more preference than homogenous catalysts. They are neither consumed nor are dissolved in the reaction mixture, which enhance easy separation process. Moreover, it can be easily recovered and reused, thereby reducing the associated costs and catalyst consumption. In the case of chemical/inorganic heterogeneous catalysts, the yields of methyl esters are lowered compared to homogeneous catalytic reaction. This is due to the mass transfer and deactivation of the solid catalyst as a result of poisoning, leaching, and coking. Heterogeneous acid catalysts are suitable for the catalysis of vegetable oils having high FFA because they do not promote saponification during transesterification. There are numbers of chemical heterogeneous acid catalysts

commercially available, which includes acidic zeolite, sulphated catalysts, heteropoly acids, and ion-exchange resins.

The base heterogeneous catalysts available commercially includes: metal oxides and carbonates, mixed oxides and hydrotalcite (Atadashi *et al*., 2013). Heterogeneous base catalysts show higher activity than solid acid catalysts due to their high basicity and solubility in short-chain alcohols. The major problem with the heterogeneous system is the presence of three phase system which create a diffusion difficulty and limits the mass transfer efficiency, thus hindering and reducing the rate of the reaction process (Etim *et al*., 2020). Moreover, heterogeneous chemical catalysts are faced with low number of active sites, micro porosity, leaching, toxicity and high cost of development, non-renewability and environmentally unfriendliness *(Hanis et al*., 2017). However, this can be overcome by the use of co-surfactant or an attachment of catalyst support. The activities of the heterogeneous chemical catalysts have been reviewed and summarized in paper 6.

2.4.3 Bi-functional heterogeneous catalysts

These are generally obtained via innovative technology of modifying metal oxide catalysts in order to have both the acidic and basic properties. A typical example is the organic sulfonic acid (RSO_3H). Bi-functional heterogeneous catalyst is tailored to simultaneously perform both the esterification and transesterification in a single reaction step at mild conditions. They comprise of basic and acidic sites, and they function as both in the transesterification process. They are mostly used in oils with high FFA content such as non-edible and waste oils. Thus, these class of oils are usually converted via integrated/two-step process, which are rather complex and cost consuming (Mansir *et al*., 2018a). This technique minimises several reaction steps and severe reaction conditions encountered in two-step process. The most auspicious feature of this catalyst apart from conserving time and resources is that it can be tuned to the required physicochemical properties needed to overcome the problem of high FFA and water contents in feedstock. The fact that it can be derived from waste biomass materials serves as a promising alternative to other catalysts and their associated problems and costs.

2.4.4 Biomass derived heterogeneous catalysts

Waste biological materials are essential sources of natural calcium, potassium and carbon. Their adoption into the green catalyst system is becoming attractive due to the abundant availability of mineral-rich wastes and simple process of development. Additionally, unlike chemical base catalysts, biomass derived catalysts are renewable, eco-friendly, biodegradable, nontoxic, non-

corrosive, and most importantly, their compositions are of combined active metal oxides and compounds. They are thermally stable and resilient with less leaching due to the high heat of calcination. Calcination ensures recoverability, reusability, easy separation and purification of the product (Etim *et al*., 2020; Odude *et al*., 2019). They are also cost effective and abundantly available because their input choices are majorly from waste biological materials such as animal residue and agricultural waste resources. Waste animal shells, eggshell, and bones are important natural calcium sources, while agricultural wastes are rich in potassium. Table 2.1 is the summary of most biomass materials and their effective performances in biodiesel production.

Table 2.1: Biomass derived heterogeneous catalysts for transesterification process

Waste Biomass resources	**CT (ºC) & Ct (h)**	**Oil type**	**Catalysts amount (wt%)**	**Oil/methanol ratio (molar)**	**Reaction Time (min)**	**Reaction Temp (ºC)**	**Yield (%)**	**References**
Cocoa/kola nut/fluted pumkin	500, 4 h	Yello oleander-rubber	1.5	9:1	40	55	95.02	(Falowo and Betiku, 2022)
Cocoa husk/plantain peels	500, 4 h	Honne	4.5	15:1	90	65	98.98	(Adedayo *et al*., 2020)
Plantain/cocoa/kola nut	500, 4 h	Honne/neem, rubber	1.15	12:1	6	150W	98.4	(Falowo *et al*., 2020)
Carica papaya peels	700, 4h	Used cooking oil	3.5	1:12	60	65	97.5	(Etim *et al*., 2020)
Tectona grandis leaves	700, 4h	Waste cooking oil	2.5	6:1	180	25	100	(Gohain *et al*., 2020b)
Banana peels	700, 4h	Marula oil	2.0	6:1	50	65	96.45	(Etim *et al*., 2021b)
Tectona grandis leaves	700, 4h	Waste cooking oil	2.5	6:1	180	25	100	(Gohain *et al*., 2020b)
Heteropanax fragrans (Kesseru)	550, 2h	Jatropha	7.0	12:1	65	65	97.75	(Basumatary *et al*., 2021)
Plantain peels	700, 4h	Neem	0.65	0.73:1	57	65	99.2	(Etim *et al*., 2018)
Carica papaya stem	700, 4h	Waste cooking oil	2.0	9:1	180	60	95.23	(Gohain *et al*., 2020a)
Pawpaw peels	600, 4h	Moringa oil	3.5	9:1	40	35	96.43	(Oladipo *et al*., 2020)

Moringa leaves	500, 2h	Soy beans oil	6.0	6:1	120	65	86.7	(Aleman-Ramirez *et al*., 2021)
Tucumá peels	800, 4h	Soy beans oil	1.0	15:1	240	80	97.3	(Mendonça *et al*., 2019)
Red banana peduncle	700, 4h	*Ceiba pentandra* oil	2.68	11.4:1	160	65	98.73	(Balajii and Niju, 2019)
Orange peels (solid acid)	180, 6h	Corn acid oil	5.0	19.95:1	274	-	91.68	(Lathiya *et al*., 2018)
Coco pod husks	700,4h	Neem	0.6	0.73:1	57	65	99.3	(Betiku *et al*., 2017)
Musa balbisiana colla	700, 4h	Waste cooking oil	2.0	6:1	180	60	100	(Gohain *et al*., 2017)
Snail shell	850, 4h	C*eiba pentandra* seed oil	1	9:1	60	60	56.7	(Muhammad *et al*., 2018)
Chicken bones	900, 4h	Waste cooking oil	5.0	15:1	240	65	89.33	(Farooq *et al*., 2015)
Cockle shell	900, 4h	Rubber seed oil	9	15.57:1	204	65	88.06	(Zamberi *et al*., 2016)

2.5 Characterization of the biomass generated catalysts for biodiesel production

Characterization is an essential process to determine the content and suitability of a material for a given purpose. This approach is carried out on biomass materials to investigate the effect of the process synthesis on the structure, composition and performance of the materials when exploited for a particular function. The analytical techniques commonly employed in the characterization of biomass-synthesized catalysts for biodiesel production are presented in Table 2.2.

Table 2.2: Analytical techniques applied for the characterization of the biomass catalysts (Hamze et al., 2014)

Techniques/Analysis	**Functions**
(FT-IR) - Fourier transform infrared spectroscopy	Employed to detect several functional groups presents in the catalyst
XRD - X-ray diffraction	Used to determine the crystallinity and qualitative detection of the element present in the catalyst
SEM – Scanning electron microscopy	To study the morphological structure and particle size of the catalyst
TEM - Transmission electron microscopy	Same function as SEM
EDX- Energy-dispersive X-ray spectroscopy; XRF- X-ray fluorescence; XPS – X-ray photoelectron spectroscopy	Are all used to detect and quantify the element and metal oxides present in the catalyst. Also provide information regarding the chemical state of the catalyst
BET- Brunauer-Emmett-Teller	To determine the surface area, pore volume and pore diameter/size of the catalyst
TGA – Thermo-gravimetric analysis	Thermal stability of the catalyst. Transformation of materials especially in weight, as a function of temperature increase in correlation with material vaporization and its thermal degradation.
NH_3 and CO_2 TPD – temperature-programmed-Desorption	To investigate acidity and basicity of the catalyst
Hammett indicator test and acid titration	Also used to visualize the basicity and acidity of the catalyst
MAS NMR – Magic-angle spin-nuclear magnetic resonance	To obtain information on the degree of carbonization/ aromatization of the carbonaceous materials

2.6 Transesterification pathways

Transesterification process can be carried out following one or two-step pathway depending on the free fatty acid content of the oil. Applicability of base catalyst is restricted to high FFA oils containing negligible amount of water. The presence of water in a feedstock promotes hydrolysis reaction of esters. Also, the presence of high FFA in base catalysed reaction tends to soap formation, thereby reducing the biodiesel yield and complicates the final separation and purification process, leading to additional cost of operation.

2.6.1 One-step transesterification

A one-step transesterification process is mostly applicable to oil with lesser content of FFA (usually edible oil) using base catalysts (Asri and Budiman, 2013). Homogeneous base catalyst can easily catalyse oils with FFA content ranging from 0.5 – 1 % while heterogeneous base catalyst (especially biomass derived) can perform effectively in oil with FFA ranging from 2 - 3 % (Yusup *et al*., 2017). Typical example is the transesterification of waste oil with FFA of 3% catalysed by CaO catalyst derived from eggshells (Tshizanga *et al*., 2017).

2.6.2 Two-step transesterification of non-edible oil

This method is usually possible when dealing with feedstock containing high free fatty acids most especially the second-generation feedstock. The acid value of this class of oil ranges from 10 to 45 mg KOH/g (Atabani *et al*., 2013). However, this oil type cannot undergo a one-step transesterification process. To avoid wastage of resources via soap formation, an integrated or a two-step pathway process is possible, which involves esterification of oil with acid catalyst prior to base transesterification. The first step involves the conversion of high FFA to alkyl ester using acid catalyst. The reaction step reduces the FFA content of the oil to the barest minimum while transesterification with base catalyst can be performed. The second step is the base catalysed stage, which takes lesser time than the first step due to higher activity of the base catalyst. At the end of every reaction step of the process, distinct layers are formed; the methyl ester or ethyl ester, depending on the type of alcohol used and the glycerol as the by-product. The methyl or ethyl ester obtained are further purified to obtain a quality biodiesel. Various studies conducted using this technique have been proven effective with higher yields of biodiesel ranging from 90 – 99 % (Betiku *et al*., 2017, 2016a; Bokhari *et al*., 2016; Etim *et al*., 2018; Harsha Hebbar *et al*., 2018; Joshi *et al*., 2018; Tan *et al*., 2019a; Tran *et al*., 2016; Yadav *et al*., 2016). There are factors influencing the transesterification process, these are reaction

temperature, reaction time, catalyst concentration and methanol/oil molar ratio. These factors are mostly optimised to achieve good conversion yield.

2.6.3 Combined step transesterification

Recently, research in the processing methods of biodiesel production has increased via the application of sophisticated technologies in order to make the process cost effective and sustainable. A two-step transesterification is considered a waste of time and resources due to the complicated steps of the reaction process and more equipment requirement. A simple and more economical transesterification pathway for a high FFA oils has recently been developed through the application of heterogeneous bi-functional catalysts, to perform simultaneously the esterification and transesterification in one-step. This is achievable with the presence of strong acid-basic strength of the catalyst. A bi-functional catalyst consists of both acidic and basic sites, the acidic site favours the esterification reaction while the basic site favours the transesterification simultaneously in a single reaction process. A bi-functional catalyst of Bi_2O_3-La_2O_3 was used in a combined step transesterification of *Jatropha curcas* oil with FFA of 14 % and 93 % biodiesel yield was achieved in the studies of Nizah *et al*., (2014). A palm fatty acid distillate with a high FFA of 92.37 % was converted to biodiesel via heterogeneous bi-functional catalyst (CAWS-$_7$ SO_4) modified from waste calcined angel wing shells, 98% biodiesel was obtained (Syazwani *et al*., 2019). Another researcher also conducted an experiment using a bi-functional catalyst (TiO_2/$PrSO_3H$) in a combined step transesterification with high FFA waste cooking oil, and 98.3 % was achieved under mild operating condition (Gardy *et al*., 2017). Although this process is competing in yields and more economical than the two-step process, the catalyst employed is energy intensive in their process development.

2.7 Transesterification modelling techniques

Biodiesel feedstocks are made of a broad range of long chain fatty acid, significantly affecting the transesterification reaction and the downstream processes. Although transesterification is widely recognised as the simplest operating route for biodiesel production, the chemical process complexity is governed by many factors such as feedstock type, catalyst type, alcohol type and concentration, mode of operation and reactor type (Aghbashlo *et al*., 2021). Proper modelling technique can therefore address these issues, making the process effective. Modelling techniques for prediction and optimization in biodiesel production are designed to cover the exact view of phenomena and sequences that occur during biodiesel production and application. While predictive modelling estimates the probability of outcome and simulate the process based

on the statistical data, optimization process serves as the key step to bring significant improvement in the efficiency of the process (Elkelawy *et al*., 2020). Modelling in biodiesel can be carried out in two ways: modelling of the production and simulation process of the transesterification reaction based on the modelled parametric conditions and modelling of the biodiesel combustion and simulation process of various fuel properties to predict engine performance and emission parameters. The process of modelling is of great importance in biodiesel as it aids in reducing several numbers of experiment and eliminate high cost of engine testing and emission analysis.

2.7.1 Response surface methodology (RSM)

RSM is a set of arithmetical techniques employed for modelling and analysing problems, which aim is to optimise the responses influence by several factors (Hariharan *et al*., 2020). It is extensively employed by researchers in various fields because of it flexibility for various processes. RSM is predominantly employed in the experimental design and appraisal of the synergetic effect of process variables, and in determination of optimal conditions that produce desired responses. RSM can also describe the relationship between the quantifiable responses and empirical parameters presumed to affect the response. The most used optimization methods incorporated in RSM include Taguchi design (TD), Central composite design (CCD), and Box-Behnken design (BBD). TD is used to optimise the magnitude of different process control variables. It allows for investigation of only a few pairs out of all the parametric combination set. It has the least number of experiments and allows for the assembling of data set in order decide for the most influential parameter. CCD on the other hand, is used on data with many numbers of factor up to five levels. The optimum condition can be located outside the study design range. BBD is flexible, economical, and efficient with limited number of factors. It is restricted to three levels to prevent extreme values to minimise error(s) (Etim *et al*., 2021c). RSM allows for the interaction between the empirical process parameters within the range of study and enhance a good knowledge of the process with reduced cost and time. It has extensively been used to model the esterification and transesterification process parameters such as alcohol to oil molar ratio (ATOR), process reaction time, catalyst concentration, agitation speed, temperature and so on (Dhawane *et al*., 2016a; Elkelawy *et al*., 2020; Jazie *et al*., 2012; Selvaraj *et al*., 2019).

2.7.2 Artificial neural network

Artificial neural networks (ANNs) modelling techniques has gained attention over the recent years. It is a popular evolutionary computation method that imitates biological phenomena to establish a technique for prediction and optimization processes. It is a nonlinear computer algorithm that has been successfully employed in many fields of studies including bioprocesses, medicine, mathematics, engineering design and application, neuroscience, learning system and so on, with focusing areas on data prediction, molecular sequencing, pattern recognition and optimization. ANNs processes information using the knowledge of biological nervous systems. It can handle modelling and simulation of nonlinear and complex systems (Etim *et al*., 2018). It is a powerful modelling tool that is made up of a vast interconnected network configuration consisting of simple processing elements such as (neurons, nodes or units) that perform parallel computation for processing data. ANN topology generally consists of three main layers: the input layer, hidden and output layer. The capability of analysing the relationship between input and output without a prior information relating their characteristics is one of the key advantages of ANN. Once the data set is trained by neural network, it can be used to predict the output of a new set of data input (Betiku and Ishola, 2020). Prediction with ANN is faster when data are well trained as compared to conventional simulation models that uses numerical method with lengthy iteration. In ANN, the accuracy and simplicity of the model is based on the selection of appropriate neural network topology (Deh Kiani *et al*., 2009). ANN can relearn the process to improve performance if new data set are obtained. Another auspicious characteristic of this is the ability to solve problems by learning through examples. It can also predict data accurately from small data sets saving time and cost of experiments for a larger data set (Betiku and Ishola, 2020; Etim *et al.*, 2018; Hariharan et al., 2020; Jahirul *et al*., 2013; Okpalaeke *et al.*, 2020).

2.7.2.1 Neural network design

ANN model consists of numerous simple analogy processing elements which are referred to as neurons connected by synapses. The neurons received input signals, process it and generate the output signal. The neurons are connected to one another using a weight coefficient, which signifies the degree of importance of a network connection (Aghbashlo *et al*., 2021; Betiku and Ishola, 2020). The signal produced from other neuron are modelled by the input data Xj [where j = 1, 2 …m] as shown in Figure. 2.4. The modelled signals are transferred to the artificial neuron by multiplying with the related synaptic weights (W_{kj}). The synaptic weights sometimes might be negative which indicates a inhibitory impact (Aghbashlo *et al*., 2021). The addition of the bias input (b_k) to the summation of the input data is taken to be an additional input signal

to the artificial neuron. The general functioning of the principle of artificial neuron or node can be demonstrated as Eq.1 (Aghbashlo *et al*., 2021).

$$\lambda k = f\left(\sum_{j=1}^{n} X_j W_{kj} + b_k\right) \quad 2.1$$

The final summation is transferred by the activated functions to get the output of λ_k. The hyperbolic tangent sigmoid (tansig) function and linear (purelin) are commonly used activated function (Meng *et al.*, 2014). The tansig function is used for nonlinear relationship approximation and it is generally expressed as Eq (2.2). The purlin function is used for linear relationship approximation and its general form is expressed as Eq. (2.3):

$$Tansig\ (h) = \frac{2}{1 + e^{-2h}} - 1 \quad 2.2$$

$$Purelin\ (h) = h \quad 2.3$$

Figure 2.5 depicts the general flowchart of the ANN model procedure (Aghbashlo et al., 2021). The key step for ANN modelling development is the training procedure, where the weight and the biases are adjusted to minimise the variations between the ANN predicted and actual values (Meng *et al.*, 2014). The mean square error (MSE) is usually employed to describe the variations between ANN output and the actual values. The training process is achieved through training algorithms. One of the most popular training algorithms is the back-propagation algorithm and it has different learning options such as Levenberg-Marquardt (LM) algorithm (trainlm), scale conjugate gradient (trainscg), resilient back-propagation (trainrp), variable learning rate (traingdx). Trainrp is a bit faster than traingdx but has the same storage requirement (Deh Kiani *et al*., 2009). The fastest among other algorithms is trainlm. LM is an estimation of Newton's method. It converges faster than the original back-propagation and it is suitable for moderate sized feedforward neural network. It has been extensively used, validated and reported to be accurate in most cases (Al-Shanableh *et al*., 2016; Baghban *et al*., 2018; Betiku *et al*., 2016b; Hariharan *et al*., 2020; Hosseinpour *et al*., 2016; Selvaraj *et al*., 2019).

Overfitting is another important aspect to be considered during the training procedure. This occurred when the obtained ANN memorises the training examples and does not have the ability to generalize the unseen data (Meng *et al*., 2014). However, early stopping can solve this

practically. For this to be achieved, the available data are randomly selected into training set, testing set and validation set. While the training set is used to train the network, the validation set prevent over-training on the training set. The testing set is an unseen data used to obtain the final test of the trained ANN and cannot be used for the training. Errors on the training and validation sets are simultaneously monitored. The training stops when the validation error keeps increasing for a specific number of iterations. The use of early stopping method gives the ANN model a better generalization capacity.

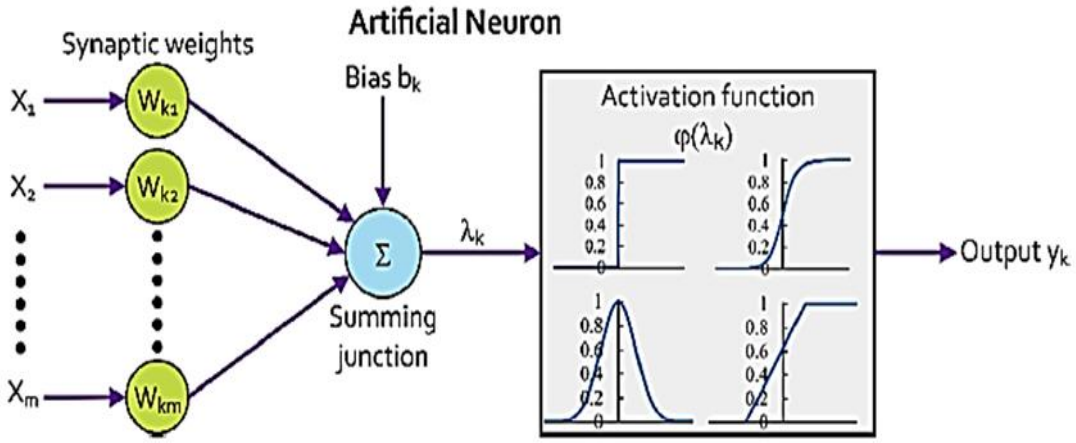

Figure 2.4: Schematic representation of the working principle of artificial neuron (Aghbashlo *et al*., 2021)

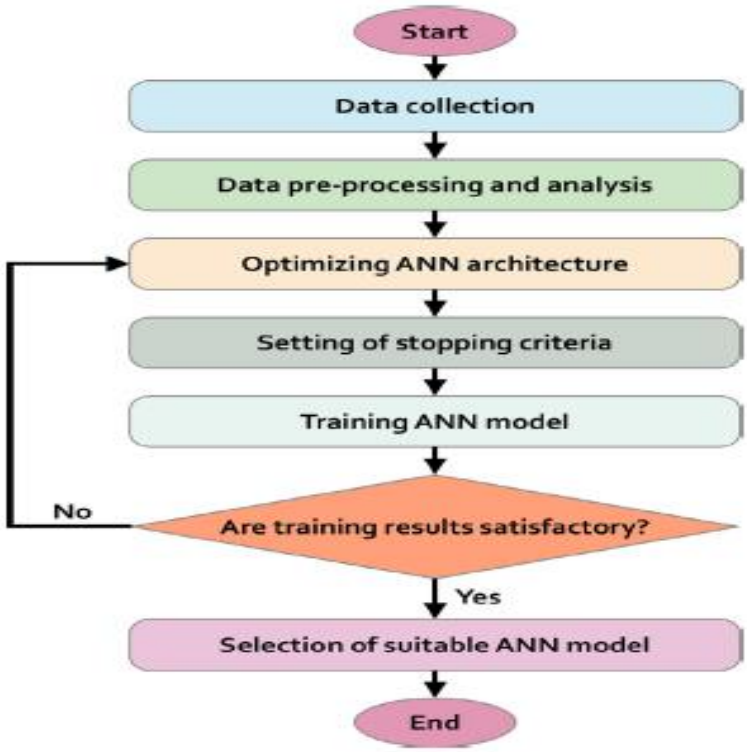

Figure 2.5: The flow chart of general procedure for ANN model development

2.7.3 Kinetic modelling for transesterification

Kinetic modelling is used to develop the reaction mechanism to study and to obtain useful information regarding the chemical transformation process in the reaction medium during biodiesel production. It shows what transpired in the reactor within the materials used for the production. It is the most crucial step to be considered in the reactor design and the applicable simulation process. Kinetic model is necessary in the optimization of chemical processes involving heating and separation steps. It is used in selecting the most favourable production conditions that could maximise biodiesel yield(s). It can also be employed in different biodiesel production processes such as homogenous, heterogeneous and enzyme catalysed reactions. A well-developed kinetic model is a useful predictive means in large-scale biodiesel production as it gives details of stages and predictive capabilities of the applicable methods taking into consideration the mass and heat transfer processes and the thermodynamic equilibrium attainable (Tin et al., 2015). To develop a suitable kinetic model, reactor design is necessary to determine certain parameters such as concentration, temperature and pressure profile, which could assist in generating important information for the process scale ups.

2.8 Transesterification process intensification techniques

The conventional heating process generally involves the use of hot plates, heating mantles and water baths as the source of heat during reaction and it is the most widely used approach in transesterification process. Although effective but limited in certain areas in terms of costing and full-scale production. There are cases of heat losses to the surroundings, long reaction time and high temperature to attain reaction completion, soap formation due to inadequate heat dissipation and mass transfer restrictions and longer separation time (usually up to 24 h) are associated with the conventional heating process (Thoai *et al*., 2019). Hence, the introduction of novel chemical engineering approach that leads to equipment scale-down, cleaner, and sustainable technologies to enhance production with less energy consumption and waste generation. These technological approaches include the use of microwave irradiation (Silitonga *et al*., 2020), ultrasonic assisted (Sharma *et al*., 2020), hydrodynamic cavitation (Mohod *et al*., 2017), and electrolysis (Rafati *et al*., 2019). This technology in biodiesel production is an essential factor towards achieving effective biodiesel production.

Several types of sophisticated reactors have been introduced recently in the biodiesel production systems to facilitate the production process intensities and to improve the heat dissipation in

the system. However, these reactors are employed to enhance superior performance in their activities during biodiesel production such as high mass and heat transfer rates within shorter molecular diffusion distance. Conventional reactors have been reported to associate with longer reaction time and other material consumption in large amounts. Intensified reactors offer rapid reaction rates through improved heat efficiency and mass transfers, high surface area/volume ratios and short distances of diffusion (Santacesaria *et al*., 2012). The activities of various conventional and intensified reactors during transesterification process are presented in Table 2.3. Although, there are differences in the process designs and costs but all constitute to the major aim of achieving a cleaner process in biodiesel production.

Table 2.3: Various reactor types employed in biodiesel synthesis

Type of reactor	**Oil used**	**Cat. / concentration**	**Catalyst loading**	**Alcohol Type/ratio to oil**	**Reaction time**	**Temp**	**Yield**	**Ref**
Packed microchannel reactor	Refined palm oil	CaO (activated)		Methanol (24:1)	8.9 min	65	99	(Chueluecha et al., 2017)
Membrane (liquid-liquid film integrated)	soybeans	NaOH	(0.2 wt%)	Methanol (9:1)	120	55	99.3	(Noriega et al., 2018)
Batch reactor	Beef tallow	HCl	(0.5%)	Methanol (6:1)	1.5 h	60	92.04	(Ehiri et al., 2014)
Batch reactor	Canola	KOH/$CaAl_2O_4$	(3.5 wt%)	Methanol (12:1)	4h	65	96.7	(Nayebzadeh et al., 2016)
Batch reactor	Canola oil	Sol-gel La_2O_3-ZrO_2	-	30:1	240	60	56	(Salinas et al., 2018)
Batch reactor	Refined palm oil and waste cooking oil	Biomass fly ashes	10 wt%	9:1	180 min	60	96%	(Vargas et al., 2019)
Zig Zag micro channel	Soy beans oil	NaOH	-	methanol	28sec	-	99.5	(Wen et al., 2009)
Continuous Micro-channel reactor	Rape seed oil	CaO/MgO	(7.87 wt%)	Meth (1.75:3)(Hexane) Co-solvent (0.575:1)	10 min	70	99.31	(Mohadesi et al., 2017)
Continuous flow microwave reactor	Palm oil	NaOH	-	Meth (12:1)	1.75 min	70	99.4%	(Choedkiatsakul et al., 2015)

Micro tube reactor	Waste cooking oil	H_2SO_4 (esterification process)	1 wt%	Meth (9:1)	5 sec	65	FFA conversion (3.96 mg KOH/g)	(Tanawannapong et al., 2013)
HC reactor	**Waste cooking oil (Palm oleoic)**	KOH	1%	Meth (6:1)	15 min	60°C,	98.1%	(Chuah et al., 2017)

2.9 Applied technologies in biodiesel purification

The full conformity of the biodiesel properties cannot be met with the standard specifications (EN 14214, ASTM D6751and SAN 833) until purification processes are performed. Crude biodiesel products obtained from both conventional and membrane reactors comes with impurities such as unreacted triglycerides, glycerol, soap, excess methanol and residual catalysts (which need to be removed after transesterification). The presence of these impurities in biodiesel fuels could lead to serious engine problems and damages (Atadashi, 2015). The impurities can be removed through several technologies such as conventional separation and purification. This includes: the wet washing and the dry washing techniques. Wet washing is the simplest and widely used technology in biodiesel purification. It involves repeating addition of water to the crude biodiesel product and decanting until a colourless water is obtained (Atadashi *et al*., 2011). This to ensure the elimination of remaining salt and soap formation due to their solubility. Although this technique is efficient, it links with increase in production time and cost, difficulty in biodiesel removal from water. It also leads to increase in spent water discharge and create environmental problems due to increase in pH values, high content of biological and chemical oxygen demands (Atadashi, 2015). Additionally, water washing technique increases the fuel water content higher than 1000 ppm, making the removal of water complicated and time consuming. Dry washing technology is introduced to substitute the disadvantage of wet washing. It is industrially accepted and adaptable, although the chemistry behind performance is yet to be fully understood. It involves the use of adsorbents such as magnesol powder, cellulosics, purelite, trisyl, activated carbon, activated clay, activated fibre and ion exchange resin to obtain purified biodiesel product (Atadashi *et al*., 2011). Refining operation is performed at 65 °C and lasted for 20-30 min (Sundus *et al*., 2017). This technique is waterless, therefore minimises washing time and generate no spent water, which could further reduce production cost and time. The dry process enhanced biodiesel quality and due to the fact

that it is waterless, there is the possibility of achieving water content level below 500 ppm to meet the requirement of ASTM D6751 specification. Due to the strong affinity of the composition of the adsorbents to the polar compound, it can easily be integrated into an existing plant (Veljković *et al*., 2015). However, the major challenge of this technology is the generation of spent adsorbents, which are not regenerated. The issues encountered with the wet and dry washing technology has given rise to the implementation of a more sophisticated technology such as the application of a membrane system. This system allows for the study of basic features of operation under reasonable conditions. It is more environmentally friendly and advantageous than the other two washing technologies as it regenerates no spent water, less energy intensive and significantly removes the glycerol and unreacted triglycerides. Membrane process is capable of producing biodiesel product with glycerol content of 0.007 wt% which is lower than the value prescribed by EN 14214 , ASTM D6751 and SAN 833 specifications (Ambat *et al*., 2018).

2.10 Analytical and quantification methods of biodiesel Product

There are several analytical methods developed to characterize biodiesel products. They include: the nuclear magnetic resonance (NMR), the spectroscopic method such as gas chromatography (GC) and infrared (IR). The GC method is extensively employed in biodiesel analysis because of high sensitivity in component segregation and quantification. It aids in determining the ester content and other specific contaminants such as the unconverted triglycerides, free glycerol and so on. The technique also provides adequate information on the biodiesel product and suitable for large-scale laboratory analysis. In the GC technique, helium is mostly used and widely preferred as a carrier gas over compressed hydrogen gas because of its lightweight and inert properties (Ramos *et al*., 2009). Safe storage guarantees usage as a carrier and auxiliary gas for the flame-induced detector (FID). Hydrogen can be used as ignitable gas in an FID but not preferred due to high thermal gas conductivity and flammability. The use of hydrogen as a carrier gas might lead to reaction with some molecules during the process. Nitrogen can also be used because it is cheaper, available and safer among the gases used but deficient in terms of selectivity. However, the general drawback of these techniques are; the extensive sample preparation, aging standards, baseline drift, overlapping signal and expensive cost of maintenance and configuration (Hamze *et al*., 2014). Other chromatographic techniques for biodiesel quality evaluation include: gas-liquid chromatography (GLC) (Rashid and Anwar, 2008), thin-layer chromatography-flame ionization detector (TLC-FID) (Rahman *et al*., 2019), and high-performance liquid chromatography-gel permeation chromatography

(HPLC-GPC) (Ambat *et al*., 2018). They are sensitive techniques and usually helpful in quantifying the FAME product and by-products such as mono- and di-glycerides, together with unreacted triglycerides. Near-infrared spectroscopy (NIRS) is widely used for biodiesel fuel quality survey and monitoring transesterification reaction progress due to ease of operation, rapidity of measurement and low cost of analysis (Balabin *et al*., 2011).

2.11 Biodiesel properties and characterization

Several factors influencing the fuel properties of biodiesel are feedstock type and quality, fatty acid compositions, production methods, purification process and post- production issues (Singh *et al*., 2019). The fuel properties of biodiesel can be grouped based on their influences on engine performance and operability. These are thermal properties such as cetane number and calorific value. Cold weather properties: cloud point, pour point and cold filter plugging point. Transport and storage: oxidative and hydrolytic stability, flash point, induction period, filterability and temperature limit. Wear of engine parts: viscosity, lubricity, cleaning effect and compatibility and other production related contaminants: FFA, residual alcohol and catalysts, free and total glycerol. All these properties must conform to the stipulated standards established for the commercial biodiesel use.

Characterization ensures the basis for a successful long-term utilization and acceptability of any fuel or biofuels. The establishment of biodiesel standard and specifications is geared towards improving the biodiesel properties by addressing critical quality issues that are linked to production. Biodiesel can only be accepted as a standalone or hybrid fuel (blends with petrol diesel) if properties meet the quality standard specifications of various global regions. The variations in the global climatic conditions affect demands and usage. For this reason, the property assessment is appropriate in order to restrict certain feedstocks, which can negatively influence fuel quality, combustion and performance characteristics. Quality regulation enables identification of feedstocks and blends limit for effective engine performance suitable for various regions in the world. The variation in biodiesel properties is linked to the fatty acid esters composition of the feedstock of production, refining, post-production and storage processes (Aghbashlo *et al*., 2021). While the physico-chemical properties affect the ignition and combustion efficiency, the structural features such as hydrocarbon chain length, the degree of saturation and unsaturation affects the fatty acid esters profile (Hoekman *et al*., 2012a). These factors clearly influence the biodiesel properties and its performance as automotive fuel. The main criterion of the biodiesel quality is the inclusion of the physical and chemical properties into the requirements of the adequate standards. Standards for biodiesel are continuously

updated due to the evolution of compression ignition engines (CIE) and revaluation of feedstocks eligibility. Biodiesel quality regulations are according to regions/countries, the existing diesel fuel standards, the common type of diesel engines available in a region, climate conditions and emission regulations governing the region/countries.

2.11.1 Chemical composition of biodiesel

Biodiesel is composed solely of fatty acid methyl esters. The composition is made up of carbon, hydrogen, and oxygen atoms that form the linear chain molecules with single and double carbon-carbon bonds. The fatty acid ester takes the form *Cnc:nd* (lipid number) where *nc* is the number of carbon atom in the fatty acid and *nd* is the number of double bonds in the fatty acid (e.g. 18:1 indicates 18 carbon atoms and one double bond). The fatty acid ester molecules with double bonds are unsaturated. The highest concentration of fatty acids are C18:1, C18:2, C18:3, followed by C18:0. Biodiesel with the highest concentration of fatty acid with lesser carbon atoms: C12:0, C14:0 and C16:0 are more volatile than others. The physicochemical properties of biodiesel produced from a given feedstock are determined by the properties of the ester content(s). Due to the significant oxygen content (about 10-11 %), biodiesel has lower carbon and hydrogen contents compared to petro-diesel. The variation in biodiesel produced from different feedstocks can be explained extensively by the following two properties which greatly influence the overall behaviour and suitability of FAME as a diesel blend-stock are; the size distribution of the fatty acid (FA) chains and the degree of the unsaturation within these FA chains (Hoekman *et al*., 2012b).

2.11.2 Cetane number

Cetane number (CN) is dimensionless, and it is a prime indicator of ignition quality of fuels. It is determined by comparing ignition delay of fuel sample to that of hexadecane (high quality standard) with a cetane number of 100 and heptamethylnonane (low quality standard) with a cetane number of 15 based on an established standard cetane scale (Knothe and Razon, 2017). This explains how CN decreases with decreasing chain length and increasing with branching. It relates to the time required for liquid fuel to auto-ignite rapidly after injection into a compression ignition (CI) engine. The CI engine combustion of the fuel-air mixture is initiated by compression ignition of the fuel. It is the primary indicator of the fuel quality as it defines the ease of fuel self-ignition. Ignition delay is elapsed during the injection of fuel into the combustion chamber and self-ignition of the air-fuel mixture. The upper and lower limits of the cetane number ensure the proper functioning of the engine. Very low cetane number causes

ignition difficulties especially at low temperatures, irregular function, slow warming, noise, incomplete combustion and increased hydrocarbon emission pollution (Habibullah *et al*., 2014; Knothe, 2014; Yesilyurt *et al*., 2020). Biodiesel has higher cetane numbers in comparable with the petro-diesel due to higher oxygen contents, which result in higher combustion efficiency (Ozcanli *et al*., 2013). High cetane number indicates a short ignition delay and good engine performance. It also enhances a working performance in cold weather conditions, promotes complete combustion and limits the formation of white smokes, hydrocarbons, carbon monoxides, NO_X and particulate matter emissions (Knothe and Razon, 2017). Extremely high cetane numbers can lead to premix of fuel leading to incomplete combustion and increase of the exhaust smoke, overheating, injector nozzles plugging as a result of unburnt fuel particles. The minimum CN number for biodiesel prescribed by ASTM D675 and EN 14214 standards are 47 and 51 respectively. CN numbers of biodiesel depends on the concentration of the ester contents. The CN number decreases with the number of double bonds (*nd*) in the fatty acid molecules and increases with the number of carbon atoms (*nc*). The CN numbers of biodiesel is higher than those of the vegetable oils which are between 39 and 67 (Barabas and Todoru, 2012).

2.11.3 Calorific Value

The calorific value otherwise called heating value or heat of combustion is the measure of the fuel energy content of any fuel. It is the total energy content generated when a substance is combusted completely in the presence of air or oxygen (Ozcanli *et al*., 2013). It is obtained by oxygen calorimeter as the product obtained from the combustion of the latent heat of moisture. It is the quantity of heat liberated when a unit quantity of the fuel is burnt in oxygen in an enclosure of constant volume. The heating value of the fatty acid esters increases with molecular chain length (i.e. the number of carbon atoms) and decreases with the degree of unsaturation (number of double bonds) (Agarwal *et al*., 2010). The presence of oxygen in the ester molecules decreases the heating value of biodiesel by approximately 10 – 13 % compared to diesel. This helps in proper combustion in an engine and decreases the oxidation capacity. EN 14214 standards prescribes a heating value of 35.00 MJ/kg in biodiesel for heating purposes (Bora *et al*., 2018). The calorific value of petro-diesel is 46 MJ/kg (Mahmudul *et al*., 2017). Unsaturated FAME has lower energy mass than the saturated.

2.11.4 Density of biodiesel

Density is an important fuel property which affects the performance of fuel atomization in the CI engines. It is defined as the mass of unit volume of any liquid at a specific temperature (Atabani *et al*., 2013). The air-fuel ratio and energy content within the combustion chamber are influenced by the fuel density (Saxena *et al*., 2013). The density of a fuel is directly affecting the performance quality as it is linked to some other properties such as cetane index, heating value and viscosity. It also affects atomization and combustion in the cylinder. The stipulated range of density for biodiesel by EN 14214 at 15 ^{o}C is from 860 – 900 kg/m^{3}. Density above the specification limit leads to excess biodiesel fuel pumping, which tends to affect the air-fuel ratio, engine performance and combustion characteristics. Biodiesel is denser than petro-diesel but less compressible due to higher molecular weights. The density of biodiesel depends on the fatty acid composition of feedstock, the method of oil extraction and the degree of fuel purity (Bhuiya *et al*., 2014). High density leads to large spray injection, increase in the wall temperature of the combustion chamber and reduces ignition delay. Contaminants such as the presence of residual methanol can cause reduction in density. Therefore, density can be an indicator of fuel contamination during storage. FAME density is strongly affected by the degree of unsaturation. The higher the degree of unsaturation, the higher the density. It is also depending on the chain length and tends to decrease with higher chain length.

2.11.5 Viscosity of biodiesel

Viscosity measures the resistance to fluid flow or internal fluid friction that opposes the dynamic change in fluid motion. It is a vital fuel property that affects the fuel flow behaviour in the injector, pipelines, orifices as well as spray atomization mostly at low temperatures (Knothe and Razon, 2017). Fuel viscosity has both upper and lower limits. Based on the American and European standards, the acceptable limits of kinematic viscosity at 40 ^{o}C for biodiesel are 1.9 – 6.0 and 3.5 – 5.0 mm^{2}/s respectively. The upper limit guarantees smooth fuel flow in cold weather conditions while the lower limit prevents the potential power loss of fuel in the engine (Ozcanli *et al*., 2013). Highly viscous fuels lead to increase in combustion chamber deposits, increase in wear of pump and injector element due to higher mechanical effort and also the prolongation of combustion duration (Agarwal *et al*., 2017a). Higher viscosity also causes operational problems at low temperatures because viscosity increases with decreasing temperatures. High temperature decreases the viscosity of the biodiesel due to the weakening of the intermolecular forces thus allowing for a free flow of molecules *(Shahir et al*., 2017). Higher kinematic viscosity of biodiesel significantly affects fuel spray, droplet size

distribution, droplet evaporation rate and spray atomization process, resulting in slower burning leading to longer combustion duration (Agarwal *et al*., 2017a). The lower the viscosity, the easier it is to atomize and achieve finer droplets. The fuel with too low viscosity leads to insufficient penetration and the formation of black smoke specific to combustion in the absence of oxygen (Barabas and Todoru, 2012). Very low viscosity provides insufficient lubrication for precision fit of the fuel injection pumps, leading to leakages (Ozcanli *et al*., 2013). Biodiesel viscosity is generally impacted by some structural configuration such as the chain length, the number and nature of double bonds. Viscosity increases with the increasing number of CH_2 moieties and the degree of saturation (Knothe and Razon, 2017). The degree of unsaturation has less influence on the viscosity and are useful in improving the cold-flow properties without significant effect on other properties (Hoekman *et al.*, 2012a). The viscosity of biodiesel also depends on the hydrolytic oxidation and extent of polymerization. The viscosity of biodiesel is higher than petro-diesel due to the polarity of biodiesel as a result of the presence of electronegative oxygen (Barabas and Todoru, 2012).

2.11.6 Acid Number

This is otherwise called neutralization number and is an indicator of the FFA content level in biodiesel. It is the amount of KOH (mg) required to neutralise a unit mass of FAME in (g). The maximum allowable limit certified by ASTM, EN and SAN standards for biodiesel is 0.5 mg KOH/g. Acidic component in biodiesel may occur as FFA, organic acids, unremoved acid catalysts and as by-product of oxidation (Veljković *et al.*, 2015) The purification process after biodiesel production helps to reduce the acid value. Higher acid value is an indicator of fuel deterioration during storage. It causes corrosion of metal components and deposits in the fuel supply system and reduces filters and fuel pump durability.

2.11.7 Oxidative stability

This is one of the most important fuel properties that relates to the in-use performance of biodiesel. The chemical changes that occur during extended storage of biodiesel indicates fuel deterioration. Instability in fuel can leads to formation of gums, increase in viscosity, sediment and deposits. It is determined not only by the fuel composition alone but also has to do with the age of the biodiesel and the storage conditions. Oxidative stability is influenced by the degree of unsaturation, the higher the unsaturation, the poorer the stability.

2.11.8 Iodine number

This measures the degree of unsaturation of fatty acids based on the alkyl double bond in biodiesel. It is the quantity of iodine needed to saturate the fatty acids in 100 g of a biodiesel sample (Caldeira *et al., 2017)*. It varies with the feedstock type and can be determined based on the classic chemical method using Wij's solution (Chuah *et al*., 2016). High iodine value relates to a high degree of unsaturation due to double bonds. A fuel with high iodine number is prone to oxidation, which is characterized with polyunsaturated fatty acids. This in turn can promote the formation of engine deposits related to the double bond polymerization of glycerides (Islam *et al*., 2015). High iodine value impacts the engine operation negatively as in the case of increased of carbon residue formation, injectors polymerization, piston rings, grooves, reduced lubrication quality and nozzle clogging (Imdadul *et al*., 2016). The EN14214 specification standard for biodiesel iodine number is 120 (g I_2/100g), SANS 833, is 140 (g I_2/100g) and ASTM standard has no limit for iodine number.

2.11.9 Flash point

Flash point is the minimum temperature at which the fuel ignites when exposed to air or flame. It is an essential property used for safety evaluation during transportation and storage. Flash point of biodiesel is higher than petro-diesel making it less a volatile fuel for transportation and storage. Higher flash points in fuels may lead to incomplete combustion and formation of carbon deposits in combustion chambers. Flash point standard must be in line with insurance and fire regulations. This serves to specify limit for the concentrated residual methanol (< 0.2 wt%) to protect the engine and to avoid the attack on some metals and elastomers in the fuel system (Knothe and Razon, 2017). The flash point of pure biodiesel should not be less than 93^{o}C to ensure a complete eradication of alcohol during the process of production.

2.11.10 Cold flow properties

This is the most significant quality of biodiesel that allows for usability in a broad geographical region and seasons. Cold climatic conditions may lead to crystallisation of liquid fuel particles due to strong intermolecular interaction below their melting points. Lower cold flow properties may cause clogging of fuel pipes and pump resulting in improper engine operation (Verma and Sharma, 2016). The cloud point (CP), the pour point (PP) and the cold filter plugging point (CFPP) or low temperature flow test (LTFT) generally characterize the cold flow performances of fuels. Cloud point is the temperature at which wax formation begins to plug the fuel filter. It

measures the temperature of the initial wax formation when the fuel is cooled. The solid crystals formed thickens and clog the fuel filters and injectors in the engine.

Pour point measures the fuel gelling point. It is the lowest temperature at which the fuel is no longer able to flow or are pumpable as a result of the amount of wax precipitated out of the solution (Verma *et al*., 2016). Cloud point is always higher than the pour point. Biodiesel has a poor cold flow property (higher cloud point and pour point) than petro-diesel.

CFPP is the minimum temperature at which a liquid fuel is able to pass through a standard filtration device under a specified testing condition due to gel formation by the fuel element (Atabani *et al*., 2013). It measures the lowest temperature at which the fuel could no longer flow in a fuel system. In some countries, it is the only criteria for evaluation of the cold flow properties due to direct better correlation with operability functionality than cloud and pour points. CFPP is directly linked to the long chain saturated ester content in biodiesel fuel. The longer the saturated chain, the lower the CFPP performance (Manaf *et al*., 2019b). High saturated fatty acid in a fuel lead to poor cold flow properties. Thus, cold flow properties can be improved by increasing the chain branching and decreasing the chain length (Agarwal et al., 2010). This can easily be achieved through hybridization strategies or genetic modification of feedstock of production.

2.11.11 Sediment and water content

Water and sediment are vital parameters in biodiesel production that hinders ester yield, promote soap formation and separation difficulty and deactivation of catalyst. Sediments are formed as dirt particles suspension during long-term storage due to oxidation. Thus, this can hinder the fuel flow from tank to the combustion chamber. Biodiesel is hygroscopic in nature. It absorbs water from the atmosphere when stored for a long time and also retains traces of wash water during its purification step (Manaf *et al*., 2019a). Biodiesel is insoluble in water and tends to separate inside the tank and settle at the bottom. High water content in biodiesel is associated with lots of disadvantages such as: encourages microbial growth, corrosion of storage tank, increase fuel consumption, decrease of heating value, emulsion formation and hydrolytic oxidation (Knothe *et al*., 2006; Manaf *et al*., 2019b; Yesilyurt *et al*., 2020). Low water content leads to phase separation in blends with petro-diesel, constituting operational problem in engine. Proper drying of the final product and tight storage containers including nitrogen blanketing can minimize high moisture content in biodiesel. According to EN 14214, water concentration in biodiesel must not exceed 500 ppm or 500 mg/kg (0.05 wt%).

3 CHAPTER THREE: Bio-alkaline synthesis from biogenic waste and their hybrids

3.1 Introduction

Waste biological materials are essential sources of minerals such as calcium, potassium, magnesium and sodium. These are the basic ingredients for the preparation of base heterogeneous catalysts. Their adoption as green catalysts are becoming of recent interests due to the abundant availability of mineral-rich waste and simple process of development. In the catalytic system of biodiesel production, catalysts play a vital role in increasing the rate of reaction and facilitating the mixing process by increasing the contact area of the immiscible reactants. Biodiesel production process can be catalysed by either acid or base. Base catalysts are highly preferred and used much rapidly due to their fast reactivity and solubility in alcohols (Hanis et al., 2017). Conventional biodiesel synthesis basically takes place at moderate conditions (60 ^{o}C, 1 atm) in the presence of alkaline homogenous catalysts such as potassium and sodium hydroxide and methoxide (Mohammed *et al*., 2018). Although these catalysts displayed fast reaction rates, their use in transesterification are limited due to some related technical issues such as voluminous spent water generation, high toxicity, saponification reaction, difficulties in separation and purification processes.

Heterogeneous catalysts have some outstanding economic advantages over homogenous, which include recoverability from the product mixture and recyclability (Papargyriou et al., 2019). Effective catalysts can be developed from waste biomass materials for economically viable and environmentally friendly biodiesel production process. Wastes biomass are generated in large quantities in South Africa with little or no economic values and constitute immensely to environmental pollution. Several wastes biomass mostly from animal and agricultural materials have been investigated and reported for their high catalytic activity in biodiesel production. Waste animal resources include; eggshells, chicken bones, fish bones, shrimp shells, crab shell, snail shells, goat bones (Corro *et al*., 2016; Marwaha *et al*., 2018; Tan *et al*., 2019a). Agricultural wastes include sugar cane bagasse, coco pod husk, and trunks, papaya peels, stem and truck, plantain peels, rice husk, coconut shell, *Brassica nigra* plant, *Moringa oleifera* leaves, *Tectona grandis* leaves and many others. A review paper published from this study contains the summary of most biomass materials and their activities in biodiesel production (Etim et al., 2020).

Animal waste resources are rich in natural CaO while aagricultural wastes are reported as the major source of potassium-based compounds such as K_2CO_3, K_2O, KCl, K_2SO_4 and so on, with high catalytic performance converting up to 90-99% biodiesel yield (Etim et al., 2021c). Oxides of alkaline earth metals such as CaO, MgO, ZnO and SrO show strong basic sites. However, this class of metal tends to leach into the reaction mixture, creating problems such as longer production time, difficulties in separation and purification process (Tan *et al*., 2019*a;* Wong *et al*., 2015). The most widely used in the transesterification reaction is CaO, due to its low cost, easy obtainability, high basic strength and recyclability characteristics. The support of CaO is ideal due to high surface area and large number of pores on its surface (Marwaha *et al*., 2018). To address the problem of leaching and other related issues associated with CaO, it is basically modified in vast literature studies with attachment of chemical compounds such as CaO-KOH, CaO-NaOH, CaO-Na_2SO_4 and CaO-H_2SO_4 to enhance effective catalytic activities and purity product (Dhawane *et al.*, 2016b; Nisar *et al*., 2017; Ogbu *et al*., 2018). This also gives rise to attractive innovation of producing an effective bi-functional catalyst, which can be used to transesterify high FFA oils. Moreover, doping of these catalysts with alkali metals such as Li-CaO, CaO/Al_2O_3, CaO-CeO_2, CaO-SiO_2 and others has also been investigated to enhance catalytic activity and increase recyclability (Wong *et al.*, 2015).

Most of the studies conducted on the biomass derived catalyst synthesis were done individually, however the purpose of feedstock blending is introduced to achieve improved properties and to generate more quantities. Most of the biomass materials are scarce in some locations. Thus, to make the process more efficient, advances towards blending of only biomass derived catalysts are considered a promising approach to an effective and standalone green process of biodiesel production. To this effect, blending of chicken and fish bones to improve their basicity and catalytic functions was investigated by Tan *et al*. (2019b), and was reported effective with increased surface area, high basic strength and significant reusability cycles. Agro-waste material blending have also been recently studied to achieve improved properties and higher catalytic functions in biodiesel production: the blending of cocoa pod and plantain peels was investigated with honne-oil biodiesel production with maximum conversion of 98.98 % (Adedayo *et al*., 2020). The mixture of coca pod, plantain peels and kola nut husk on a blend honne-rubber-neem oil biodiesel production was studied by Falowo *et al*. (2020), with maximum yield of 98.48 %. Again, a mixture of cocoa pod, kola nut and fluted pumkin waste for heterogeneous catalyst for transesterification of yellow oleander-rubber seed oil was investigated by Falowo and Betiku (2022), the highest biodiesel yield of 95.02 % was obtained. However, the exploration of biogenic waste combination such as animal waste and agricultural

waste materials has not been investigated and reported. A typical example and first contribution to this novel approach is from the experiment carried out in this study. This was conducted using chicken eggshells and *Carica papaya* peels (paper 2). This chapter investigates the exploitation of chicken eggshells, banana peels, papaya peels and their hybrids for a green heterogeneous catalyst development for effective biodiesel production. The characterization analysis was performed to evaluate their physical and chemical properties. The study contributes immensely to effective biomass valorisation and sustainable biodiesel development.

3.2 Waste materials of study and their availability

3.2.1 Eggshells

Eggshells are abundantly available waste found anywhere in the world. Places such as restaurant and bakeries in South Africa produces waste eggshells in several tons per day. Globally, eggs production amounts up to about 8.3 million tons yearly and approximately 2.4 MT of the shells are ending up in landfill. However, the unique composition of the shells such as 95 % content of calcium and 3.4 % of protein gives it special characteristics. Eggshell has wider applications such as a source of calcium supplements for both animal and humans, as bio adsorbent for waste water treatment and as source of CaO for biodiesel production (Gupta and Rathod, 2018; Risso *et al.*, 2018).

3.2.2 Banana peels

Banana is the most popular fruit consumed globally with over 100 million metric tons produced annually in tropical and sub-tropical countries. According to the world market report by FAO 2021, 116.78 million metric tons of banana are produced annually. In 2019, Asia was ranked the highest producer with 63.14 million metric tons, followed by Africa with 21.48 million metric tons, out of which South Africa produced 416.5 thousand metric tons. Although banana is a tropical crop and well adaptable in any region, it is limited due to climatic and cultivation area challenges in South Africa. The peel is rich in carbohydrate, protein and fat. Banana peels contain high amount of potassium and other mineral compositions in the order of K > Na > Mg > Ca > Cu > Fe > Zn > Pb. It is reported as being utilized as a carbon source for citric acid production and as bio-sorbent for heavy metals removal from wastewater (Betiku *et al*., 2016a). The peels and other part of the banana plant such as trunk and peduncle have been investigated and reported as good source of solid heterogeneous catalyst for biodiesel production (Balajii and Niju, 2020; Betiku *et al*., 2016a; Rajkumari and Rokhum, 2020).

3.2.3 *Carica papaya* (pawpaw) peels

Carica papaya fruit commonly known as pawpaw is an economical tropical fruit from herbaceous plant belonging to caricaceae family. It is commonly found in tropical and subtropical regions of the world and is believed to originate from Mexico and Central America (Oladipo et al., 2020). Papaya fruit pulp is high in carbohydrate and the most freshly consumed fruit globally, due to its high content of sucrose and other macro and micro minerals such as K, Na, Mg, Ca, Mn, Cu and Zn. Figure 3.1a shows the fresh papaya fruit. It is a good source of antioxidants (such as carotenes, vitamin C, B, K, thiamine, riboflavin and niacin) and digestive enzymes, papain, which is used as additive for various industrial purposes. The world production of papaya fruit increases from 13.24 million metric tons in 2018 to 13.74 million metric tons in 2019. Figure 3.1b depicts the world statistics of papaya production from 2000 to 2019. Among this, South Africa has a little production in the last two years. The annual production volume of papaya in South Africa decreases by 10.4 thousand metric tons in 2018/2019 as against 13.5 thousand metric tons of the previous year. When compared to the fruit production in 2001/2002, there is a dramatic decrease from 22.2 thousand metric tons in 2001/2002 to 10.4 thousand metric tons in 2018/2019. This is attributed to the non-ideal climatic challenge for its production in South Africa. Figure 3.1c, presents papaya fruit production trend in South Africa from 2000 – 2019. A typical papaya fruit is reported to have a percentage composition of 8.5 % seed, 12 % skin and 79.4 % pulp (Oladipo *et al*., 2020). With the huge global production of papaya fruit, the peels disposal becomes a concern as it contributes to environmental waste pollution. Aside utilization of the peels as food additive and supplement, there is inadequate information regarding other industrial utilization of the waste peels. It is reported that the peels contain potassium as the major ingredient in its mineral composition up to 504.33 – 516.33 mg/kg with other elements such as Ca (16.23 mg/kg), Zn (1.93 mg/kg) and Fe (2.73 mg/kg) (paper 2). However, the presence of high content of potassium in its mineral content suggest that it is a good source of potash and could be developed as a green catalyst for transesterification reaction.

(a) Fresh papaya fruit

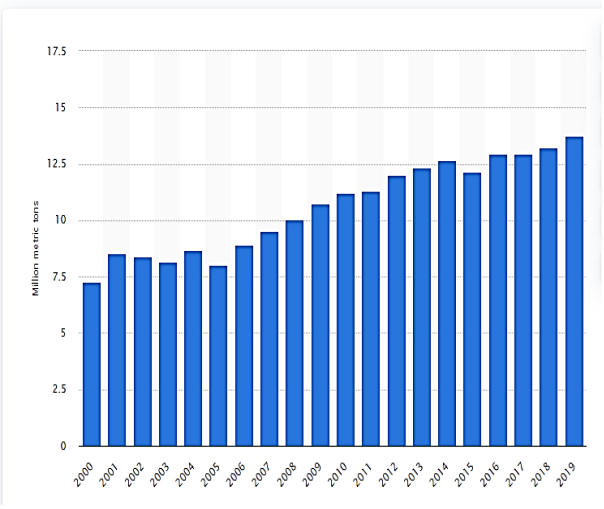

(b) Global papaya production from 2000 – 2019

(c) Papaya production in South Africa from 2000 – 2019

Figure 3.1 (a-c): shows the fresh papaya fruit, the statistics for the global papaya production and South Africa

3.3 Preparation of catalysts from biomass waste materials

The waste materials (eggshells, banana peels and pawpaw peels) were washed with distilled water to remove all debris at the surface of the materials. The washed materials were dried in an oven for 48 h at 80 ^{o}C to constant weight. The dried eggshells were crushed to powder, sieved to obtain fine particle size of less 75 µm, and further calcined in a programmable muffle furnace [Havells, B 25, DHMCBSPF025] at 900 ^{o}C for 3 h to generate natural CaO, labelled as calcined eggshell (CE-CaO). The dried banana peels and pawpaw peels were burnt individually in open air and ground into fine powder using a porcelain mortar and pestle and then sieved with 75 µm mesh size to obtain fine char. The resultant powder of each material were further calcined at 700 ^{o}C for 3 h to obtain calcined banana peels (CBP) and calcined pawpaw peels

(CPP) respectively according to the method adopted by Betiku et al.(2017) and Etim *et al.* (2018). Each calcined char sample was stored in an air-tight bottle and kept in a desiccator for further analysis

3.3.1 Preparation of biogenic hybrid catalysts

The hybrid process was performed by modifying the calcined char of each agro-waste material (CBP and CPP) with CE-CaO via wet impregnation method. Equal proportion of the CE-CaO and CBP were bonded by dissolving 1g of CE-CaO in a 100 ml of warm distilled water followed by the addition of 1g of CBP. The suspension was subjected to vigorous agitation for 1 h using a magnetic hot plate set at 60 ^{o}C, in order to obtain a slurry. Similarly, CE-CaO and CPP were also bonded with different ratio proportion; 7CE-CaO: 3CPP and then stirred vigorously for 1 h. The resultant slurries of each hybrid obtained were dried over 120 ^{o}C for 24 h to remove moisture. The dried sample of CE-CaO:CBP hybrid were pulverized and further activated via calcination at 800 ^{o}C for 2 h in the furnace. Similarly, the dry cake of 7CE-CaO: 3CPP hybrid were activated at 600 ^{o}C for 2 h to generate effective nano-particles (NPs) respectively. Each synthesized hybrid nanoparticles catalyst were labelled CE-CaO:CBP-800 NPs and 7CE-CaO:3CPP- 600 NPs respectively. Figures 3.2 and 3.3 show the procedure and the general flow chart of all the synthesized catalysts.

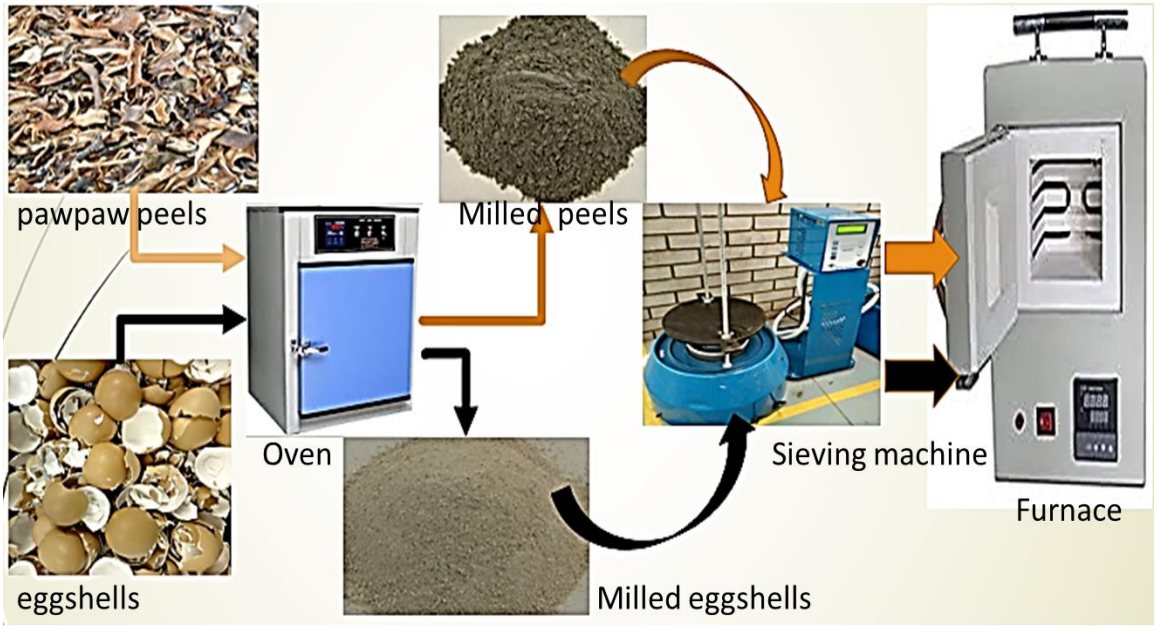

Figure 3.2: Procedure for the synthesized bio-alkaline catalyst

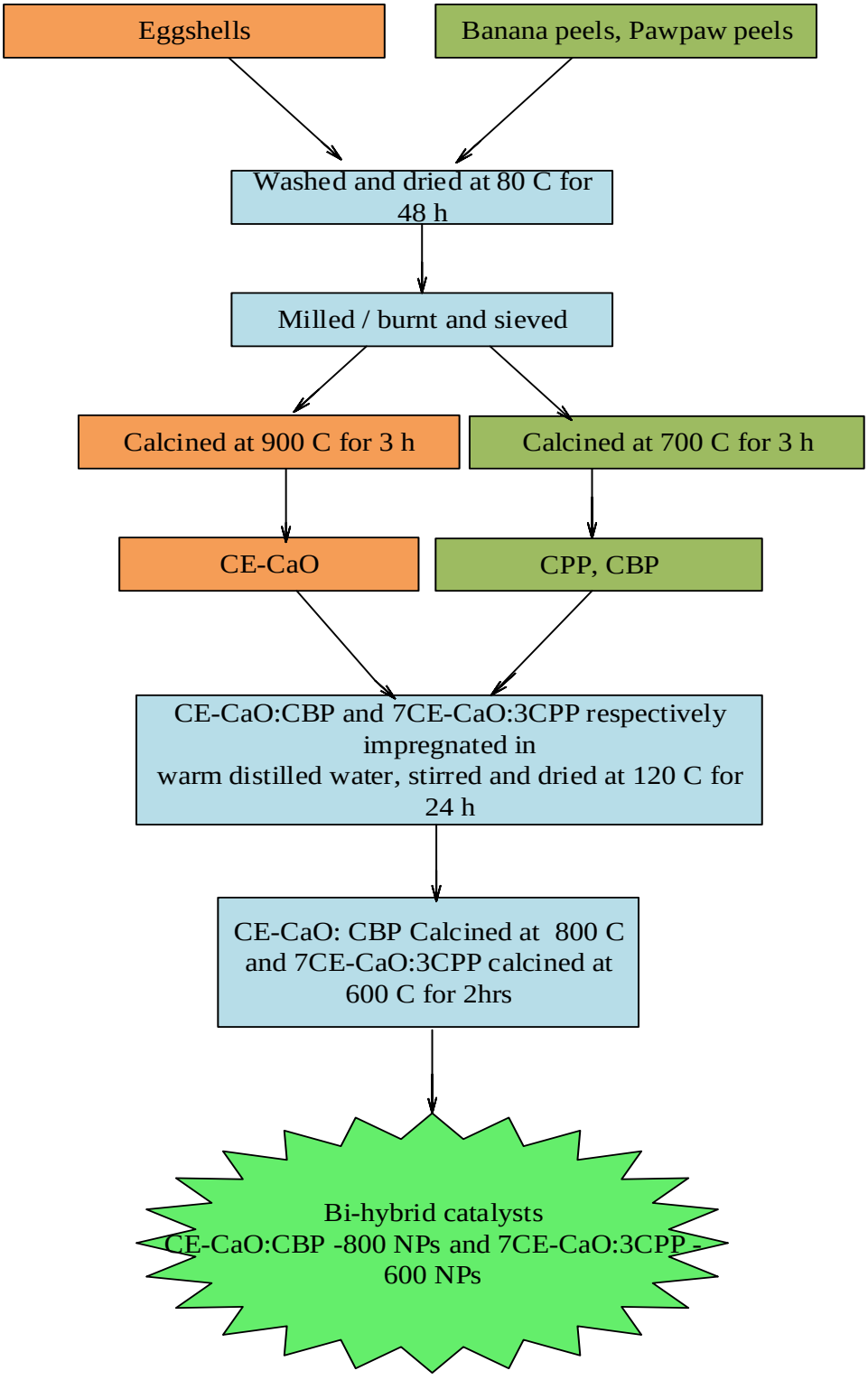

Figure 3.3: General flow chart of the synthesized bio-alkaline catalysts

3.4 Catalyst characterization

3.4.1 Basic strength

The basic strength of the synthesized catalysts was determined by Hammett indicator method. 25 mg of each catalyst was dispersed in 10 ml of methanol solution in a Hammett indicator and left to equilibrate for 3 h respectively and the colour changes were observed. The Hammett indicator used was phenolphthalein (H_9.8) (Pathak *et al*., 2018; Tshizanga *et al*., 2017).

3.4.2 IR spectra Analysis

All the synthesized catalyst samples were analysed for active functional groups using Fourier transform infrared (FT-IR) spectroscopy at the wavelength of 4000 – 500 cm^{-1}, using an FT-IR spectrometer (PerkinElmer spectrum 100). The X-ray diffraction XRD was used to detect the crystalline compounds of the samples in a D-8 advanced diffractometer with CU-Kα radiation, fitted to a PSD detector (Bruker AXS Karlsruhe, Germany), with an electron beam generated at 40 kV and 30 mA at ambient temperature, in the scanning angle of 2θ ranging between 10-80 ^{o}C. The surface morphology and composition of the calcined chars were determined with a high-resolution scanning electron microscope – Energy dispersive X-ray (SEM-EDX) by AURIGA (Zeiss Germany).

3.5 Reusability study of the catalysts

The reusability of the synthesized single and hybrids bio-alkaline catalysts were studied by investigating the number of reusable cycles. The investigation was done for single and hybrid catalysts under the optimal conditions. The catalysts were recovered by separating the spent catalyst after each reaction cycles via centrifugation and washed with solvent (n-hexane) to remove the physio-sorbed oil. The washed catalysts CBP and CPP were dried in oven respectively and reused without further reactivation. While the hybrids (7CE-CaO:3CPP-600 NPs and CE-CaO:CBP-800 NPs) were further reactivated by calcining at high temperature of 800^{o}C for 2 h respectively. The regenerated bio-alkaline single and hybrids catalysts were investigated for their reuse in subsequent transesterification.

3.6 Results and Discussion

Hammet indicator test conducted for the basicity determination for the synthesized catalysts showed the basic strength of H_10.9 for CE-CaO, H_12.0 for CBP, H_17.5 for CPP, H_22.8 for CE-CaO:CBP-800 NPs and H_25.4 for 7CE-CaO:3CPP-600 NPs were taken to be higher than the weakest indicator (H_9.8). The increase of the basic strength of these catalysts are attributed to the major concentration of the alkaline metal oxides present (Gohain et al., 2020a; Rajkumari and Rokhum, 2020). The higher basic strength observed for the hybrid catalysts are due to the combined strength of the two major active basic ions (K^+ and Ca^+). The efficiency of the heterogeneous base-catalysed transesterification reaction is enhanced due to the strong basic sites on the surface of these catalysts, which is responsible for their high catalytic activities in the conversion process.

3.7 Characterization of CE-CaO, CBP and CE-CaO:CBP-800 NPs Hybrid catalyst

3.7.1 FT-IR Analysis

The FT-IR analysis is important to determine the active surface functional groups of compound present in the catalysts. The combined FT-IR plots for CE-CaO, CBP and CE-CaO: CBP-800 NPs are shown in Figure 3.4. The bands at 3642 cm^{-1} are attributed to (—OH) of absorbed moisture on the surface of catalyst samples (Chen *et al*., 2015). This was obvious in CE-CaO and more intense in CE-CaO:CBP-800 NPs samples due to water absorbed during the synthesis process as a result of the hygroscopic nature of CaO. Although not clearly visible on CBP samples, but can still be observed around 3500 - 3000 cm^{-1} (Rajkumari and Rokhum, 2020). The characteristic band around 1411 and 873 cm^{-1} in CBP samples can be accredited to the carbonyl (O-C-O) vibration of metal carbonate entities resulting in the K-O and Ca-O vibrations at high calcination temperatures. The band around 600 in CBP are attributed to K-O. The band around 500 cm^{-1} could be accredited to vibratory stretching of Ca-O and are clearly visible in CE-CaO, and CE-CaO:CBP-800 NPs spectra. The EDX result (Table 1) corroborates the observed functional groups identified in the IR spectra of each sample.

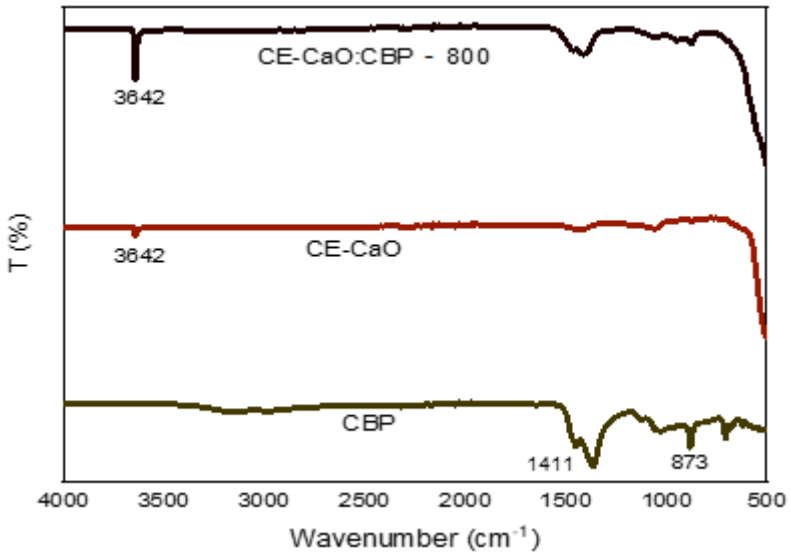

Figure 3.4: Combined FT-IR plot for CBP, CE-CaO and CE-CaO:CBP-800 NPs

3.7.2 The XRD Analysis

The XRD analysis was performed to on the catalyst samples to determine their mineral compositions at the crystalline phase. The combined XRD spectra of CE-CaO, CBP and CE-CaO/CBP-800 NPs are shown in Fig.3.5. The X-ray diffraction (XRD) intensity plot shows the crystalline characteristics of the catalyst structure of CE-CaO, CBP and CE-CaO:CBP - 800 NPs catalysts. The obtained peaks were compared with the Joint Committee on Powder Diffraction Standards (JCPDS) database. In CE-CaO, CBP and CE-CaO:CBP-800 NPs samples, distinct peaks were observed between 14-55^{o} and this can be attributed to the efficacy of the calcination temperature. The calcined eggshells (CE) diffraction peak showed CaO as the dominant and active compounds present in eggshells (JCPDS: 00-037-1487). However, there are other minor peaks indicating the presence of $Ca(OH)_2$. This is due to the hygroscopic nature of CaO when exposed to air and moisture. The peak intensity was found to decrease at high temperature of calcination attributable to the increasing formation of CaO. Thus CaO peaks increase as a result of the greater crystallinity of the catalyst (Tan *et al*., 2019b). In CBP sample, calcination led to the decomposition of compounds present in CBP to KCl, K_2CO_3 and $MgCaSiO_4$. The XRD pattern indicates the dominant peak of the face centred cubic (FCC) lattice structure of KCl corresponding to 2θ^{o} at 28.3^{o}, 40.5^{o} and 50.2^{o}. A crystal monoclinic structure of K_2CO_3 observed at the degree of 12.8^{o}, 25.7^{o}, 26.8^{o}, 32.6^{o}, 39^{o} and 41.8^{o}; and the orthorhombic structure of $MgCaSiO_4$ was also detected as corresponding to 15.9^{o}, 21.2^{o}, 24.47^{o}, 27.9^{o}, 30.4^{o}, 33.5^{o} and 34.6^{o}. The result showed that the new compounds $HN_4Al_3(SO_4)_2(OH)_6$

and Na K Cl were formed as a result of the impregnation in the X-ray diffraction pattern of CE-CaO:CBP-800 NPs hybrid. The peaks at 17.65º, 29.57º, 47.43º 52.16º can be ascribed to the presence of rhombohedral structure of Ammoniolunite – Ammonium Aluminium Sulphate ($HN_4Al_3(SO_4)_2(OH)_6$). While the peaks at 28.6º, 40.9º, 50.7º and 67º indicates the presence of FCC lattice structure of sodium potassium chloride (Na K Cl). This clearly indicates that these mineral particles were properly absorbed on the surface of the CaO through impregnation process and are responsible for the effective catalytic activity of the hybrid catalyst.

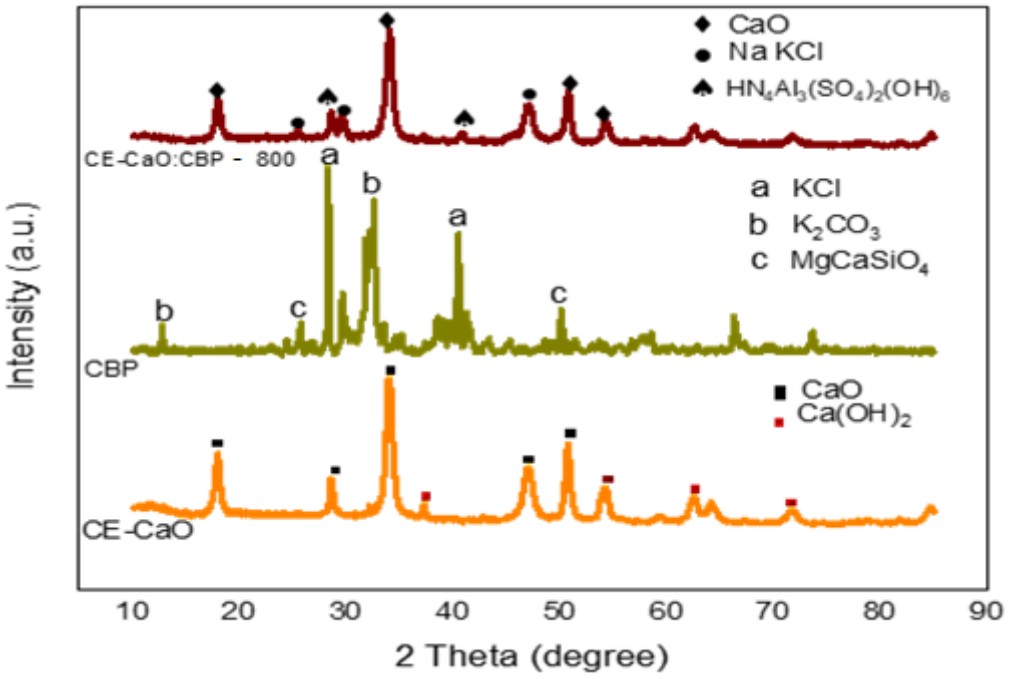

Figure 3.5: combined XRD spectra of CE-CaO, CBP and CE-CaO:CBP-800 NPs

3.7.3 SEM-EDX Analysis

The SEM analysis was conducted on the synthesized catalyst samples to examine their morphological structure. The micrograph displaying the morphology of the powdered CE-CaO, CBP and CE-CaO:CBP-800 NPs is depicted in Fig 3.6. The calcined eggshells consist of irregular micro morphology of stone-like structures while calcined banana peels consist of a number of aggregates of microporous structure due to calcination effect. The hybrid nano particles catalyst CE-CaO:CBP-800 shows the aggregate of numerous porous and spongy nature of the ash mineral particles as a result of high temperature of calcination. The particle size distribution of the non-uniform structure on the surface of the hybrid catalyst might be attributed to the merging effect of the two biogenic materials during synthesis, which clearly indicate the modified surface structure of pure CaO as result of the attachment of other mineral

particles from CBP catalyst. Moreover, the EDS analysis as shown in Table 3.1, indicates that CE contains only two major elements which are Ca and O while CBP was found to be mainly composed of high content of K, O and Cl with trace amounts of P, Mg and Si. However, the hybrids of the two biogenic materials CE-CaO:CBP-800 was found to contain majorly of high content of O, Ca, K with small amounts of Cl and Si. The content of Ca was observed to increase which was minimal in CBP. The existence of the increased content of K and Cl was found present in pure CaO surface, indicating the effectiveness of impregnation and calcination processes.

Table 3.1: EDS result of CE-CaO, CBP and CE-CaO:CBP-800 NPs

Calcined catalyst	**Temp & time**	**Element Composition (%)**								
		O	Ca	K	Cl	P	S	Mg	Na	Si
CE-CaO	900 °C, 3 h	49.2	50.8	0.00	0.00	0.00	0.00	0.00	0.00	0.00
CBP	700°C, 3h	38.5	1.21	44.11	14.17	0.38	0.00	0.72	0.00	0.92
CES/CBP-800°C	800°C, 2 h	44.39	34.93	18.62	1.41	0.00	0.00	0.00	0.00	0.65

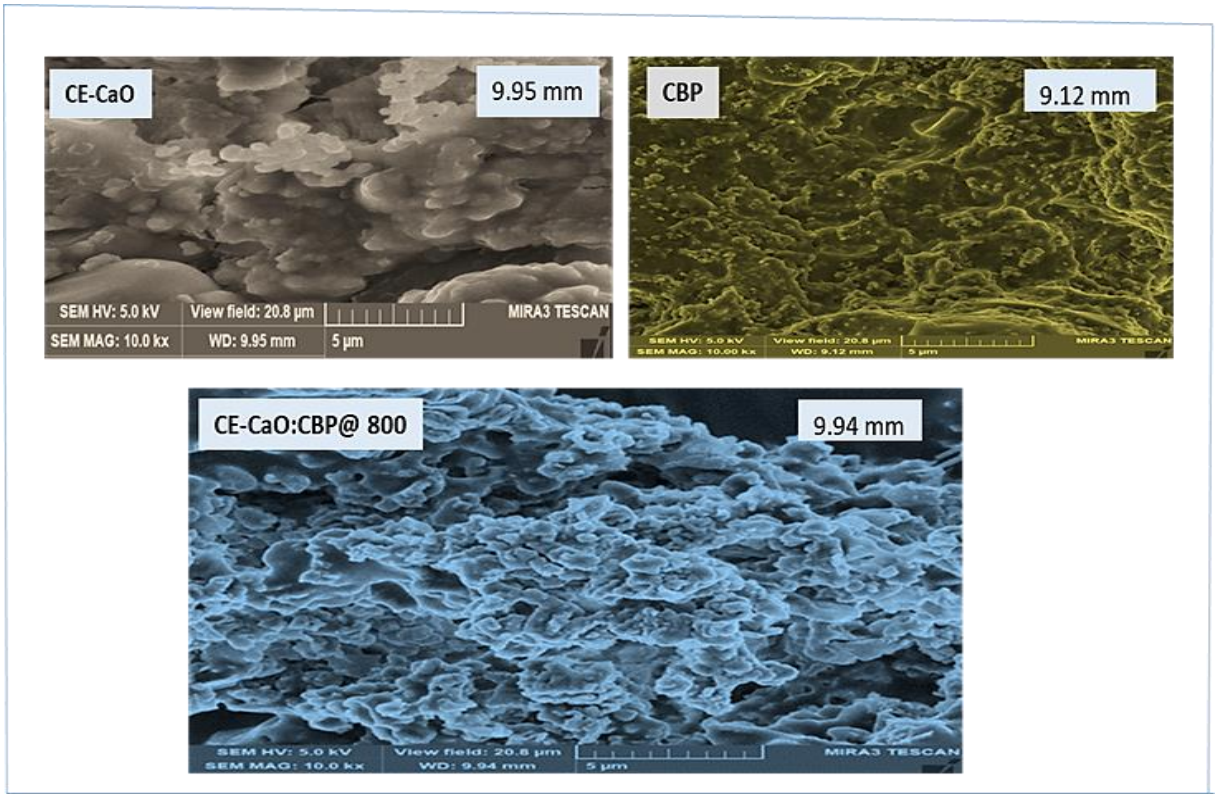

Figure 3.6: The SEM images of CE-CaO, CBP and CE-CaO:CBP-800 NPs

3.8 Characterization of CE-CaO, CPP and CE-CaO:CPP-600 NPs Hybrid catalyst

3.8.1 FT-IR Analysis

The infrared (IR) spectra of CE-CaO, CPP and 7CE-CaO:3CPP-600 NPs is depicted in Figure. 3.7, which shows the bands of available functional groups. The O-H group broad band at 3642 cm^{-1} designates the presence of absorbed water molecule. It is less obvious in CPP due to high heat treatment and well pronounced in CE-CaO and 7CE-CaO:3CPP-600 due to high hygroscopicity of CaO. The characteristic bands around 1418 cm^{-1}, and 1046 cm^{-1} are corresponding to –C-O stretching vibrations, suggesting the presence of metal carbonates entities such as Ca-O and K-O. The absorbed band around 868 cm^{-1} is due to the presence of CO_3^{-2} group and was also indicated in CPP ash and other calcined biomass chars reported by Falowo and Betiku, (2022). The band at 500 cm^{-1} is accredited to the vibratory stretching of oxide of Ca, indicating the presence of CaO. This is mainly contributed by eggshells, and clearly indicated in the CE-CaO and 7CE-CaO:3CPP -600 spectra.

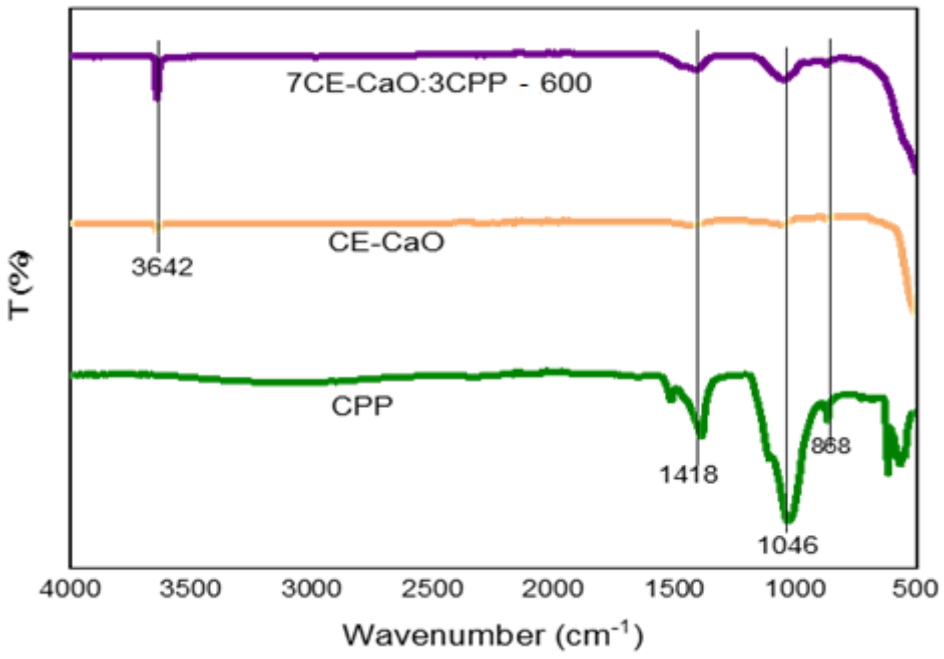

Figure 3.7: FT-IR spectra of CE-CaO, CPP and 7CE-CaO:3CPP-600 NPs

3.8.2 XRD Analysis

Figure 3.8 displays the combined pattern of CE-CaO, CPP and 7CE-CaO:3CPP-600 NPs. The X-ray diffraction pattern of CPP shows the prominent crystalline peaks of cubic structure of KCl at 2θ value of 28.3, 40.5 and 50.1. Orthorhombic crystal structure of K_2SO_4 at 2θ value of 21.3, 29.7, 30.7, 30.9, 43.3 and the hexagonal structure of $KCaPO_4$ at 2θ value of 30.3, 32.5, 45 and 56.5°. The X-ray diffraction of the 7CE-CaO:3CPP-600 NPs hybrid showed the proper absorption of the newly found mineral particles on the surface of CE-CaO as a result of the impregnation process. The pattern shows the mixtures of three inorganic compounds viz CaO, KCl and NaO_2. The presence of CaO can be identified with the prominent peaks at 2θ value at 19.30, 30.51, 40.65, 50.55, 60.45 and 70.31. This is the main constituent compound and it is contributed by eggshells. The existence of $Ca(OH)_2$ was also identified as a result of the moisture absorbed by the CaO due to its natural hygroscopic properties. CE only constitutes CaO as the only available compound, thus the presence of KCl is contributed from the pawpaw peels. Other minor peaks indicating the presence of NaO_2 were found to exist. Thus, the attachment of KCl on the surface of CaO, due to impregnation of the two biomass materials increases the basicity property and the surface area of CaO, boosting its activity for effective transesterification process. The XRD shows that the calcination process is efficient in extracting and successfully improving available minerals present in the material. The observed crystalline composition is clearly in congruence to the EDS outcomes (Table 3.2).

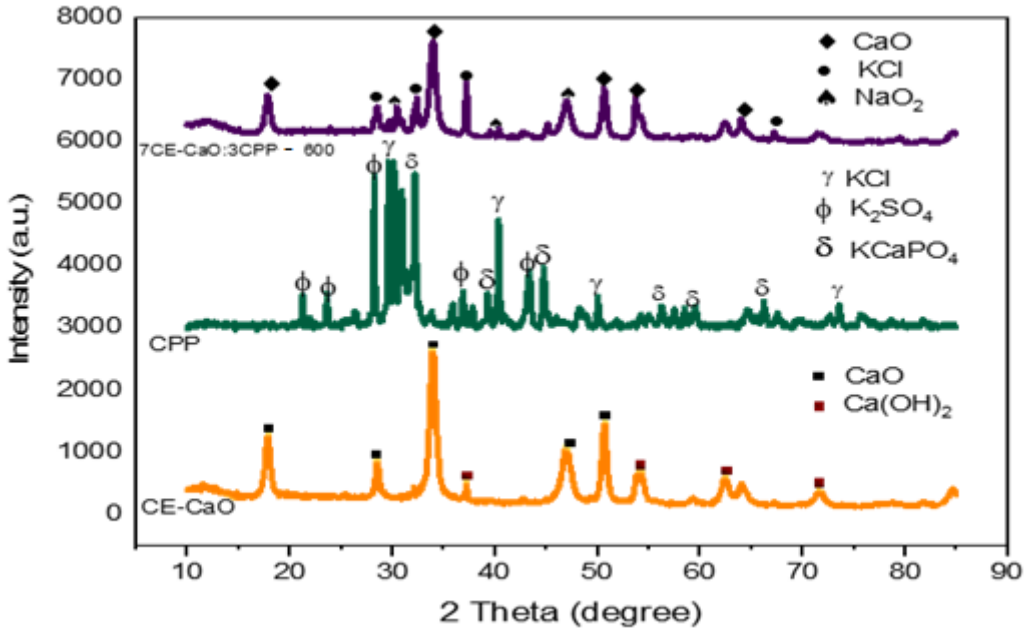

Figure 3.8: XRD spectra of CE-CaO, CPP and 7CE-CaO:3CPP-600 NPs

3.8.3 SEM-EDS Analysis

Fig. 3.5.3 shows the surface morphologies of the CE-CaO, CPP, and 7CE-CaO:3CPP - 600 NPs catalyst hybrid. CPP morphology displays a complex network of pores of irregular particle size distribution. The hybrid displays the irregular particle agglomerated into lump, indicating the modified structure of CaO as a result of impregnation and calcination. The EDS characterization shown in Table 3.2 clearly defines the content of the single and hybrid catalysts. The CPP composed majorly of K, Cl, Ca, P, S and small quantity of Mg, Na, and Si. The hybrid of 7CE-CaO:3CPP -600 composed mainly of Ca and K, with minimal quantity of P, Mg and S. The Ca content are contributed mainly from CE while other essential elements such as K and Cl are contributed by CPP.

Table 3.2: EDS of CE-CaO, CPP and 7CE-CaO:3CPP-600 NPs

Calcined catalyst	**Temperature & time**	**Element composition (%)**								
		O	Ca	K	Cl	P	S	Mg	Na	Si
CE-CaO	900°C, 3 h	49.2	50.8	0.00	0.00	0.00	0.00	0.00	0.00	0.00
CPP	700°C, 3 h	44.10	3.64	30.74	10.30	4.22	4.31	1.16	0.82	0.71
7CE-CaO:3CPP	600°C, 2 h	49.96	40.96	8.57	0.00	0.62	0.30	0.52	0.00	0.00

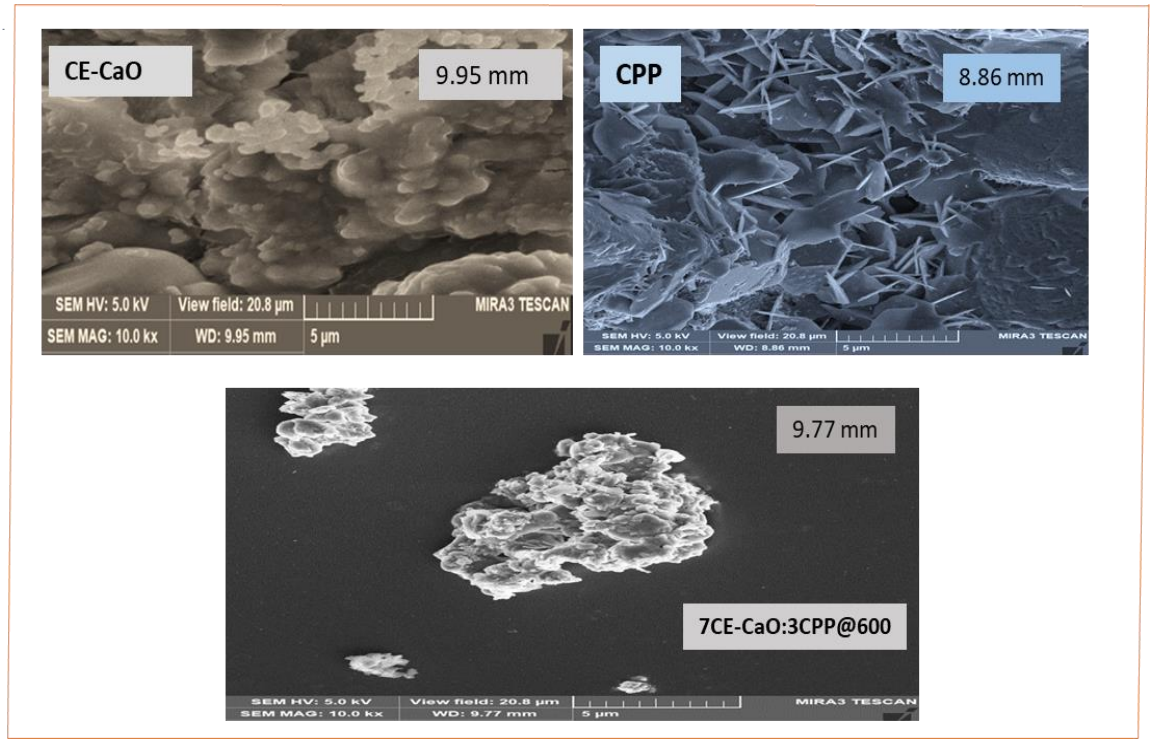

Figure 3.9: SEM images of CE-CaO, CPP, and 7CE-CaO:3CPP-600

3.9 Reusability potential of the catalysts

Reusability is the major attribute of heterogeneous catalysts. CaO is one of the most promising heterogeneous catalysts with high basicity and performance in biodiesel production, but it is susceptible to deactivation due to the leaching of the active ion Ca^{2+} which can also lead to the contamination of biodiesel product. To enhance stability, catalytic activity and reusability they are often mixed with other chemical compounds. In this study, those compounds are supplied from the same biomass materials such potassium-based compounds in banana and pawpaw peels. The catalysts were recovered by separating the spent catalyst after each reaction cycles via centrifugation and washing with solvent (n-hexane) to remove the physi-sorbed oil. The washed catalysts CBP and CPP were dried in oven and reused while the hybrids 7CE-CaO:3CPP-600 and CE-CaO:CBP-800 were further reactivated by calcining at high temperatures of 600 ^{o}C and 800 ^{o}C for 2 h respectively (Yusuff *et al*., 2017) . Their activities in biodiesel production are presented in the next chapter. Figure. 3.10 – 3.13 depicts the reusability plots of each catalyst. The regenerated CBP and CPP and their respective hybrids catalysts were investigated for their reuse in subsequent transesterification (Figure.3.10 and 3.11). The single synthesized catalysts (CBP and CPP) could be reused up to 3 - 4 cycles with the minimum biodiesel yield range of 88 to 91.2 % at the end of the last cycles. While the hybrids (7CE-CaO:3CPP-600 and CE-CaO:CBP-800) (Figures 3.12 and 3.13) were reused for

up to 5 - 6 cycles with minimal decrease in yield of 4 – 5% after the last cycles. However, a significant decrease in yield was observed in 7CE-CaO:3CPP@600 sample at the fourth and fifth cycle (Figure 3.12). This might be attributed to the deactivation of the catalyst by oil, moisture, CO_2 and other trapped impurities. The leaching of soluble content and active elements of the solid base catalysts is one of the drawbacks of heterogeneous catalyst. The effect of leaching and deactivation were observed to be stronger in hybrid catalysts than the single due to the hygroscopicity of CaO, which can lead to carbonates and hydroxide formation. Re-calcination of used catalysts at high temperature after washing with solvent enhances the catalytic activity in order to maintain biodiesel yield in subsequent reuse (Yusuff *et al*., 2017).

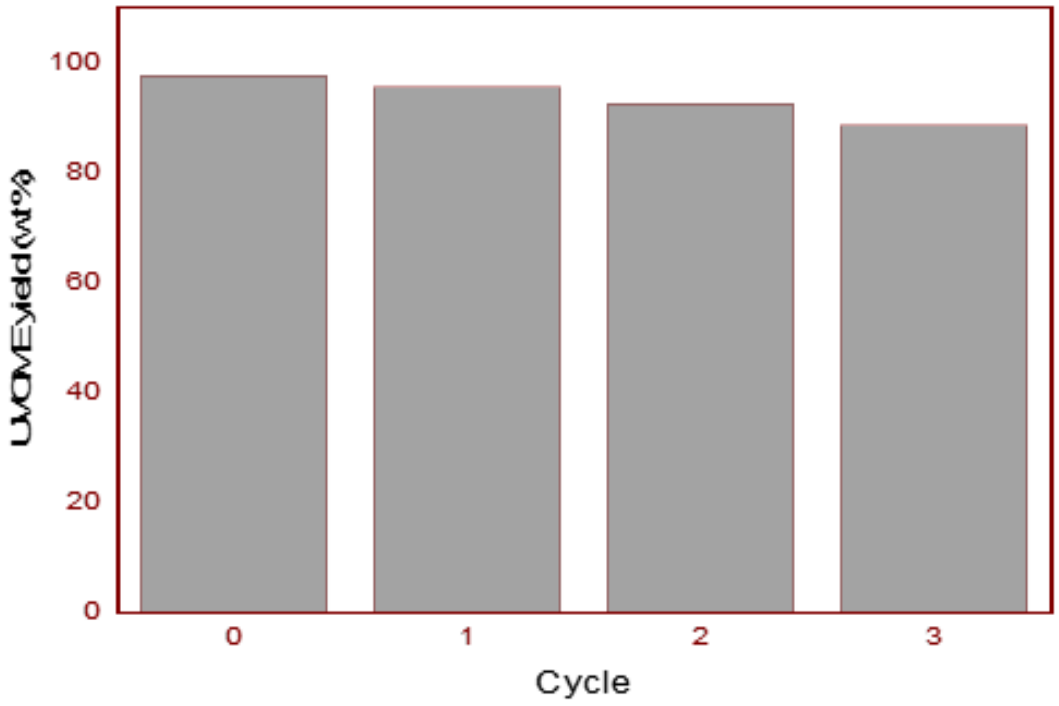

Figure 3.10: Reusability test of CPP catalyst

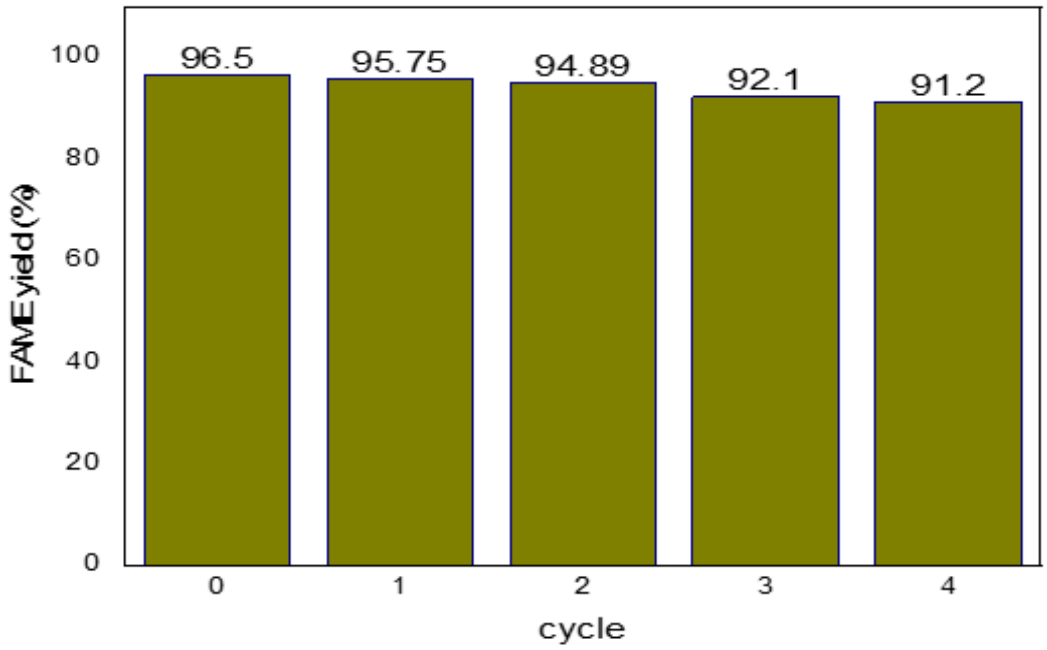

Figure 3.11: Reusability cycle of CBP

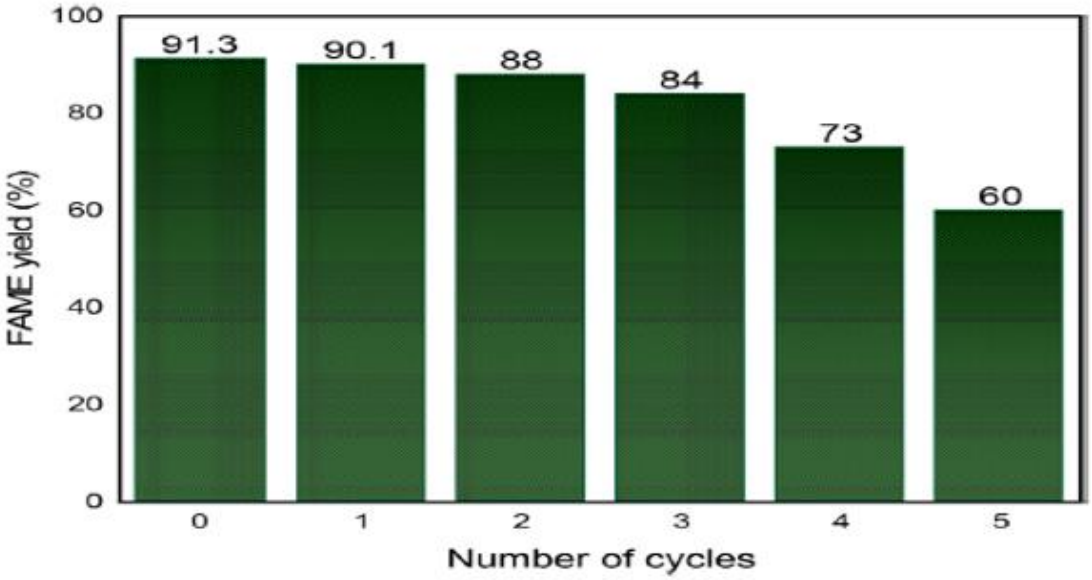

Figure 3.12: Reusability test of 7CE-CaO:3CPP-600

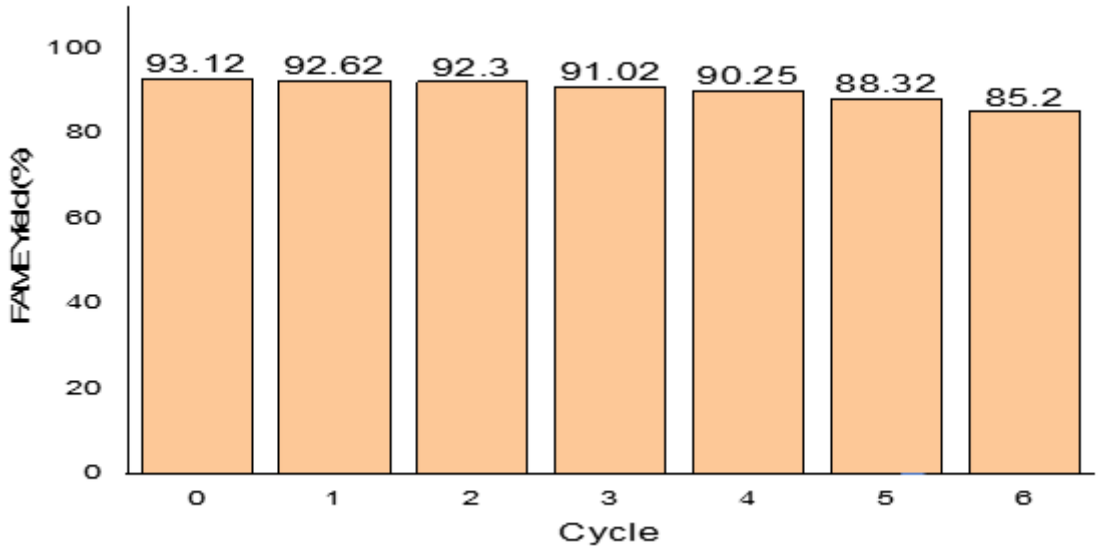

Figure 3.13: Reusability test for CE-CaO:CBP-800 NPs

3.10 Conclusion

The study emphasized the recycling of naturally available biological waste materials in the production of single and hybrid heterogeneous catalysts for biodiesel production. The characterization studies were carried out on individual synthesized catalyst using Fourier transform infrared ray (FT-IR), scanning electron microscopy – energy dispersive X-ray (SEM-EDX) and X-ray diffraction (XRD). The results confirm eggshell ash as the riches source of calcium oxide (CaO) while banana peels, papaya peels ashes contain potassium salts related compounds. Impregnation process was found to improve the basic strength of the catalyst. Potassium and calcium ions being two highly active base, when added together by impregnation becomes a desired and competitive base catalyst for effective transesterification of oil at lower operating conditions. The granular and porous texture of the fine crystal particles confirm the good catalytic efficiency and increase surface area of the catalyst produced. The reusability test confirms that washing and high heat treatment of the spent catalyst can improve the catalytic activity of the catalyst for several reuse. The simple process synthesis of highly active heterogeneous catalysts from low cost, waste and renewable materials can offer a solution to the associated problem encountered in homogenous catalysts. The study demonstrate that these waste materials are viable candidates for efficient bio-alkaline catalysts syntheses for effective biodiesel production.

4 CHAPTER FOUR: Advanced biodiesel synthesis via application of single and hybrid waste-based bio-alkaline catalysts in the optimized transesterification of used sunflower oil and other tropical plant oils

4.1 Introduction

The effect and significance of biomass-based diesel fuel (BDF) has lately been noticed as a suitable alternative fuel, after much dependence on fossil energy. The BDF aside being an indigenous fuel is endowed with auspicious characteristic in engine combustion and performance. It is renewable, non-toxic, biodegradable, highly lubricating and eco-friendly in nature. The BDF commonly called biodiesel is generally obtained from plant oils, waste cooking oil, microalgae and animal lipids. The wide acceptable route of production is through a simply process, called transesterification. A process where oil is reacted with alcohol (mostly short carbon chain) in the presence of a suitable catalyst. The downside of BDF is the high cost compared to petrol-based diesel fuel (PDF). Biodiesel production requires homogenous or heterogeneous catalysts. Homogeneous catalysts such as sodium, potassium hydroxide and methoxides tend to soap formation because of side reaction with the free fatty acid of the oil. The use of heterogeneous catalyst obliterates these shortcomings by some advantageous characteristics such as recoverability, reusability, easy separation and no soap formation (Betiku *et al*., 2017). Agricultural waste could serve as a viable low-cost heterogeneous catalyst feedstock for biodiesel production. Feedstock is outlined the major contributor of the high cost of biodiesel fuel, as it contribute 85 % of its total production cost (Mansir *et al*., 2018b). This is because the major input feedstock source is edible plant oils, which are high in prices. From the research view point, more than 90 % of the globally biodiesel produced are sourced from edible vegetable oils such as soybeans, sunflower, rapeseed, palm, coconut, olive, canola and peanut oils (Mardhiah *et al*., 2017). They are prioritised as the major oil source due to high percentage oil content and compositions. However, the conflict between food supply and energy is the paramount hindrance as both economies keep competing for the same resources such as arable land accessibility. This leads to the complete phase out of edible oil sources for a long-term biodiesel feedstock usage. Economical raw materials such as non-edible oils, waste cooking oils and biocatalysts have been highlighted as the possible solution to high cost of production. To address this issue, current interest in research have been engrossed on the non-edible oils sources for biodiesel production. Despite the short coming of the non-edible oils

such as complex production processes and resources consumption, their potentiality are still pursued to be standardized for future long term usage. However, technologies such as modelling and optimization of their production process parameters and application of various process intensifications are put in place to make their production economically viable.

The optimization of process parameters is identified as one of the economic measures of biodiesel production that can possibly slashed down the exorbitant price of biodiesel production. This helps to identify the set of parameters that influences the transesterification process, which needs to be optimised in order to maximise the yield of the fuel produced. This could be achieved through the application of effective modelling and statistical tools such as response surface methodology (RSM) in the transesterification process. RSM has widely been used for this purpose with different oil compositions to achieve effective results. This could be facilitated due to the ability to define the relationship between the operational input parameters and the response using empirical data. Apart from this, RSM can optimize the multivariant problems with limited number of experiments and allows for the interaction of the process parameters with the response. As compared to the traditional method of optimization using one factor at a time (OFAT) which is considered a waste of time and resources, RSM simultaneously model the effect of single and combined factors affecting the response. It was employed to optimise the esterification and transesterification experiment of waste cooking oil and 95.37 % yield was achieved (Dhawane et al., 2018). It was also used in neem oil methyl ester transesterification to achieve 99.3 % (Etim *et al*., 2018). RSM was used in the optimization of the process parameters in used vegetable oil transesterification to achieve a maximum yield of 97.5 % (Etim *et al*., 2021a) and many others. Moreover, from the reported studies, it can be concluded that the optimal condition for biodiesel production differs considerably based on oil compositions.

Beside the traditional raw material for biodiesel production, this study investigates and explores the utilization of other available and underutilised oil feedstock for biodiesel production. These include used sunflower oil, linseed, marula, baobab and *Trichelia emetica* seed oils using the single and hybrid waste biomass derived catalysts developed in the previous chapters. Among these, oil such as marula, baobab and *trichilia emetica* have not been extensively studied and reported for biodiesel production. RSM was employed to optimise the transesterification process in order to achieve effective results. This study contributes greatly to the development of green biodiesel production process from biomass resources.

4.2 Feedstock sources

Southern African region is endowed with numerous oilseeds bearing plant of high economic value, which can be utilized for various purposes. Information about them is scattered in literature with rich history of local exploitation of different parts (such as leaves, fruits, roots and stems) as sources of food, medicine and cosmetics. The seed oil of most of these plants are reported to having limited commercial applications. Some of these tree-plants includes marula (*Sclerocarya birrea*), baobab, linseed, and *Trichilia emetica*. Research has that the seed oil of these plants is underutilized aside little quantity being used for cosmetics. Although classified as edible oil, they require several refining processes in order to be used as food. Due to this, the interest of their food adoption is minimal. Increasing interest in their adoption as biodiesel feedstock is supported by the fact that their physio-chemical properties are comparable to those of the traditional edible oils such as sunflower, soybeans, rapeseed, canola, peanut oil and so on. The images of all the oilseed of study are depicted in Fig. 4.1.

4.2.1 Marula (*Sclerocarya birrea-spp cafra*)

Sclerocarya birrea -spp caffra, generally known as marula is a home-grown deciduous savanna tree that belongs to the *Anacardiaceae* family. It is distributed widely throughout sub-Saharan Africa, from the tropical, central to Southern Africa. It usually grows up to 18 - 20 metres in height and adaptable to a sandy loam soil woodland habitat and are leafless during winter (Nndwammbi *et al.*, 2018). The fruits are yellow in colour and are edible. It has a plain tough skin and gummy flesh which enfolds 2-3 white kernels that are rich in oil and protein (Nyoka *et al.*, 2015). The nut contains 90 % of shell and only 10 % of kernel. The seeds contain up to 56 % oil per kernel and the energy value of 2699 to 2703 kJ per 100 g kernel (Ejilah *et al.*, 2012). The seed oil has been found to contain majorly of the fatty acid of oleic, palmitic, stearic and linoleic acid, which are excellent for biodiesel production. The seeds have not been used for any major economic purposes except for cosmetics, traditional medicine and alcoholic creams (popular amarula liquer). Hence, this underutilized seed oil with high level of unsaturated fatty acids could be considered a good precursor for biodiesel production.

4.2.2 Baobab (*Adansonia digitata*)

Baobab is a deciduous tree species scientifically called *Adansonia digitata.* It belongs to the family of *bombacaceae* originated from the large family of *Malvaceae*. It is the largest succulent plant in the world and commonly found in tropics such as Southern African, northern part of Nigeria, Madagascar and Australia. It normally grows and distinguished with a huge

trunk diameter of 10 – 12 cm and 25 m height. It is well adapted to a semi-arid region, dry woodland and low rainfall regions. The leaves are present only for three months in the year. The fruits are rich in vitamin C and a mature tree can bear up to 30 kg of fruits. The leaves and fruits have been reported to be used for food especially in the Northern part of Nigeria (Birnin-Yauri and Garba, 2011), while the seed are being discarded. The properties of baobab oils are comparable to the common edible oils such as peanut and sunflower oils. The oil is known to be highly monosaturated and reported to compose mainly of oleic, linoleic and palmitic acids (Vermaak *et al*., 2011). The seed oil has no major commercial value except in traditional medicine and cosmetics. The seed-oil plant image is shown in Figure 4.1b.

4.2.3 Linseed or flaxseed

Flax (*Linum usitatissimum*) is an economic herbaceous annual plant belonging to Linaceae family. It is widely cultivated for fibre, which are used as raw material for linen and fabric manufacturing. The plant has an average height of 0.9 to 1.2 m with slender stalks of 2.5 to 4 mm with branches clustered at the top (Figure 4.1c). It has a small and lance-shaped leaves alternating on the stalk. The plant has blue flower and at times white or pink, that develops into fruits with small dry capsules comprising of five lobes. The plant is adaptable to different soils and climates but do well in a sandy loam and temperate climates. The linseed oil obtained from the ripen seed is yellowish in colour. The oil is reported to be highly unsaturated with mostly linolenic fatty acid (C18:3) and considerable amount of oleic and linoleic acid. It is a drying oil due to its unique hydrophobic properties, which implies it can polymerize into solid form.

4.2.4 *Trichilia Emetica* (Mafura butter)

Trichilia emetica commonly known as Natal mahogany or mafura butter is an evergreen tree that belong to the family of *Maliaceae*. It usually grows up to 20-35 m in height, with a swollen trunk at the base and non-aggressive root. It is a multipurpose tree used throughout centuries. It has a red-brown or grey-brow bark colour with dark greenish leaves at the upper surface. It has a round hairy red-brown fruit capsule that contains 3-6 shiny black seed with a large fleshy orange-red aril. The tree is a widely distributed and mostly found in lowland regions of the Southern Africa and extends to the tropical and the western part of Africa. In South Africa, it is mostly found in KwaZulu-Natal, Mpumalanga, Limpopo etc. The tree grows well in a well-drained alluvial or sandy soil. A matured tree produces average seeds of 64.7 kg annually. The medicinal value of *T. emetica* is obtained from the leaves, bark and the root extracts while the

seeds oil are unconventional and underutilized, except for candle and soap making. The seed oil is poisonous and bitter but can be used as food source if refined (Grundy *et al*., 1993).

The seeds contain two different natural oils, pericarp or the nut husk or coat with about 20-25% oil content and the kernel which has about 65-77 % oil content (Vermaak *et al*., 2011). The kernel oil (butter) is more viscous and are reported to be rich in fat with high percentage of palmitic and oleic acid, which make them quality oil for cosmetic and other scientific purposes. However, there are fewer information relating to other scientific applications of the seed oil. The seed oil images are shown in Figure 4.1d.

4.3 Oil Extraction process

Various extraction techniques have been employed in obtaining oil from seeds and other essential component from plants. These include mechanical expulsion, Soxhlet extraction, ultra-sonic extraction, microwave-assisted extraction and extraction by shaking and stirring (Balasubramanian *et al*., 2011). However, these are used to overcome one technical issue, or another associated with the use of each technique such as longer extraction time, large solvent requirement, additional treatment process, and high-energy inputs. Extraction by solvents is widely employed to achieve higher oil efficiency. Solvents such as polar and non-polar can be used. However, the choice of selection depends on the polarity of the compound of interest. The non-polar solvents such as hexane have extensively been used due to low cost and boiling point. In this study, hexane was used to extract oils from the seeds. The dried kernels were milled with the aid of a mini grinding machine. The seed kernels powder of certain amounts was poured into a well-sealed bucket and then a certain quantity of n-hexane was added to ensure the powder are well soaked. The mixture was vigorously stirred within a short time and left overnight after which it was filtered. The filtrate containing the oil and the solvent was separated with the aid of a distillation column. The process was repeated twice to ensure no oil is left in the cake. At the end of the extraction, the solvent was recovered, and the oil obtained was further heated to ensure no trace of solvent is left behind. The oil was then kept in a plastic bottle for further analysis and for biodiesel production.

(a) Fresh marula fruit Dried seeds kernels

(b) Fresh baobab fruit Dried seed Kernels

(c) Linseed fruit Mature fruits Dried seeds

(d) *Trichilia emetica* seeds Dried seeds Kernels

Figure 4.1: Photos of oilseeds of study

4.4 Chemicals and reagents

Labo Equip, Springfield, KwaZulu Natal, South Africa, supplied the commercial linseed oil, baobab, and marula oil while *Trichilia emetica* seeds were picked from Durban University of Technology, Steve Biko campus environment and then extracted. Used sunflower oil was collected from the students' cafeteria from the same campus. Chemicals and reagents used such as methanol (98 %), ethanol (98 %), diethyl ether, n-hexane, potassium hydroxide, hydrochloric acid, cyclo-hexane, monochloride solution, potassium iodide, phenolphthalein and starch were all of analytical grades.

4.5 Oil Analysis and characterization

The quality and suitability of oils for any purpose is determined by their physico-chemical properties. The properties such as density, viscosity, iodine value, acid value, saponification value, cetane number and calorific value of each oil was determined using standard methods. Acid value of the oil with its corresponding percentage free fatty acid (FFA) is the major determining factor of the transesterification pathway to be adopted.

Gas Chromatography analysis was carried out to determine the fatty acid composition of each oil. The fatty acid of the vegetable oils depends on the species and the growth condition of the plant (Hebbar et al 2018). Shimadzu GCMS-QP2010 Ultra coupled with mass spectrometer with column capillary (RXT-5, 30 m ×, 0.25 mm × and 0.25 µm) was used to analyse the fatty acid compositions of the oils. Helium gas was used as a carrier gas with a flow rate of 60 (mL/min) and the sample volume of 1.0 µL was injected using a split-less mode at injection temperature of 220 ^{o}C. The oven temperature was set at 70 ^{o}C for 1.50 min before ramping up at 10 ^{o}C/min to 320 ^{o}C and maintained at 10 min.

4.6 Experimental setup

A conventional batch transesterification method was adopted in this study. The apparatus used include of 250 mL three necked round bottom flask reactor, water cold reflux condenser to prevent the evaporation of volatile reactants like methanol, a thermometer for monitoring the temperature of the content, a magnetic hot plate as a source of heat and agitation. Fig. 4.2 shows the complete apparatus setup for all transesterification experiments carried out in this study.

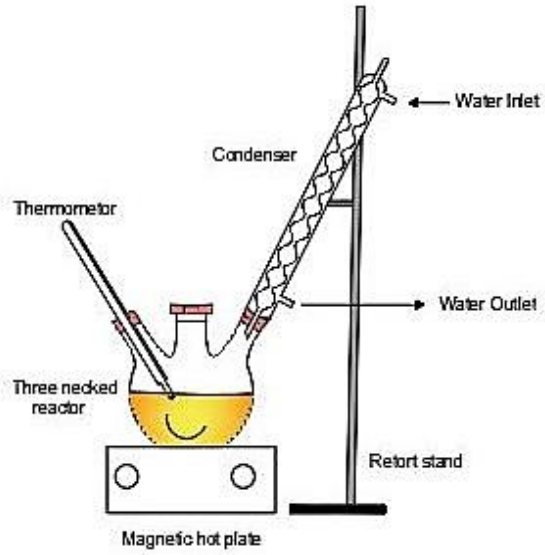

Figure 4.2: Apparatus setup for the transesterification process

4.7 General procedure for the transesterification process execution

A one-step transesterification pathway was adopted for all the oils used in this study. This is because their FFAs were within the recommended range for solid-base catalysed transesterification (≤ 2.5%) (Kumar *et al.*, 2015). The reaction was carried out using the setup in Fig 4.2 and followed the pattern flow chart in Fig.4.3. The influential transesterification reaction parameters such as methanol-to-oil molar ratio (MTOMR), catalyst loading (CL), reaction time (RT) were modelled and optimised by response surface methodology (RSM) while temperature and agitation speed was held constant at 65 ^{o}C and 450 rpm respectively (Balajii and Niju, 2020; Betiku *et al*., 2017). The design guide generated using the stipulated range of each parameter considered were used as standard for each round of experiment. The parameter such as methanol and catalyst quantities were calculated based on the weight of the oil in grams, using weight per weight method as described in paper 1. The reaction started by discharging a specified amount of crude oil into the reactor and allowed to heat up to 60 ^{o}C. A measured amount of methanol was added to the oil in the reactor followed by the addition of a calculated quantity of catalyst after 5 min. The reaction was monitored following the design guide generated by the RSM. At the end of each reaction condition, the resulting mixture was transferred into the separating funnel and allowed to stand overnight for gravitational settling and phase separation.

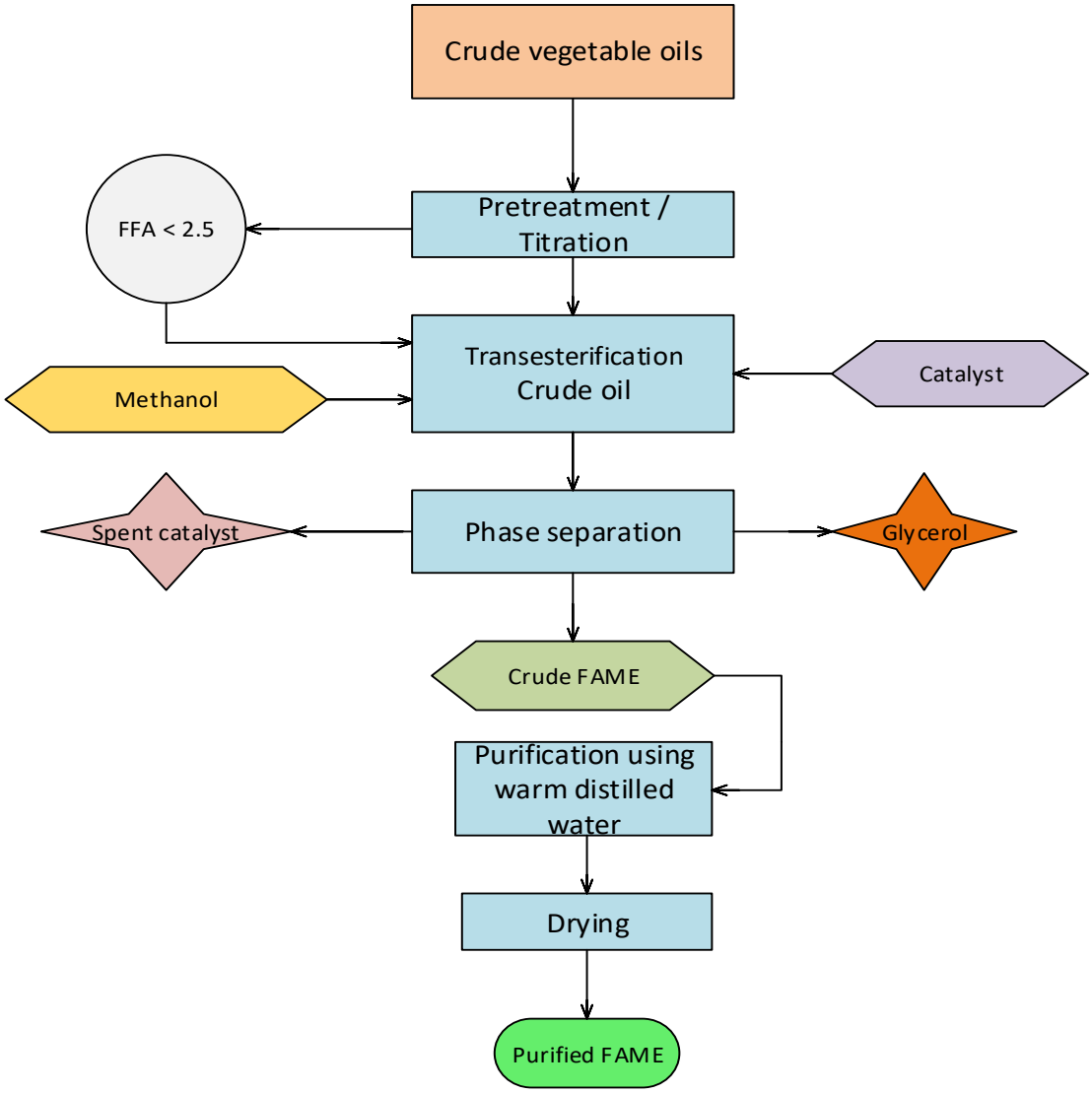

Figure 4.3: General flow chart of the biodiesel production via transesterification process

4.8 Purification and characterization of biodiesel

After each separation process, the three-layers were formed as a result of solid catalyst used, which include the crude biodiesel, glycerol and spent catalyst layers. The glycerol and catalyst layers were decanted and stored, the crude biodiesel layer left behind in the separating funnel were further washed thrice with warm distilled water at 50 ^{o}C to remove the trapped residual methanol, glycerol and catalyst remaining in the biodiesel product. The washed biodiesel were further dried to remove trace of water trapped during the washing process. The purified biodiesel obtained were stored in corked bottles for quality characterization analysis. The purified biodiesel yields were determined gravimetrically using Eq. 4.1. The quality of the

biodiesel produced was determined by comparing the result obtained with the biodiesel standards (ASTM D6751, EN 14214 and SAN 833).

$$FAME\ (\%) = \frac{weight\ of\ FAME\ produced\ (g)}{weight\ of\ oIl\ used\ (g)} \times 100 \qquad 4.1$$

4.9 Empirical design and statistical analysis for the transesterification of USO, LO, BO and MO using CBP catalyst

Four oil samples were simultaneously modelled using the same empirical design and transesterified with calcined banana peels catalyst (CBP). They include used sunflower oil (USO), linseed oil (LO), baobab seed oil (BO) and marula seed oil (MO).

A central composite design (CCD) with three factors five levels was used to investigate the effect of transesterification reaction parameters on four responses (USOME, LOME, BOME and MOME). CCD was used to create 20 experimental runs [i.e. 2^n+2n+6, where n is the 3 number of independent parameters], which includes 8 factorial points (2^n), 6 axial points (2n) and 6 replicates at the centre to estimate the pure error (Hebbar *et al*., 2018). Table 4.1. shows the process independent parameters, their levels and ranges viz methanol to oil molar ratio (6:1 – 14:1), catalyst loading level (1.5 – 5.5 wt%), reaction time (40 – 80 min) and a constant reaction temperature of 65 ^oC. Table 4.2. shows the respective actual and coded level factors of independent variables. Zero (0) value represents the centre point for the variables while -1 and +1 represent the lower and upper value of the three process variables. - **α** and + **α** represent the lowest and highest value suggested by the model for every parameter within the range studied. The quadratic polynomial model terms of the variables were fitted through multiple regression equation. Both analysis of variance (ANOVA) and the significance test at 95 % confident level were deployed to establish the features of the model. The second order mathematical equation that describes the fitness of the polynomial response model is given in Eq. 4.2

$$Y = \text{Ϙ}0 + \sum_{i=1}^{n} \text{Ϙ}_i X_i + \sum_{i=i}^{n} \text{Ϙ}_{ii} X_i^2 + \sum_{i=1}^{n-1} \sum_{j=2}^{n} \text{Ϙ}_{ij} X_i X_j + \varepsilon \qquad 4.2$$

By expansion

$$Y = \text{Ϙ}_0 + \text{ϘA} + \text{ϘB} + \text{ϘC} + \text{ϘAB} + \text{ϘAC} + \text{ϘBC} + \text{Ϙ}A^2 + \text{Ϙ}B^2 + \text{Ϙ}C^2 + \varepsilon \qquad (4.2.1)$$

Where Y is the predictive response (biodiesel yield), Q_0 is the intercept value, Q_A, Q_B, Q_C are the coefficients of the independent terms, Q_{AB}, Q_{AC}, Q_{BC} are the interaction coefficient terms and Q_A^2, Q_B^2, Q_C^2, represent the quadratic coefficients and A, B and C represent the independent variables and ε is the random error. The parity plot that shows the consistencies between the experimental and predicted values are depicted in Figure 4.1. The transesterification reaction and purification process were performed as outlined in the earlier section. The yield of each biodiesel produced was calculated according to Eq. 4.1. The quality characterization of the biodiesel produced was done in accordance with the standard methods.

Table 4.1: Experimental range and level of independent variables

Factors	**Symbols**	**Coded factor levels**				
		-α	**-1**	**0**	**1**	**+α**
Methanol/oil molar ratio	A	6	8	10	12	14
Catalyst loading (wt%)	B	1.5	2.5	3.5	4.5	5.5
Reaction time (min)	C	40	50	60	70	80

Table 4.2: operational conditions with actual and predicted yields for four biodiesel produced

Run	**A**	**B**	**C**	**UFOME (%)**		**LOME (%)**		**BOME (%)**		**MOME (%)**	
				Act	**Pred**	**Act**	**Pred**	**Act**	**Pred.**	**Act**	**Pred**
1	0	0	0	93.47	94.10	94.00	93.60	94.10	94.47	91.65	91.30
2	**- α**	0	0	93.03	92.91	91.70	92.10	92.65	93.03	90.5	90.89
3	1	-1	1	96.04	96.15	93.95	93.89	95.85	96.04	97.6	97.73
4	0	0	0	94.47	94.10	93.80	93.67	94.75	94.47	91.2	91.30
5	1	1	-1	92.63	92.88	93.50	93.86	92.60	92.63	87.00	87.45
6	0	0	0	94.47	94.10	92.05	91.87	94.95	94.47	91.30	91.30
7	0	0	**- α**	95.41	95.46	92.25	92.16	95.35	95.41	89.00	89.14
8	0	**- α**	0	97.25	97.45	94.85	94.98	96.50	97.25	90.90	91.36
9	2	0	0	91.55	91.46	95.20	94.98	92.10	91.55	97.60	97.59
10	0	**α**	0	91.58	91.18	96.55	95.96	91.80	91.68	87.40	87.31
11	0	0	**α**	93.52	93.26	92.10	92.13	93.40	93.52	92.00	92.24
12	0	0	0	94.47	94.10	91.85	91.71	95.35	94.47	91.30	91.30
13	-1	1	1	90.86	91.28	94.70	94.98	91.85	91.46	89.90	90.10
14	-1	-1	-1	94.67	94.64	94.85	94.98	94.85	94.67	90.30	90.28
14	-1	-1	1	95.69	95.64	93.60	93.55	96.15	95.69	88.50	87.68
16	1	-1	-1	95.01	94.79	94.55	94.89	95.05	95.01	94.50	93.93
17	-1	1	-1	94.73	94.83	95.51	94.98	94.25	94.73	91.30	90.80
18	0	0	0	94.47	94.10	90.55	90.33	94.25	94.47	90.60	91.30
19	0	0	0	93.47	94.10	91.90	91.83	94.55	94.47	91.40	91.30
20	1	1	1	89.45	89.69	94.82	94.98	88.50	89.35	93.50	93.15

Act- Actual value; Pred – predicted value

4.10 Result and discussion

4.11 Physicochemical properties of the oils

The results of physico-chemical properties and fatty acid compositions of the oils used in this study are presented in Table 4.3. The properties of the oil are directly reflected by the fatty acid compositions. The density of the oils were high and were varied based on their compositions. LSO has the highest density of 0.949 g/cm^3 followed by USO because they are strongly unsaturated. The viscosity of all the oils were high and are not suitable to be used directly in CI engines. The viscosity of TEKO was exceptionally high because it is rich in saturated fatty acids and it sometimes form solid in cold weather. The acid values of the oils were low, except TEKO with 5.61 mg KOH/g. The fatty acid compositions of the oils are also shown on the Table. Linseed oil (LSO) is highly rich in linolenic acid (C18:3) with a percentage of 55.1 %, used sunflower oil (USO) contains linoleic acid (C18:2) and oleic (C18:1) with 65.3 % and 22.7 % respectively, baobab oil (BO) is rich in oleic and linoleic, 42 and 30 %, marula oil (MO) contains mainly of oleic (70 %) and *Trichilia emetica* kernel oil (TEKO) composed mainly of palmitic (50 %) and oleic (43 %).

Table 4.3: Physical and chemical properties of oils

Properties	**USO**	**LSO**	**BSO**	**MSO**	**TEKO**
Colour	Dark brown	Light yellow	Golden yellow	Clear pale	Dark brown
Refractive index	1468	1465	1463	1462	1467
Density (g/cm^3)	0.948	0.949	0.942	0.939	0.944
Viscosity (mm^2/s)	23.87	16.43	12.69	15.86	40.1
Acid value (mg KOH/g)	2.25	3.60	2.17	4.35	6.10
IV (g I_2/100g oil)	78.68	94	78.3	72	79.1
SV (mg KOH/g)	198	196	192	209	191
Calorific value (MJ/kg)	38.6	38.7	38.24	39.5	38.12
		Fatty Acid Composition (%)			
Palmitic	6.8	5.1	20.0	10.5	50.0
Stearic	3.9	2.5	8.0	8.0	3.0
Oleic	22.7	18.9	42.0	70.0	43.0
Linoleic	65.3	18.1	30.0	7.0	4.0
Linolenic	0.2	55.1	-	0.7	-

4.12 Modelling and parameter optimization of the transesterification process of USOME, LOME, BOME and MOME

The experimental conditions based on the process variables investigated using CCD for the five level three factors with four responses including actual and predicted yield value are shown in Table 4.2. The model significance level and various parameters influencing the yields of each biodiesel produced were determined by the analysis of variance (ANOVA) and are displayed in Table 4.4- 4.7. The significance of each model was confirmed with the F-values, P-values and other fit statistics as presented in Table 4.7. The quadratic regression model that best defined the relationship between the processes parameter with the responses are given by Eq. 4.3 - 4.6

UFOME $$Y = 94.10 - 0.3612A - 1.57B - 0.5488C - 0.5250AB + 0.0875AC - 1.14BC - 0.4791A^2 + 0.0522B^2 + 0.0647C^2 \quad (4.3)$$

LOME $$Y = 92.53 + 0.335A + 0.6238B - 0.0838C - 0.1175AB + 0.7225AC + 0.92BC + 0.6405A^2 + 0.953B^2 + 0.043C^2 \quad (4.4)$$

BOME $$\mathrm{Y} = 94.63 + 0.1\mathrm{A} - 1.38\mathrm{B} - 0.4625\mathrm{C} + 0.375\mathrm{AB} - 0.1125\mathrm{AC} - 0.6\mathrm{BC} - 0.4483A^2 + 0.333B^2 - 0.0108C^2 \quad (4.5)$$

MOME $$Y = 91.3 + 1.67A - 1.01B + 0.775C - 1.75AB + 1.6AC + 0.475BC + 0.733A^2 - 0.492B^2 - 0.1545C^2 \quad (4.6)$$

Where Y is the FAME yield (wt%), A is the methanol to oil ratio (MTOR), B is the catalyst amount (wt%) and C is the reaction time (min). The positive (+) and negative (-) signifies the high and low level of the parameters and their interactions.

Table 4.4 – 4.7 showed the results of the ANOVA test performed to evaluate the statistical significance of the developed model. The F-value and p-value shown in Table 4.8 for USOME, LOME, BOME and MOME production implies that the models are statistically significant at 95 % confidence level ($P < 0.05$). The values of $P < 0.05$ indicates the model terms are significant.

To test the fit of the model, the coefficient of determination (R^2) was evaluated, which has been recommended to be at least 0.8 for the good fit of a model (Betiku *et al*., 2017). The R^2 values obtained in this study were computed and presented in Table 4.8. The R^2 of all the models were

close to 1, which indicates the effectiveness of the models in explaining more than 97-98 % of the variability. The adjusted R^2(s) were sufficiently high to show the significance of the models. The adjusted R^2 and the predicted R^2 for models were in good agreement with the difference of less than 0.2 between them. The low F values of lack of fit of the models showed that the lack of fits was not significant relative to pure error, which is desirable for the good fit of the model. The percentage coefficient of variance (CV) for the models were computed and presented in Table 4.8. The low values observed are indicative of the model good fit. In addition, the data fitting of the models was also examined and demonstrated in Figure 4.4. The model shows the good fit of the experimental data. The figure is in support of the high R^2 of the models. This shows that the experimental and predicted values are well-correlated. For a good relationship between experimental and predicted values, R^2 should be close to 1 as possible.

Table 4.4: Test of ANOVA quadratic model for USOME

Source	**Sum of Squares**	**df**	**Mean Square**	**F-value**	**p-value**
Model	65.77	9	7.31	36.44	< 0.0001
A-Met/oil	2.09	1	2.09	10.41	0.0091
B-Catalyst Loading	39.31	1	39.31	196.01	< 0.0001
C-Time	4.82	1	4.82	24.02	0.0006
AB	2.21	1	2.21	10.99	0.0078
AC	0.0613	1	0.0613	0.3054	0.5927
BC	10.35	1	10.35	51.61	< 0.0001
A^2	5.77	1	5.77	28.77	0.0003
B^2	0.0684	1	0.0684	0.3410	0.5722
C^2	0.1051	1	0.1051	0.5241	0.4857
Residual	2.01	10	0.2006		
Lack of Fit	0.6724	5	0.1345	0.5043	0.7648
Pure Error	1.33	5	0.2667		
Cor Total	67.78	19			

Table 4.5: ANOVA quadratic model for LOME

Source	**Sum of Squares**	**df**	**Mean Square**	**F-value**	**p-value**
Model	48.58	9	5.4	47.03	< 0.0001
A-Met/oil	1.8	1	1.8	15.64	0.0027
B-Catalyst Loading	6.23	1	6.23	54.24	< 0.0001
C-Time	0.1122	1	0.1122	0.9778	0.3461
AB	0.1105	1	0.1105	0.9623	0.3497
AC	4.18	1	4.18	36.38	0.0001
BC	6.77	1	6.77	58.99	< 0.0001
A^2	10.31	1	10.31	89.85	< 0.0001
B^2	22.83	1	22.83	198.93	< 0.0001
C^2	0.0464	1	0.0464	0.4042	0.5392
Residual	1.15	10	0.1148		
Lack of Fit	0.4544	5	0.0909	0.6554	0.6729
Pure Error	0.6933	5	0.1387		
Cor Total	49.73	19			

Table 4.6: ANOVA quadratic model for BOME

Source	Sum of Squares	df	Mean Square	F-value	p-value
Model	47.84	9	5.32	51.98	< 0.0001
A-Met/oil	0.16	1	0.16	1.56	0.2395
B-Catalyst Loading	30.25	1	30.25	295.76	< 0.0001
C-Time	3.42	1	3.42	33.46	0.0002
AB	1.13	1	1.13	11	0.0078
AC	0.1013	1	0.1013	0.9899	0.3432
BC	2.88	1	2.88	28.16	0.0003
A^2	5.05	1	5.05	49.4	< 0.0001
B^2	2.79	1	2.79	27.25	0.0004
C^2	0.0029	1	0.0029	0.0286	0.869
Residual	1.02	10	0.1023		
Lack of Fit	0.4707	5	0.0941	0.8526	0.5673
Pure Error	0.5521	5	0.1104		
Cor Total	48.87	19			

Table 4.7: ANOVA quadratic model for MOME

	Sum of Squares	df	Mean Square	F-value	p-value
Model	143.35	9	15.93	58.72	< 0.0001
A-Met/oil	44.89	1	44.89	165.48	< 0.0001
B-Catalyst Loading	16.4	1	16.4	60.46	< 0.0001
C-Time	9.61	1	9.61	35.42	0.0001
AB	24.5	1	24.5	90.31	< 0.0001
AC	20.48	1	20.48	75.49	< 0.0001
BC	1.81	1	1.81	6.65	0.0274
A^2	13.51	1	13.51	49.79	< 0.0001
B^2	6.09	1	6.09	22.44	0.0008
C^2	0.6005	1	0.6005	2.21	0.1676
Residual	2.71	10	0.2713		
Lack of Fit	2.1	5	0.4201	3.43	0.101
Pure Error	0.6121	5	0.1224		
Cor Total	146.07	19			

Table 4.8: Fit statistics for the four FAME produced using CCD

FAME	Model P-value	Model F-value	R^2	Adjusted R^2	Predicted R^2	Adeq. Precision	Mean	Standard deviation	C.V. %
UFOME	< 0.0001	36.44	0.9704	0.9438	0.8915	24.4994	93.81	0.4478	0.4774
LOME	< 0.0001	47.03	0.9769	0.9561	0.9076	25.9873	93.84	0.3388	0.361
BOME	< 0.0001	51.98	0.9791	0.9602	0.9048	30.9895	94.53	0.3198	0.3383
MOME	< 0.0001	58.72	0.9814	0.9647	0.8867	28.2847	91.37	0.5208	0.57

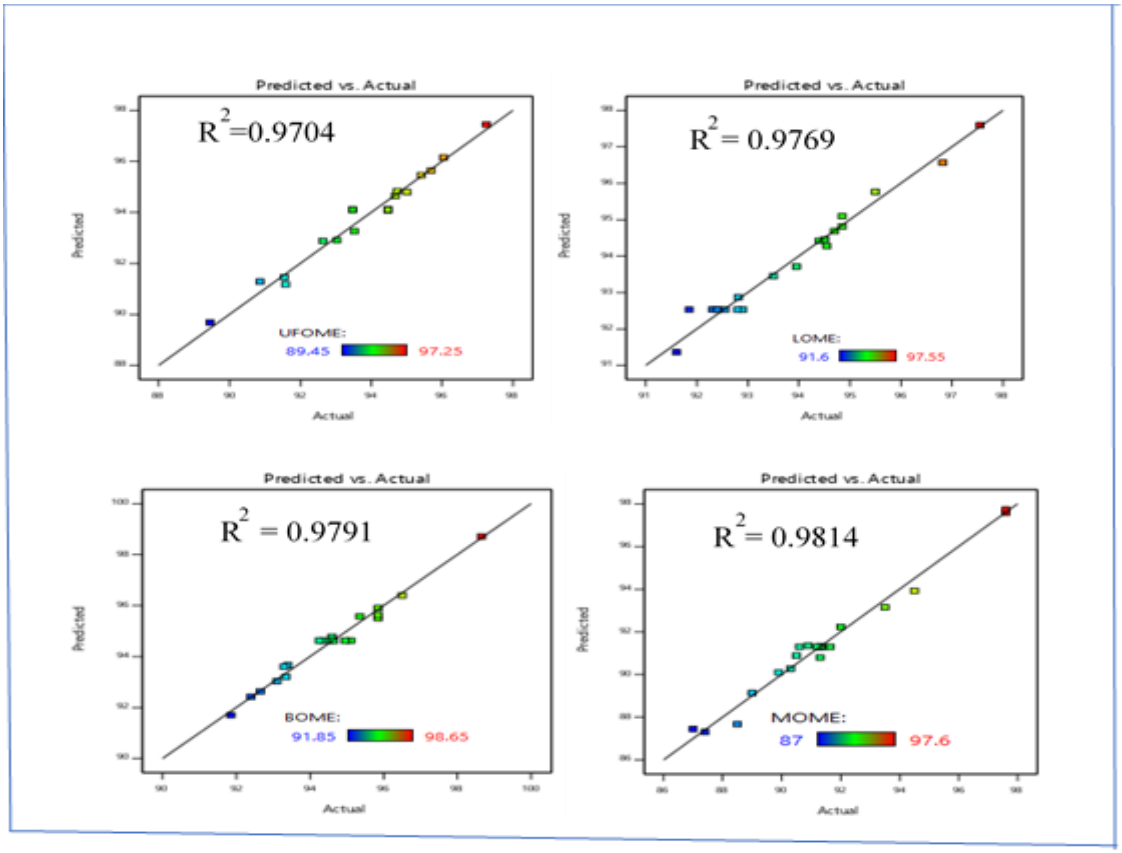

Figure 4.4: The plot actual versus predicted values for USOME, LOME, BOME and MOME

4.13 Interaction effect of parameters with the responses

Surface plots was used to visualize the effect of the process parameters and is depicted in Fig 4.5. The curvature nature of the graphs signifies the significant interaction of the operational parameters on the yields.

4.13.1 Methanol to oil molar and catalyst loading

Figures 4.5 (a_1, b_1, c_1 and d_1) show the surface plots of methanol/oil molar ratio and catalyst loadings on USOME, LOME, BOME and MOME yields. In the transesterification of oils with alcohol, methanol/oil molar ratio and catalyst amount are vital factors influencing the biodiesel yield(s). In practical situation, methanol is required in excess beyond the theoretical ratio of 3:1 to drive the equilibrium reaction of the transesterification process towards the forward direction. Immiscibility of oil and methanol decelerates the transesterification process. Therefore, catalyst is required to speed up the conversion rate with the aid temperature and agitation to ensure a successful reaction process and high yield. For the combined design, methanol/oil molar ratio used in this study was varied between 6:1- 14:1, while the catalyst loading was varied between

1.5 – 5.5 wt%. In Fig.4.5a_1, the USOME yield was observed to increase at the decreasing levels of methanol/oil ratio and catalyst loading. Methanol/oil from 6:1 – 10:1 and catalyst loading of 1.5 – 3.5 wt% favours USOME yield, but further increase of both factors beyond this point resulted in decreased yield. This might be due to the mass transfer resistance because of less contact between the reactants (Betiku *et al.*, 2019). In Figure.4.5b_1, increase in LOME yield was observed at the lower and higher levels of both methanol/oil and catalyst loading (-1, 1) while at the midpoint level (0), decrease in yield was observed. Figure 4.5c_1, displayed the interaction of these factors on BOME yield. Increase in yield was noticed at lower range of catalyst (1.5 – 2.5 wt%) and decreasing range of methanol/oil ratio. However, the problem of dilution via excess methanol should be avoided as this can lead to low product yield. In Fig.4.5d_1, MOME yield increase occurred at concurrent increase range of both factors.

4.13.2 Reaction time and methanol to oil molar ratio

Figures 4.5 (a_2, b_2, c_2 and d_2) illustrate the surface plot interaction between reaction time and methanol/oil ratio of USOME, LOME, BOME and MOME. Reaction time is another important factor that influences the transesterification of oils with alcohols. It measures the duration of interaction of the reactants. It is crucial to identify the optimum reaction time in the transesterification process. In terms of the nature of equilibrium of the transesterification process, exceeding optimum reaction time will favour the backward reaction, which will lead to the hydrolysis of alkyl esters and will promote soap formation and yield reduction (Betiku *et al.*, 2019). Time range of this study was considered from 40 – 80 min. In Figure 4.5 a_2, USOME yield increases with increase in reaction time and methanol/oil ratio and attains maximum at 10:1 in 80 min. Figure 4.5 b_2 shows that the maximum LOME yield occurred in 50 min at the highest level of methanol/oil of 14:1. In Figure 4.5 c_2. BOME yield increases with increasing reaction time and decreasing methanol/oil ratio. Figure 4.5 d_2 showed that MOME yield increases with decreasing reaction time and methanol/oil ratio and reaches its maximum in 50 min and at 6:1. Thus, the selected time range for the reaction in this study was enough for the yields to reach maximum without reverse reaction occurring.

4.13.3 Reaction time and catalyst loading

Figure 4.5 (a_3, b_3, c_3 and d_3) show the plot surfaces of interaction between reaction time and catalyst loading for USOME, LOME, BOME and MOME. In Figure 4.5 a_3, the plot shows a parallel decrease of both the reaction time and catalyst loading as leading to increase in USOME yield. USOME attained its maximum at the lowest time of 50 min and catalyst loading of 1.5

wt%. Figure 4.5 b_2 shows that LOME yield increases at lower catalyst loading of 1.5 wt% and then dropped from 2.5 - 4.5 wt% and further increases at the higher loading of 5.5 wt%. The yield was favoured at low reaction time and reaches maximum at 50 min. In Figure 4.5 c_3, the plot indicates that BOME yield is favoured at lower reaction time of 50 – 40 min and catalyst loading of 1.5 – 2.5 wt%. Further increased condition beyond this range reduces the yield. The plot surface in Figure 4.5d_3 shows that MOME yield was much favoured at increasing reaction time and decrease loading of the catalyst. Catalyst loading beyond 3 wt% will lead to a tremendous decrease in the yield of MOME. This might be due to the saturation of catalyst particles as the concentration increases. Thus, similar trend of all interactions observed in this study has been reported in literature (Ahmad *et al*., 2019; Betiku *et al*., 2019; Etim *et al*., 2018; Gupta *et al*., 2016).

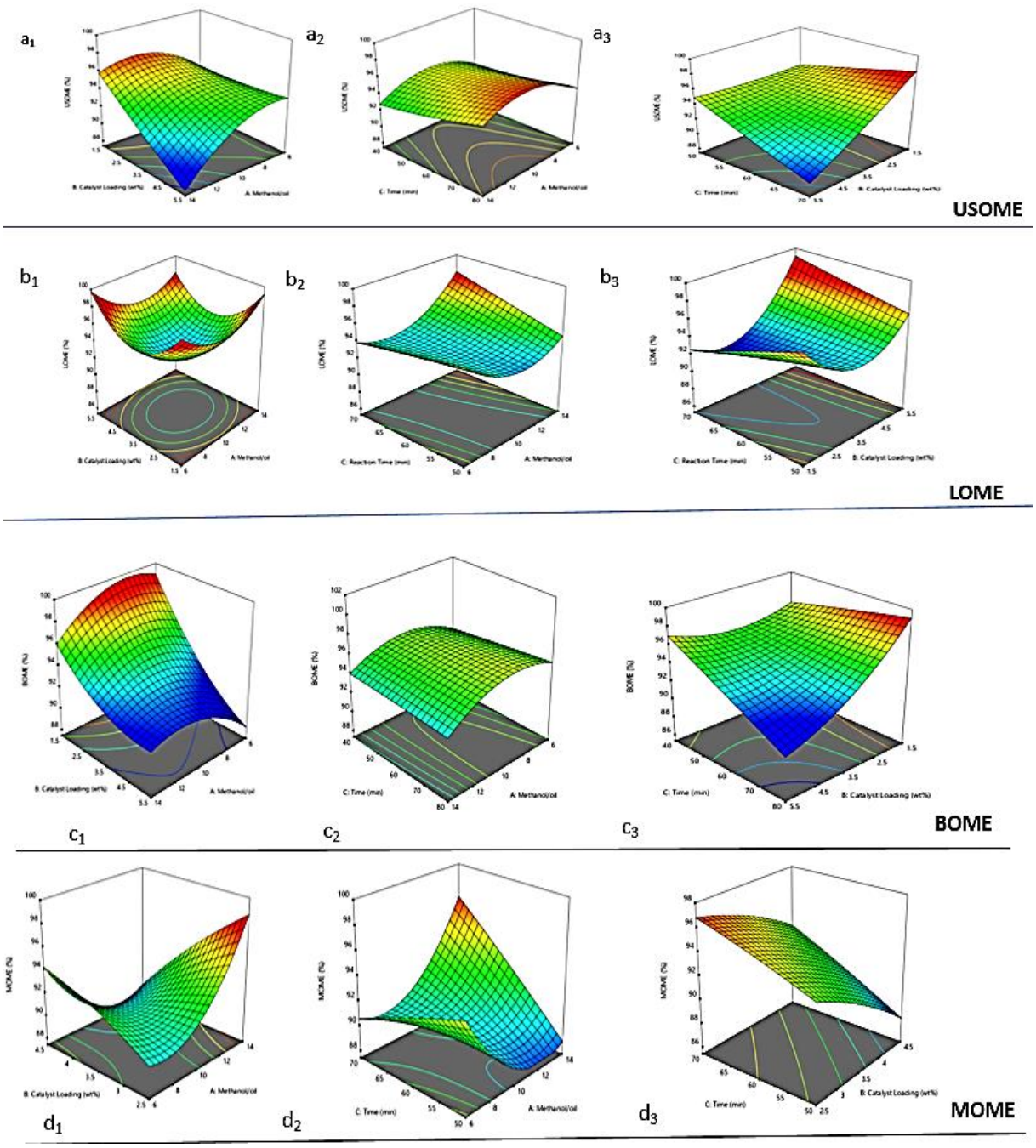

Figure 4.5: Surface plot of interaction effect of the process parameters

4.14 Numerical Optimization Process

A numerical optimization used to establish the best experimental conditions to produce USOME, LOME, BOME and MOME was obtained by solving the regression model equations (Eq.4.3 – 4.6) using the Design Expert software package, version 11.0.1 (Stat-Ease, Inc., Minneapolis, U.S.A). The optimum values were numerically predicted as MTOR of 14:1, catalyst loading of 3.5 wt% and reaction time of 60 min while maintaining the temperature constant at 65 ^{o}C. The prediction of USOME, LOME. BOME and MOME under this condition was 91.46 %, 95.76 %, 93.03 %, and 97.58 % respectively, which was validated with actual values of 94.53 %, 95.61 %, 94.86 % and 98.0 % using three independent experimental replicates under optimal condition. The obtained result proved that the regression model developed could adequately describe the transesterification process.

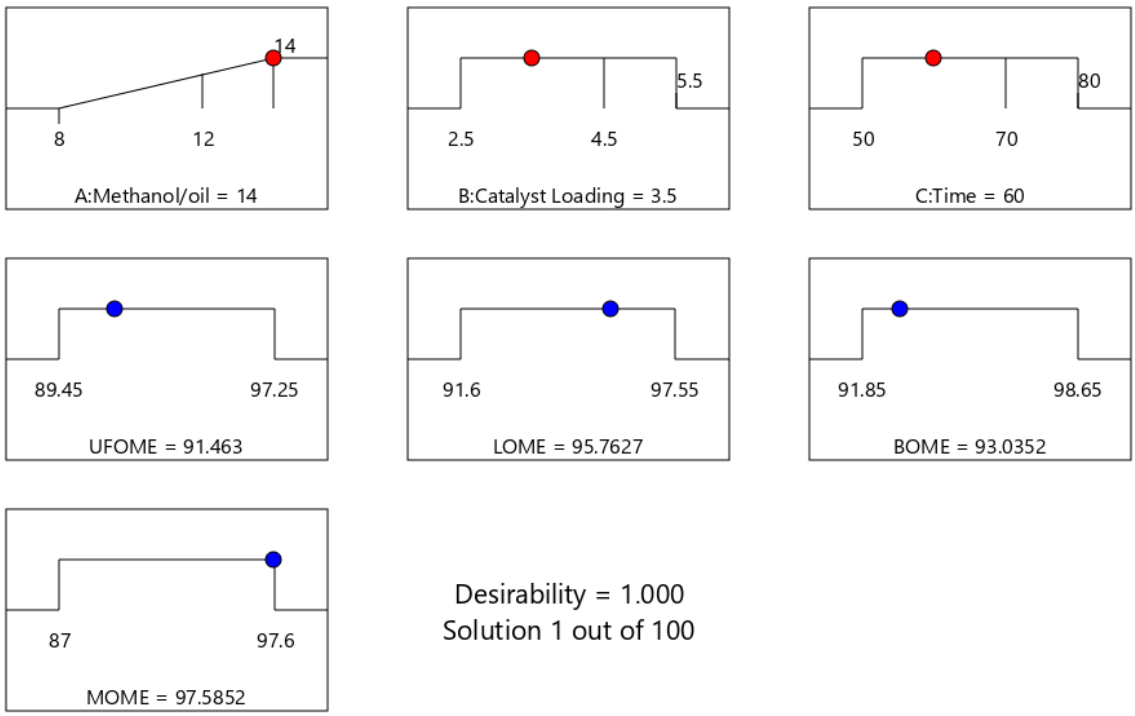

Figure 4.6: Ramp plot of optimized conditions with a desirability performance of 100%

4.15 FAME quality characterization and its fatty acid profile

The FAME produced were tested for their fuel properties and the results obtained are summarised in Table 4.9: The properties are conformable with ASTM D6751, EN 14214 and SAN 833 biodiesel specifications. The densities of the FAME were high but within the standard

range. The viscosities were all within the recommended ranges, BOME viscosity (3.40 mm^2/s) was below the EN and SAN limits. Acid values were within the limit specified except for TEKOME (0.564 mg KOH/g) which is a little above the standard limit. Higher acid values can damage the rubber and metal parts of an engine.

4.16 Application of other synthesized single and hybrid bio-alkaline catalysts in biodiesel production

Information on the application of all the synthesized catalysts presented in Chapter 3, are contained in the published/accepted papers listed in the publication section [paper 1-3, 5-8] and the summaries of their empirical design, reaction activities and reusability are presented in Table 4.10. Based on the composition of TEKO (high acid value), empirical design process parameters such as reaction time, catalyst loading and methanol to oil ratio, were a bit higher than the design of other oils. This was done to avoid soap formation as one-step transesterification process was applied for all the experiments.

The reusability test was conducted on the synthesized catalysts at optimum conditions of their established empirical design applicable to the respective oils used. The minimum yields obtained at the end of each cycle were also compared to others reported in literature as briefly summarised by Oladipo *et al*. (2020).

Table 4.9: Properties of FAME produced in comparison with the biodiesel specification standards

Properties	**USOME**	**LOME**	**BOME**	**MOME**	**TEKOME**	**ASTM D6751**	**EN D14214**	**SAN 833**
Density at 15^{o}C (g/cm^{3})	0.8913	0.8932	0.880	0.882	0.8867	0.86 – 0.9	0.85	0.86– 0.90
Viscosity (mm^{2}/s)	4.48	4.23	3.40	3.65	4.18	1.9 -6.0	3.5 – 5.0	3.5 – 5.0
Acid value (mg KOH/g)	0.457	0.352	0.35	0.423	0.564	0.5	0.5	0.5
IV (g I_2/100g oil)	97.71	95.81	85.66	84.38	90.1	120	-	140
CN	52.50	48	52.45	53.38	58.67	47 min	51 min	51 min
Calorific value (MJ/kg)	40.25	41.2	40.94	40.72	42.72	-	35	-

Table 4.10: Activities of the synthesized catalysts in biodiesel produced

Oil source	**Synthesized Catalyst**	**RSM Design**	**Optimum conditions**			**Optimum Yield (%)**	**Reusability**		**Article found**
			Meth/oil	Catalyst Loading (wt%)	Time (min)		No. of cycles	Minimum yield	
USO	CBP	CCD	14:1	3.5	60	94.53	-	-	Chapter 4
LO	CBP	CCD	14:1	3.5	60	95.61	-	-	,,
BO	CBP	CCD	14:1	3.5	60	94.86	-	-	,,
MO	CBP	CCD	14:1	3.5	60	98.0	-	-	,,
MO	CBP	CCD	6:1	2.0	55	96.45	-	-	,,
TEKO	CBP	BBD	13:1	4.5	80	95.10	-	-	,,
LO	CBP	CCD	11:1	2.7	51	96.50	4	91	Paper 1
USO	CPP	BBD	12:1	3.5	60	97.50	3	88.5	Paper 5
LO	7CE-CaO:3CPP@600	BBD	14.9:1	3.87	80	91.3	5	60	Paper 3
USO/MO Blend	CE-CaO/CBP@800	TD	15:1	2.5	70	93.77	6	85.2	Paper 7

4.17 Conclusion

Biodiesel was successfully synthesized from USO, LO, BO and MO using CBP catalysts. The modelling and optimization process was accomplished by RSM. The CCD based on three factors five levels was used to investigate the effect of the interaction of the process parameters on four responses which include: USOME, LOME, BOME and MOME. The optimal condition of methanol to oil ratio of 14:1, catalyst loading of 3.5 wt% and reaction time of 60 min, showed that 94.53, 95.61, 94.86 and 98.0 wt% yields corresponding to USOME, LOME, BOME and MOME could be achieved. The TEKOME synthesis was investigated separately using a BBD with three factors three levels. The optimum condition established was methanol to oil ratio of 13:1, CBP catalyst loading of 4.5 wt% and reaction time of 80 min with the yield of 95.10 wt%. Investigation on the application and the reusability of the synthesized catalysts such as CBP, CPP, 7CE-CaO:3CPP-600 and CE-CaO:CBP-800 on biodiesel production were also summarised and presented with yields ranging from 91.3 – 97.50 wt%. The statistical evaluation of the developed models for each experiment were accurate and resulted in good predictions. The reusability test of the produced catalyst revealed that CBP could be used for up to 4 cycles with a minimum yield of 91 wt% at the 4^{th} cycle, CPP up to 3 cycles with minimum yield of 88.5 wt% at the last cycle, 7CE-CaO:3CPP-600, 5 cycle with a minimum yield of 60 wt% and CE-CaO:CBP@800 up to 5 cycles with a minimum yield of 89.32 wt%. The properties of each biodiesel produced in all the investigations were found consistent with the standards (ASTM D6751, EN 14214 and SANS 833), which implies that they can be used in the internal combustion engines. The study demonstrates the useful protocol of utilizing biomass resources for effective biodiesel production.

5 CHAPTER FIVE: *In-situ* and *ex-situ* hybridization techniques for biodiesel production

5.1 Introduction

Biodiesel is one of the viable sources of renewable energy projected to hold important place in the global energy infrastructure. It appears to be the most promising fuel alternatives to petroleum-based fuel in motor vehicles and industrial plants due to their similarities in properties with petro-diesel fuel. However, for biodiesel to replace the major portion of the global fuel needs at present and in the near future, the input feedstock source of its production needs to be significantly increased. The major economic hurdle to the commercialization of biodiesel is the feedstock of production. Feedstock are the core determinants of the biodiesel production cost as they forms about 70 – 85 % of the total cost of production (Mansir *et al*., 2018a). Limited supply of feedstock is a serious challenge to biodiesel production, and it contribute immensely to higher price and large-scale commercialization. Plant oils are viable energy source but may not be directly use in the engine due to high viscosity and poly-unsaturated features of its bond structures. To this effect, several approaches such as biochemical and thermal conversion process are employed to make quality biodiesel fuel out of vegetable oils. Biodiesel feedstocks are different in their properties due to their sourced location and methods. They are also regionalised due to soil topographies and climates, thereby creating difficulties in sourcing for large or sufficient quantities for industrial production. This leads to uncertainties in biodiesel fuel properties. However, application of genetic engineering strategy via simple hybridization process to optimized feedstock quantity as well as improving its properties is a promising and sustainable path for adoption. Hybridization involves the blending of various feedstocks at varying proportions to generate a new product with new properties similar to the parents stock (Eloka-eboka and Inambao, 2016). The essence is to improve the fuel properties, which are mostly influenced by the fatty acid composition of each oil that comprises the mixture (Giwa *et al*., 2016). The fatty acid compositions of the oil is directly related to its physical and chemical properties (Hegde *et al*., 2015). Therefore, strategical alteration of the fatty acid profile will indeed lead to adequate scale up of the biodiesel feedstock with improve properties. Co-mingling of oil feedstock ensures quality improvement irrespective of the effect of compositional background of the oil source as a result of geographical differences and climate.

Oils containing more saturated fatty acid show low cold flow properties (cloud point, pour point). Unsaturated fatty acid rich oil shows less oxidation stability. Oils with high amount of oleic and linoleic fatty acid are reported as better feedstock in terms of the quality of the fuel properties of the biodiesel produced from them. Biodiesel synthesis from a mixture of oils has been exploited via the combination of edible, non-edible and waste cooking oils, with yields ranging from 86 – 98 %. (Almeida *et al*. 2015; Dharma *et al*. 2016; Falowo *et al.* 2020; Freire *et al*. 2012; Milano et al. 2018; Serqueira *et al.* 2014). However, information regarding the investigation of biodiesel properties by application of two-pathway hybrid process is sparse in literature.

This study investigates a two-pathway hybrid process (*in-situ* and *ex-situ*) of used sunflower oil (USO) and linseed oil (LO), baobab seed oil (BO) and marula seed oil (MO) and their respective biodiesel produced (USOB, LOB, BOB, MOB). Among these plant oils, baobab and marula oils are investigated for the first time for their prospects in biodiesel production. The *in-situ* hybrid in this study entails co-mingling of the raw oils (USO, LO, BO, and MO) prior to transesterification and *ex-situ* hybrids involve co-mingling of the produced biodiesel (USOB, LOB, BOB and MOB) after transesterification. This was used to juxtapose their physicochemical property differences for improve properties and effective applications. The transesterification process was performed under the same operation condition and catalysed by CBP catalyst. The study contributes towards an effective feedstock hybrid application for the sustainable development of biodiesel fuels.

5.2 Biodiesel and petro-diesel specification standards

For a succ**es**sful utilization and marketability of biodiesel, the establishment of the biodiesel quality specifications and testing describing their properties is a prerequisite. Hence, the development of fuel quality regulations to serve as a guarantee for engine performance is of essence. Biodiesel characteristics vary based on the fatty acid esters composition of feedstock used, by-products, and product purification, post-production, and storage issues (Atabani *et al*., 2013). Some physicochemical properties affect the ignition and combustion efficiencies of fuels whereas, structural features, namely chain length of hydrocarbon, degree of saturation, and branching impacts on the profile of fatty acid esters (Aghbashlo *et al*., 2021). These directly influence the biodiesel properties and therefore their characteristic behaviors and performances as automotive fuels. Another reason for biodiesel standards stems from the variation of the global climatic conditions as these affect the demands of biodiesel usage in a particular region. The specification standards for petro-diesel and biodiesel are listed in Table 5.1.

Table 5.1: Standard limits for diesel and biodiesel fuels

Fuel property	**Diesel [a]**	**ASTM D6751**	**EN 14214**	**SANS 833**
Moisture content (%)	-	0.03	0.05	0.05
Density (g/cm^3)	0.824	0.86 – 0.9	0.85	0.86 – 0.90
Viscosity (mm^2/s) @ 40°C	2.3	1.9 – 6.0	3.5 – 5.0	3.5 – 5.0
Acid value (mg KOH/g oil)	-	≤ 0.5	≤ 0.5	0.5
Iodine value (g I_2/100g oil)	38	-	≤ 120	140
Cetane number	45	≥ 47	≥ 51	>51.0
Heating value (MJ/kg)	46	-	35	-
Flash point (°C)	53	≥ 130	≥ 120	-
Pour point (°C	-8	-15 to 16		-
Cloud point (°C)	1	-3 to 12	-	-
CFPP (°C)	-5	5 max.	-	-4 to 3
Oxidative stability (h)		≥ 3	≥ 6	6 min

a (Acharya et al., 2017)

5.3 Experimental

5.3.1 Materials

The oil sources used in this study have been studied in chapter four. They include used sunflower (USO), linseed oil (LO), baobab oil (BO), and marula oil (MO). Their potential for biodiesel production have also been investigated individually at different optimised conditions. In this chapter, their hybrid oil via pre-transesterification (*in-situ* hybridisation) and post-transesterification (*ex-situ* hybridisation) are investigated in order to study their physical and chemical properties. The general flow chart that describes the whole process is depicted in Fig.5.1.

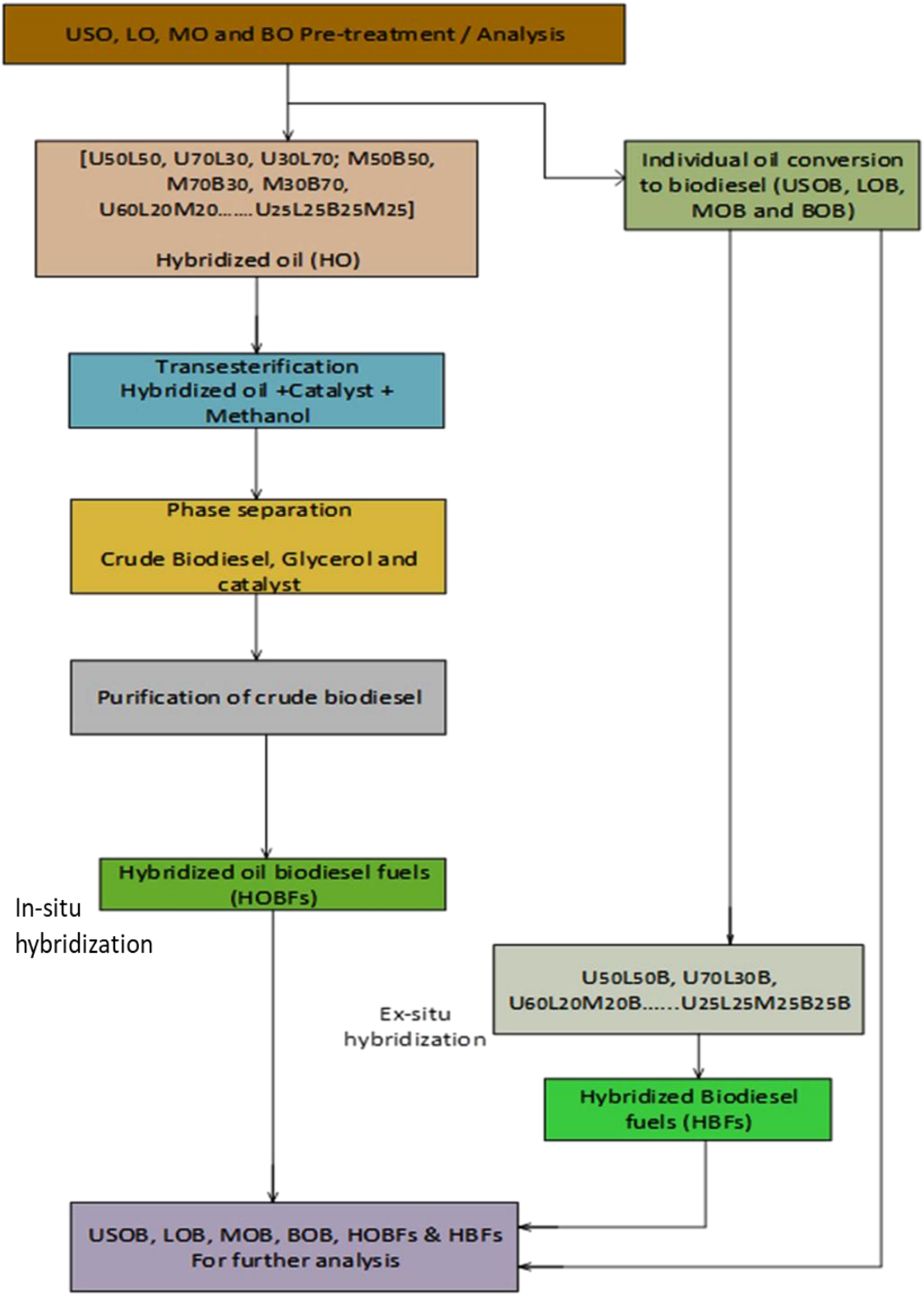

Figure 5.1: The flow diagram of the *in-situ* and *ex-situ* hybridization preparation processes

5.3.2 Preparation and co-mingling pattern

A simplex centroid design was adapted with 31 experiments, which comprises of 31 different oil contents as biodiesel feedstock, including single oils, bi-, ternary- and quaternary hybrids in different volumetric ratios as presented in Table 5.2. The sample of each oil ratio were first heated to 60 ^{o}C and then mixed to obtain a homogenous solution. They were then left to cool before their physico-chemical properties were determined.

Table 5.2: Hybrid matrix for both in-situ and ex-situ hybridization process

Run	USO (%)	LO (%)	BO (%)	MO (%)	Labelled Ratio	FAME (%)
1	100	-	-	-	U100	93.73
2	-	100	-	-	L100	95.06
3	-	-	100	-	B100	91.63
4	-	-	-	100	M100	95.50
5	50	50	-	-	U50:L50	94.00
6	70	30	-	-	U70:L30	97.23
7	30	70	-	-	U30:L70	96.01
8	50	-	-	50	U50:M50	90.43
9	30	-	-	70	U30:M70	94.34
10	70	-	-	30	U70:M30	93.65
11	50	-	50	-	U50:B50	95.82
12	30	-	70	-	U30:B70	96.81
13	70	-	30	-	U70:B30	95.33
14	-	50	50	-	L50:B50	96.46
15	-	30	70	-	L30:B70	94.10
16	-	70	30	-	L70: B30	96.42
17	-	-	50	50	M50:B50	94.31
18	-	-	70	30	M30: B70	94.59
19	-	-	30	70	M70: B30	94.64
20	-	50	-	50	L50:M50	97.50
21	-	30	-	70	L30: M70	95.20
22	-	70	-	30	L70: M30	94.81
23	60	20	-	20	U60: L20: M20	93.54
24	-	60	20	20	L60: M20: B20	95.26
25	20	-	20	60	M60: B20:U20	90.93
26	20	20	60	-	B60: U20: L20	95.40
27	25	25	25	25	U25: B25:L25: M25	92.70
28	40	20	20	20	U40: L20: M20: B20	93.08
29	20	40	20	20	L40: U20: M20: B20	96.60
30	20	20	20	40	M40: L20: U20: B20	92.52
31	20	20	40	20	B40: L20: M20: U20	94.43

Where U, L, B and M denotes the first letter of the oil used.

5.4 Physico-chemical characterization

Standard procedures were used to characterize the physico-chemical properties of the oils and the biodiesel produced. The standard properties characterised are the density, kinematic viscosity, acid value, cetane number, heating value, saponification value and iodine value. The measured properties were compared with the American standard testing methods (ASTM), European norms (EN) and South African standard (SAN) for fuel quality.

5.5 Transesterification process of crude single and hybrid oil

The free fatty acid (FFA) of the four oils and their hybrids was less than 2.5 mg KOH/g oil, therefore a one-step transesterification process was employed (Mendonça et al., 2019), using calcined banana peels catalyst (CBP). The transesterification reaction process was performed under an optimal condition established in chapter 4. Briefly, 200 g of oil were poured into a round bottom flask equipped with a water-cooled condenser, placed on a magnetic hot plate. A calculated amount of methanol to oil molar ratio (MTOR) of 14:1 and catalyst loading of 3.5 wt% was added and the reaction was allowed to run for 60 min at a constant temperature and agitation speed of 65 ^{o}C and 450 rpm (Balajii and Niju, 2020). At the end of the reaction, the content was transferred to a separating funnel and allowed to stand for 6 h for fractional settling and phase separation. The top phase containing methyl ester was purified by washing with warm distilled water at 50 ^{o}C and further dried by heating to remove moisture. The methyl ester yield was determined gravimetrically using Eq 4.1. This was done to all the oil samples in Table 5.2 to obtain their corresponding methyl ester and yields. The *in-situ* hybrid oil methyl esters (HOMEs) were subjected to the physico-chemical properties analysis.

5.6 Preparation of the ex-situ hybrid biodiesel fuels

Ex-situ hybridization process involves the co-mingling of the biodiesel fuel after transesterification (post- transesterification). Biodiesel produced from single feedstock under the same operating conditions was studied in various hybrid proportions to observe the changes in their fuel properties and compositions. In this study, the methyl ester produced from the single oil (U100, L100, B100 and M100) in Table 5.1 with their corresponding methyl esters (USOME, LOME, BOME and MOME) were also hybridized using the same simplex centroid design (Table 5.1) to obtain hybridized methyl esters (HMEs). Each sample of the hybrids were

respectively heated and stirred to obtain a homogenous fuel solution and further subjected to the required physicochemical analysis.

5.7 Physiochemical properties and method of determination

Properties such as high cetane number, low viscosity, high flash point, low acid value and density are the key parameters that indicate the quality of biodiesel (Chattopadhyay and Sen, 2013).

5.7.1 Determination of density

The density of the biodiesel was determined at 15 ^{o}C using 100 ml relative density bottle (pycnometer). The measurement was performed according to ASTM 4052. The weight of the empty bottle was weighed and then filled with fuel. The bottle was again filled with distilled water at 15 ^{o}C and weighed. The differences in weights were estimated. The density was calculated using Eq 5.1 and expressed in g/cm^3.

$$Density\ (\delta) = \frac{W_3 - W_1}{W_2 - W_1} \times \delta H_2 0 \qquad 5.1$$

Where W_1 = Weight of empty bottle (Pycnometer 100 ml)

W_2 = weight of bottle with water

W_3 = weight of bottle with fuel

$\delta H_2 0$ = density of water

5.7.2 Determination of kinematic viscosity (η)

Viscosity is that property that measures the resistance to fluid flow. The kinematic viscosity was determined according to the ASTM D445 using Cannon Fenske routine viscometer. The viscometer was filled with sample at 40 ^{o}C and immersed in a water bath of a constant temperature to maintain the temperature. The viscosity was calculated by multiplying the time of sample flow through the capillary tube with the viscosity being constant. It was expressed in mm^2/s.

$$Viscosity\ = time\ (s) \times viscosity\ constant \quad \text{5-2}$$

5.7.3 Determination of acid value

Acid value indicates the FFA content of the oil or biodiesel fuel. It was determined according to ASTM D664 and EN 14104 (Almeida *et al*., 2015). The method is based on titration wherein samples were diluted with ethanol-diethyl ether mixed in the ratio of 1:2, titrated with potassium hydroxide using phenolphthalein as indicator to detect the endpoint. The result was calculated according to Eq. 5.3 and expressed in milligrams of potassium hydroxide per gram of sample (mg KOH/g).

$$AV = \frac{(C \times V \times 56.1)}{m} \quad \text{5.3}$$

Where C = the concentration of the KOH (0.1 N)

V = the volume of KOH

M = mass of the sample (g)

5.7.4 Determination of Iodine value

This is the measure of unsaturation of oils and fats. High iodine value relates to high unsaturation in the oil. The iodine value of the oil and biodiesel samples were determined by AOAC method using monochloride solution.

$$Iodine\ value = \frac{[B - S] \times N \times 12.69}{Weight\ of oil\ sample} \quad \text{5.4}$$

Where N is the concentration of sodium thiosulphate used for determination, B is the volume of the sodium thiosulphate used for the blank; S is the volume of sodium thiosulphate used for the determination.

5.7.5 Determination of Cetane number

This is determined the ignition quality of the fuel when injected into the engine. Higher value of CN shows better ignition quality of fuel. It can be calculated following the Eq. 5.5 (Ahmad *et al*., 2019)

$$Cetane\ no. = 46.3 + \left(\frac{5458}{saponification\ value}\right) - 0.225\ Iodine\ value \quad 5.5$$

5.7.6 Determination of heating value

This is the function of saponification value and iodine value. The CV of the oil and biodiesel was calculated by the following Equation 5.6

$$HV = 49.63 - [0.041(SV) + 0.015(IV)] \quad 5.6$$

Where SV = saponification value; IV= iodine value

5.7.7 Mean molecular mass determination

The mean molecular mass was obtained using the Equation 5.7

$$Mean\ Molecular\ Mass = \frac{56}{saponification\ value} \times 100 \quad 5.7$$

5.7.8 American Petroleum Index

This was evaluated according to equation described by Equation 5.8

$$API = \frac{141.5}{Specific\ gravity\ at\ 288\ K} - 131.5 \quad 5.8$$

5.7.9 Aniline point

This helps in characterization of pure hydrocarbons and in their mixtures. It increases with the increasing molecular weight. Aniline point is used to measure the aromatic content of the

mixtures (Nadkarni, 2015). It was obtained in accordance with the ASTM D611 and determined by the Equation (Ahmad *et al.*, 2019)

$$Aniline\ point = \frac{Diesel\ index \times 100}{API} \quad 5.9$$

5.8 Results and discussion

The physiochemical properties of the single and hybrid oil were determined following the method stated above and the results are presented in Table 5.3. The properties of the hybrid oils were observed to be lower than the singles. This happens because the process of hybridization would impact on some of the properties of single stock becomes higher or lower in numerical values. Property such as density was observed to be higher in single oil than the hybrids. The viscosity of the hybrid oils is almost half that of the single oil due to the mixing effect as well.

Table 5.3: Physicochemical properties of single and hybrid oils

Single and hybrid oil	DEN	VIS	AV	SV	IV	CN	CV
U100	0.948	23.87	2.25	198.16	115.08	37.95	38.7
L100	0.949	16.43	3.60	196.05	105	50.51	40
M100	0.939	15.86	4.35	192.13	98.4	52.56	38.8
B100	0.941	12.69	2.17	209.5	88	52.55	38.4
U50:L50	0.927	16.53	2.72	195.91	87	54.58	38.6
U70:L30	0.926	16.36	2.33	196.51	112.00	51.03	38.9
U30:L70	0.911	13.31	2.14	192.7	111.00	49.5	37.8
U50:M50	0.918	17.32	3.73	196.72	109.00	50.2	38.22
U30:M70	0.912	16.26	4.47	195.31	107.51	51.96	39.14
U70:M30	0.918	16.17	2.92	195.31	108.00	50.9	38.75
U50:B50	0.923	16.98	1.53	201.91	110.00	50.8	37.83
U30:B70	0.915	14.54	1.26	198.31	113.00	51.33	38.05
U70:B30	0.919	17.25	0.69	194.11	111.00	50.65	38.25
L50:B50	0.923	14.67	1.54	198.11	99.60	49.91	38.19
L30:B70	0.917	15.91	1.77	202.13	102.51	50.24	38.52
L70: B30	0.922	12.93	2.24	196.51	108.31	49.70	39
M50:B50	0.916	14.52	5.33	201.81	110.11	48.57	38.45
M30: B70	0.911	14.5	2.38	192.9	99.53	52.20	38.11
M70: B30	0.911	13.96	3.37	195.91	106.13	50.28	38.05
L50:M50	0.924	12.26	5.61	194.31	104.91	50.78	37.91
L30: M70	0.915	10.59	4.77	191.91	107.20	50.62	38.08
L70: M30	0.921	12.97	3.22	189.51	104.81	51.51	38.7
U60: L20: M20	0.922	14.71	2.52	192.31	109.11	50.13	38.44
L60: M20: B20	0.918	13.31	3.03	194.51	106.59	50.37	39.09
M60: B20:U20	0.911	15.22	3.34	193.72	108.54	50.05	38.14
B60: U20: L20	0.917	11.6	1.52	198.91	110.65	48.84	38.9
U25: B25:L25: M25	0.916	13.6	2.81	197.31	111.49	48.87	39.36
U40: L20: M20: B20	0.917	13.22	3.49	195.91	109.73	49.47	38.11
L40: U20: M20: B20	0.917	12.88	2.58	194.51	110.54	50.78	40.14
M40: L20: U20: B20	0.916	12.44	3.34	193.91	101.20	51.09	38.73
B40: L20: M20: U20	0.917	12.36	2.58	198.51	102.00	50.1	38.88

Den- density, AV – Acid value, Vis- Viscosity, SV-saponification value, IV, iodine value, CN-cetane number and CV- calorific value

5.8.1 Fuel properties evaluation of *in-situ* and *ex-situ* hybridization process

The comparison of the two-pathway hybridization processes was carried out by graphical illustration depicted in Figures 5.1 – 5.5.

5.8.2 Density

Density is a very important fuel property. It affects the functional efficiency of fuel atomization in a CI engine. The stipulated range by EN14214 standards for biodiesel at 15 ^{o}C is from 860 – 900 kg/m^3. Fuels that exceed the density limit specification incur injection of a large mass of biodiesel, which may affect the air-fuel ratio, engine combustion and performance characteristics (Ashraful *et al*., 2014). High density gives rise to large spray injection with the tendency to form a rich mixture in the engine cylinders. Higher density of biodiesel results in the formation of large fuel droplets during the process of atomization, which also affects the emission and performance characteristics of the engine (Aghbashlo *et al*., 2021). Biodiesel density is mostly dependent on the composition of the fatty acids in the feedstock and the degree of purity of the fuel. The densities of the single and hybrid biodiesel fuels in comparison are presented in Figure 5.2. The densities of some single fuels were found higher (USOB and LOB) than others (BOB and MOB). This also reflects in their hybrid fuels, by reducing the densities. A drastic decrease in density to a value less than 0.85 g/cm^3 occurred at the bi-hybrid of BOB and MOB. This is because the densities of their single fuels are lower compared to others. The *in-situ* hybrid fuels were a bit higher in density than the *ex-situ* fuels, but all were within the specified standard limits. This implies that hybridization of oil can re-structure the fatty acid composition of oil giving rise to improved properties.

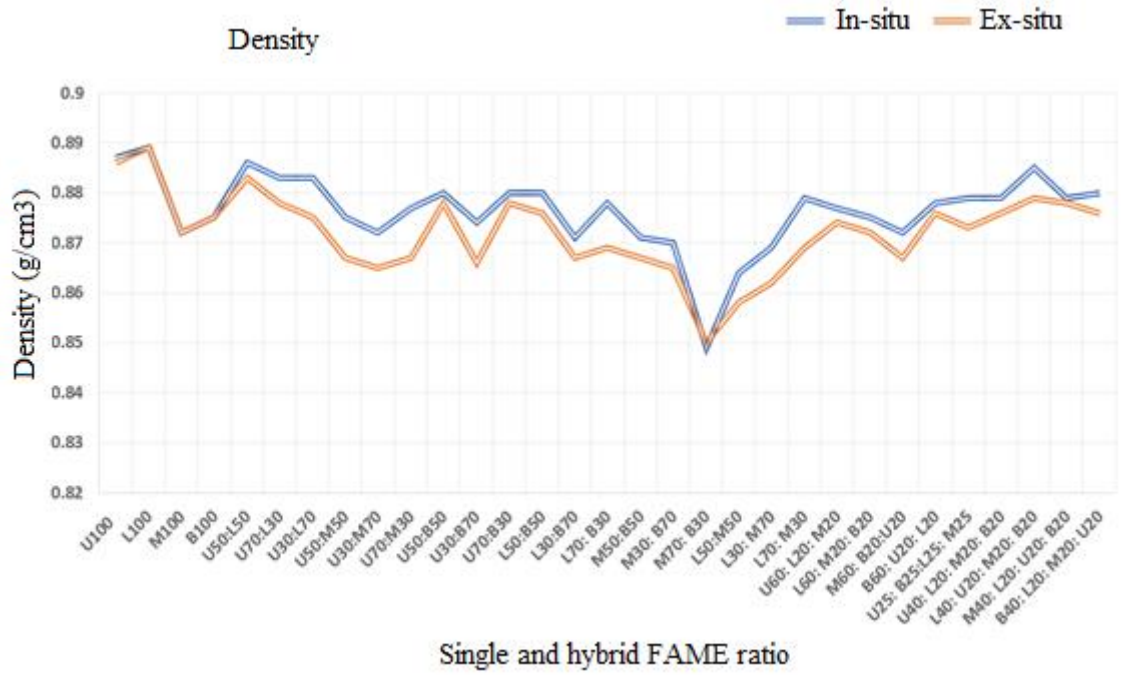

Figure 5.2: *In-situ* and *ex-situ* hybrid fuel Density

5.8.3 Viscosity

Viscosity measures the flow resistance of a fluid or internal fluid friction. It influences the fuel flow behaviour in pipelines, orifices and spray atomization mostly at low temperatures. Fuel that is highly viscous tends to produce large spray droplets on injection leading to poor fuel atomization and promotes engine deposits, resulting in a more energy input fuel pumping (Shahir *et al*., 2017). According to the American and European standards, acceptable limits of kinematic viscosity at 40 ^{o}C for biodiesel are 1.9 – 6.0 and 3.5 – 5.0 mm^2/s respectively. The lower limit prevents the possibility of power loss in engine while the upper limits ensures smooth cold flow conditions (Ozcanli *et al*., 2013). Lower viscosity guarantees easy pumping and finer droplets. High viscosity influences cold engine start-ups and ignition delays. Insufficient lubrication resulting in a very low viscosity leads to leakages (Agarwal *et al*., 2017b). Figure 5.3 shows the graphical representation of the single and hybrid fuel properties. The order of increase in viscosity of single fuel is U100 > M100 > L100 > B100, and falls in the range between 3.0 – 4.5 mm^2/s. The hybrid fuels viscosities were observed to be lower than the singles and tend to decrease as the ratio of hybrid biodiesel fuel blends increase. *In-situ* hybrid fuels viscosities were less high in some of the ratios than the *ex-situ* fuels. All the viscosities of the biodiesel produced were within the ASTM D6751 limits but some especially the poly-hybrids were below the EN 14214 standard limits. This also depends on the differences in their chemical compositions. The analysis shows that the viscosities of all biodiesel fuels

produced can be pumped easily when used in CI engine without much power losses or engine deposits.

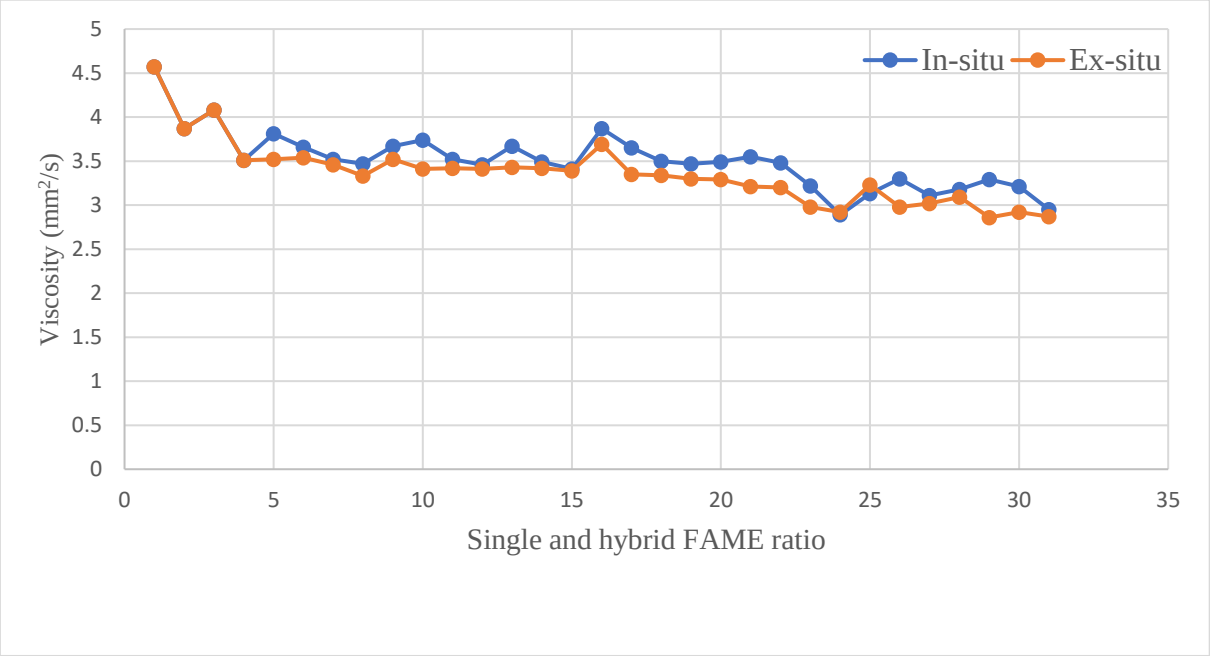

Figure 5.3: *In-situ* and *ex-situ* hybrid fuel viscosity

5.8.4 Acid value

Acid value indicates the level of FFA in a biodiesel fuel. It is the amount of KOH (mg) required to neutralise a unit mass per gram of FAME. The maximum acid value certified by ASTM, EN and SAN standards for biodiesel is 0.5 mg KOH/g. Acid constituents in biodiesel exist as organic acid, FFAs, by product of oxidation and unremoved acid catalyst (Singh *et al*., 2019). High acid value tends to corrode metal components of the fuel supply system and also causes fuel deposits, reduction in filters and pump life (Yesilyurt *et al*., 2020). Acid values of all the produced biodiesel fuels under the same optimum condition were lower than the specified limits. The values of hybrid fuels were lower than the singles. Alternate trends were observed in some part of the bi-hybrid ratios of the two processes due to the differences in composition of the new oils formed. Thus, acid values of the two processes were found decreasing with increasing ratios of the hybrids (Figure 5.4).

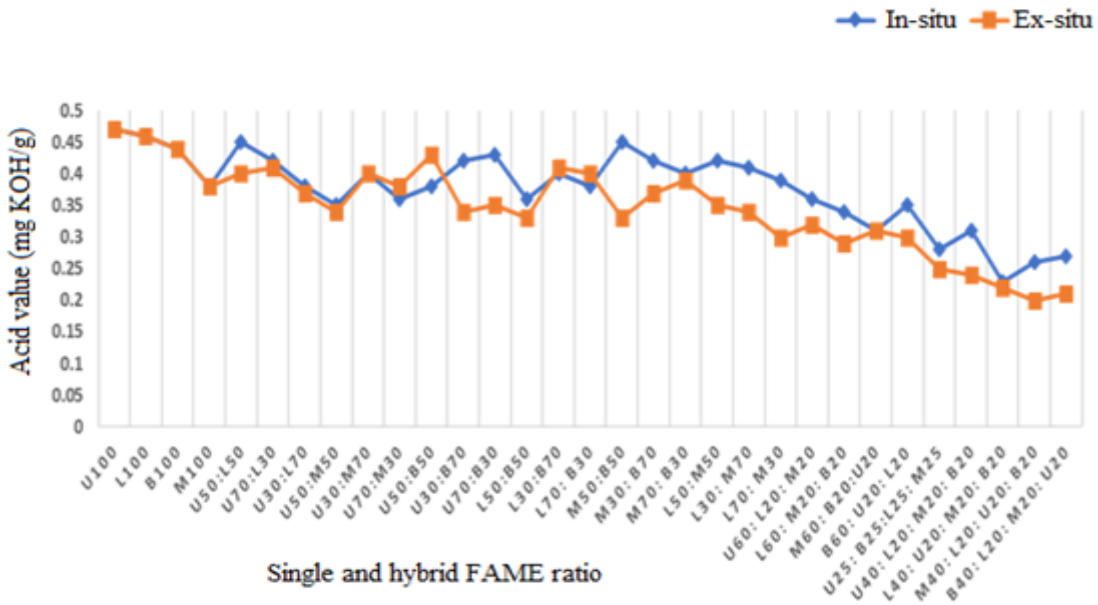

Figure 5.4: *In-situ* and *ex-situ* hybrid fuel acid value

5.8.5 Cetane number

Cetane number extensively influences the ignition delay. A high cetane number indicates a short ignition delay and it is favourable for an effective engine performance. High cetane number offers good engine performances in cold weather conditions, promote complete combustion, minimized white smoke formation, hydrocarbons, NOx, carbon monoxide, and particulate matter. The ASTM D6751, EN 14214 and SAN standards specify a minimum of 47 and 51 respectively for biodiesel. Generally, the cetane number of biodiesel is higher than petro diesel due to higher oxygen contents, which also results in higher combustion efficiency of biodiesel. Figure 5.5 shows the graphical comparison of the two-hybrid processes together with the single oil biodiesel produced under the same condition. It is obvious from the plot that the cetane number of the hybrid fuels are much higher than the singles. The cetane number were found to increase with increasing ratios of hybrids. In comparison with the hybrid pathways, *ex-situ* hybrids were observed to be higher than *in-situ* along the bi-hybrids ratios, but both appears almost similar in poly hybrids. All the cetane numbers of the biodiesel produced were within the specified limits.

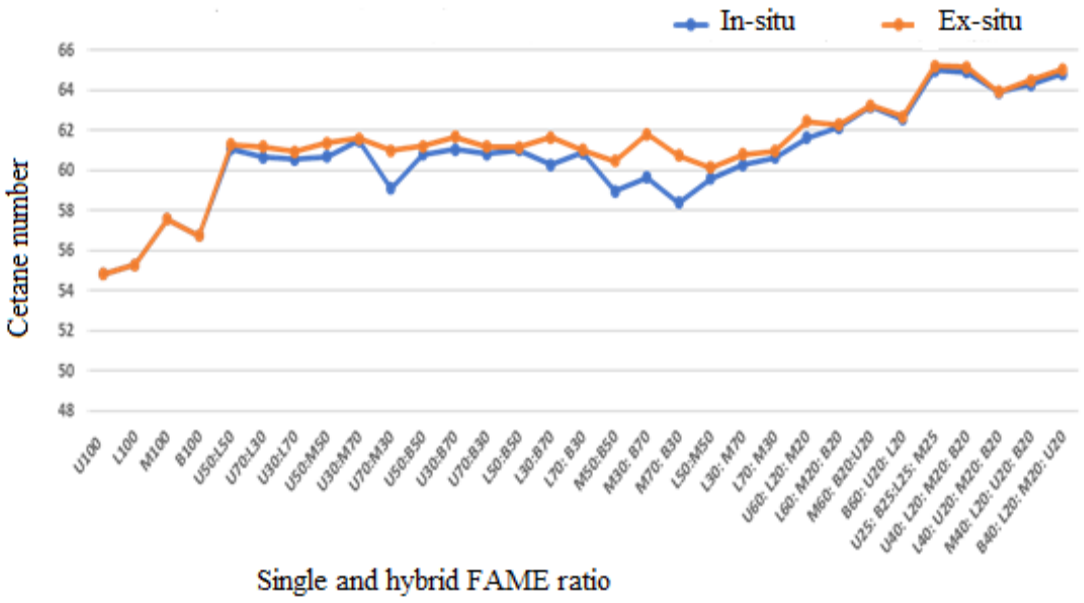

Figure 5.5: In-situ and *ex-situ* hybrid fuel Cetane number

5.8.6 Calorific or Heating values

Calorific value is a standard for measuring the optimal engine operation. It measures the total energy content (heat) produced when a substance is combusted completely in the presence of air or oxygen. Due to the higher oxygen content of the biodiesel, its calorific value is relatively lower, ~ 12 and 14 % lower in energy content (MJ/kg) on a mass basis compared to petro-diesel (Chattopadhyay and Sen, 2013). Thus, for heating purposes, a minimum calorific value of 35.00 MJ/kg was prescribed in the EN14214 standard for biodiesel, but most FAME exceeds this value due to their fatty acid compositions and structures. There is no prescribed limit reported by ASTM and SANS, probably due to uncertainties of climatic conditions in some regions. The comparison of the single and the two pathway hybrid fuels are illustrated in Figure 5.6. The plot clearly depicted the increase in calorific values of the hybrid fuels than the singles. All the calorific values of the biodiesel obtained are above the EN 14214 minimum limits. The calorific values of single fuels ranges from 40 - 41 MJ/kg while the values obtained for the hybrids tend to increase above to 43 MJ/kg. Thus, this is competing as compared to petro-diesel with 46 MJ/kg. The differences in hybrids are clearly based on the composition of new oils created in the process. In comparison, the two-pathway processes displayed almost the same thing but with little increment in some ratios of the *ex-situ* than *in-situ*. This could also be supported by the fact that the transesterification process increases the cetane numbers and heating values of the biodiesel while reducing the viscosities, acid values and the densities of the raw vegetable oils (Selvan and Nagarajan, 2013).

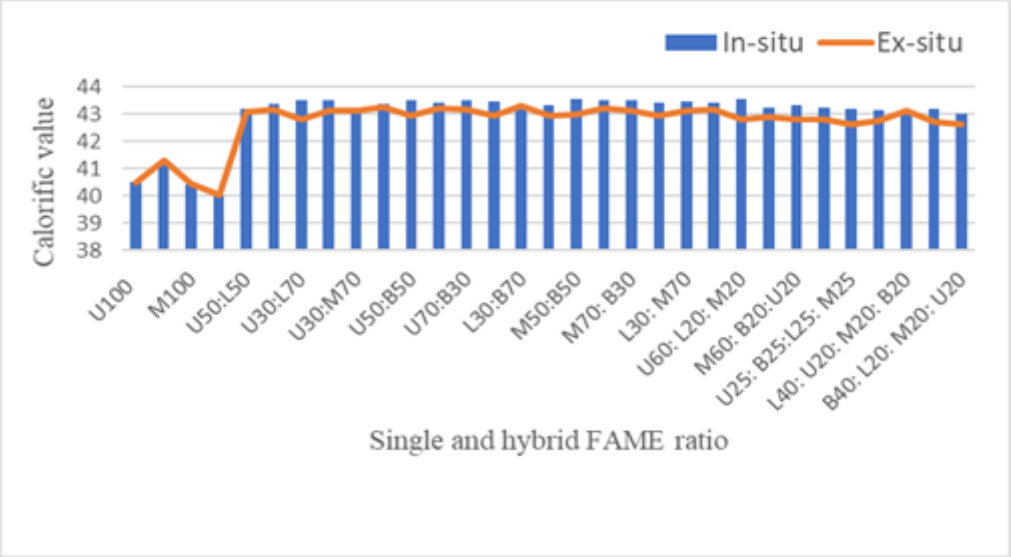

Figure 5.6: In-situ and ex-situ hybrid fuel calorific value

5.8.7 Conclusion

Biodiesel was developed from used sunflower oil, linseed oil, baobab oil and marula seed oil and their bi-, ternary- and quaternary hybrid oil under the same operational conditions. As the feedstock availability is limited, the possibility of using hybrid feedstock was investigated. The oils contain low free fatty acids and similarly the hybrids. Therefore, one-step transesterification was performed using bio-alkaline heterogeneous catalyst (calcined banana peels) to obtain their methyl esters. The yield(s) obtained for the single and hybrid oils ranged from 90 – 98.5 %. High conversion yields were also observed from hybrid feedstock, which shows that the transesterification process is impartial to the number of ratios of oil mixture or any specific oil. All the biodiesel produced were within the international and SANS standard specifications. The two-process pathway of hybridization are indeed very effective and economical. They enhanced the properties that are appropriate with regards to the upper and lower limits of standard specifications. Properties such as viscosity, acid value and density were found to be decreasing with the progressive number of hybrid ratios while the cetane number and the calorific value were increasing with increased number of hybrid ratios. *In-situ* hybrids were observed to be a bit higher in physical properties while *ex-situ* was a bit higher in thermal properties. Thus, at industrial level, the protocol can be adopted to ensure sufficiency and improvement of feedstock for biodiesel production in the face of scarcity.

6 CHAPTER SIX: Application of machine learning technology in modelling and computing biodiesel properties

6.1 Introduction

Biodiesel fuels obtained from plant and animal resources are endowed with auspicious characteristics such as renewability, biodegradability, nontoxicity, benignity and safety. Despite these attributes, some detrimental features of their physico-chemical properties are of concern to researchers and to industries. The physico-chemical properties of biodiesel are directly dependent on the fatty acid compositions. This greatly affects production, transportation, handling, storage, combustion and performances. Therefore, biodiesel fuel must comply with the international and local acceptable standards such as ASTM D6751, EN 14214 and SANS 833, to certify fuel quality before commercialization. The cetane numbers, heating values and oxidative stability plays important role in the combustion process. While the cetane number influences the ignition quality of the biodiesel, calorific value measures its heat content of the combustion process and oxidative stability indicates the tendency of deterioration due to chemical changes as a result of extended period of storage. Fatty acid composition has a direct effect on the physical and chemical properties of biodiesel. Oils from different sources have different fatty acid compositions with variations in carbon chains length and numbers of unsaturation. The degree of unsaturation, chain length, chain branching, double bond number and configuration are the key structural features of a particular fatty ester molecule affecting physico-chemical properties (Aghbashlo *et al*., 2021). The cold flow properties of biodiesel are higher than petro-diesel due to higher concentration of high-melting point saturated long-chain fatty acids (Singh *et al*., 2019). Improvement in the cold flow properties of biodiesel can be achieved by decreasing chain length and increasing degree of saturation. Biodiesel is a chemical and thermodynamic complex system. Therefore, the study of its compositions and properties based on experimental data can effectively be addressed by the application of machine learning approach. One of such is the use of artificial neural network (ANN) in modelling and prediction of its properties.

Artificial neural network (ANN) is a data processing system motivated by biological neural system. It is an intelligent-based technique used in a computational modelling of extremely complex systems. Unlike other modelling system such as RSM, ANN does not require the complex equations to perform the computational modelling but can rather be developed wholly from past process dataset (paper 4). ANN that is properly trained can be used as a model to

predict a specific application. It has a generalized advantage of specifically predicting responses for a new set of data input. It also can concurrently estimate multiple input–output relationships (Betiku and Ishola, 2020). The development of methods used in predicting biodiesel properties has increased recently. ANN model was used to predict density, kinematic viscosity and cetane number of biodiesel (Rocabruno-Valdés *et al*., 2015). The prediction of exhaust emission in transient conditions of diesel engine fuelled with animal fat biodiesel was carried out by Domínguez-Sáez *et al*. (2018). ANN was also used in predicting the heating values of vegetable oil based ethyl esters biodiesel (Najafi *et al*., 2011). A comprehensive review on machine learning application for investigating biodiesel properties was reported by Aghbashlo *et al*. (2021). In this study, ANN was deployed to model and predict the thermal properties of biodiesel (cetane and calorific values) based on empirical data. The two-pathway hybrid processes were used as focal points for comparison purposes. This was achieved by using the empirical data of other properties in order to investigate their predictions based on the uncertainty of the hybrid technology. This approach contributes to one of the effective ways of verifying the theoretical and empirical data of the physicochemical properties of biodiesel fuels.

6.2 Experimental

6.2.1 Data collection

The machine learning of the fuel properties of biodiesel obtained from this study was further investigated by the use of artificial neural network (ANN) system. The experimental results obtained for the physico-chemical properties of the *in-situ* and *ex-situ* hybridization pathways in chapter 5 were further investigated to confirm the uniqueness of the hybridization technology. The data generated from the two-pathway processes were used to establish the ANN framework model. A total number of 32 data sets were used for each process pathway to predict two responses. The input factors used were density, viscosity, acid value, saponification value and iodine value. While the output factors investigated, were the cetane number and the calorific value respectively. All the data used and their predictions are presented in Appendix A, Table 1.1 and 1.2 respectively.

6.3 ANN modelling of the *in-situ* and *ex-situ* hybrid FAME properties

The ANN model was developed using MATLAB (R2021b). To obtain the desired model for each pathway hybrid, the data sets obtained were split into three subsets where 70 % of the processed data were used for the training, 15 % for testing and 15 % for validation. A

feedforward back propagation was used with Levenberg-Marquadt training algorithm (TrainLM) and gradient descent with momentum backpropagation (Traindgm). The network topology comprises of 3 layers which include the input hidden layer 1, hidden layer 2 and the output layer. The transfer function in the hidden layer 1 was fixed with tansig and 10 neurons, while that of hidden layer 2 was optimized with different transfer function (Tansig, Logsig and purelin) and varied neuron between 10 and 20. This was done to generate the most effective network topology that leads to the desired predicted responses (CN and CV). Each network topology was evaluated with several number of iterations until the lowest mean-square-error (MSE) with the highest correlation coefficient (R) approaching one was obtained. The general form of each transfer function used in this study are given in Eq. (6.1) – (6.3). The features of the network model used for this study are presented in Table 6.1.

Tangent sigmoid function (Tansig)

$$f(t) = \frac{e^{t} - e^{-t}}{e^{t} + e^{-t}} \tag{6.1}$$

Log sigmoid function (Losig)

$$f(t) = \frac{1}{1 + e^{-t}} \tag{6.2}$$

Pure linear function (Purelin)

$$f(t) = t \tag{6.3}$$

Table 6.1: ANN modelling features for the prediction of in-situ and ex-situ hybrids fuel properties

Property	Value/ remark
Network type	Feedforward back propagation
Algorithm	Levenberg-Marquardt back-propagation (TrainLM) Gradient descent with momentum backpropagation (Traindgm)
Learning	Supervised
Number of Inputs	5
Number of outputs	2
Transfer function - Hidden layer 1	Tansig
Transfer function - Hidden layer 2	Varied (tansig, losig and purelin)
Number of hidden neurons	10 & 20
Best network structure – In-situ FAMEs	5-10-10-2
Best network structure – Ex-situ FAMEs	5-10-20-2
Best iteration for In-situ FAMEs	8
Best iterations for Ex-situ FAMEs	6
Minimised error function	MSE

6.3.1 Evaluation of ANN model over the two-pathway hybrid process

The efficacy of the developed models were statistically appraised on the two-pathway hybrid properties. This was carried out using various statistics as displayed in Eq. (6.4) – (6.11) to determine the parameter viz. R, R^2, RMSE, SEP, MAE and AAD. The result obtained were compared to determine which hybrid pathway is superior to the other. The correlation between the experimental and the predicted data for each pathway was also plotted to adjudge the accuracy of the applicable model.

Correlation coefficient

$$R = \frac{\sum_{i=1}^{q}\left(Z_{p,i} - Z_{p,m}\right).\left(Z_{a,i} - Z_{a,m}\right)}{\sqrt{\left[\sum_{i=1}^{q}(Z_{p,i} - Z_{p,m})^2\ \right]\left[\sum_{i=1}^{q}(Z_{a,i} - Z_{a,m})^2\right]}} \quad (6.4)$$

Coefficient of determination

$$R^2 = 1 - \frac{\sum_{i=1}^{q}(Z_{a,i} - Z_{p,i})^2}{\sum_{i=1}^{q}(Z_{p,i} - Z_{a,m})^2} \quad (6.5)$$

Adjusted R^2

$$Adjusted\ R^2 = 1 - \left[(1 - R^2) \times \frac{q-1}{q-h-1}\right] \quad (6.6)$$

Mean square error

$$MSE = \frac{1}{q}\sum_{i=1}^{q}(Z_{p,i} - Z_{a,i})^2 \quad (6.7)$$

Root mean square error

$$RMSE = \sqrt{\frac{1}{q}\sum_{i=1}^{q}(Z_{p,i} - Z_{a,i})^2} \quad (6.8)$$

Mean absolute error

$$MAE = \frac{1}{q}\sum_{i=1}^{q}\left|\left(Z_{a,i} - Z_{p.i}\right)\right| \quad (6.9)$$

Standard error of prediction

$$SEP = \frac{RSME}{Z_{a,m}} \times 100 \quad (6.10)$$

Average absolute deviation

$$AAD = \frac{100}{q}\sum_{i=1}^{q}\left|\frac{\left(Z_{a,i} - Z_{p,i}\right)}{Z_{a,i}}\right| \quad (6.11)$$

6.4 Results and discussion

6.4.1 ANN model

The ANN models developed comprise the density, viscosity, acid value, saponification value and iodine value as input parameters and two responses, which are cetane numbers and calorific values as the output parameters. A three-layered network topology for each pathway hybrid was used. The selection of the optimal ANN network architecture was based on studying the three transfer functions (tansig, Losig and purelin) for the input hidden layer 2 while maintaining for all training sets and output hidden layer, a constant hyperbolic tangent transfer (tansig) function. The number of hidden neurons were also studied between 10 and 20 and each were trained with several number of iterations. Table 6.2 presents the network comparison with different transfer functions of Levenberg-Marquardt back propagation with varied number of neurons in the input-hidden layer 2. There were six pairs of transfer function combinations for the *in-situ* pathway hybrid fuel properties and another six pairs for the *ex-situ* pathway hybrid properties. The best combination was selected based on the lowest and highest value obtained for MSE and R for the processes. The MSE (0.2021) and R (0.9987) were obtained for the *in-situ* pathway hybrid while (0.2799) and (0.9989) were obtained for the *ex-situ* pathway hybrid. Thus, the optimal ANN model developed for the *in-situ* hybrids is tansig-tansig–tansig transfer function with 10 neurons in the input hidden layer 2, and tansig-purelin-tansig for the *ex-situ* hybrids with 20 neurons in the input hidden layer 2. The optimal ANN framework design developed for the prediction of cetane numbers and calorific values for the *in-situ* and *ex-situ* hybrids is shown in Figures 6.1 and 6.2 with topologies of 5-10-10-2 and 5-10-20-2 respectively. This implies 5 process input parameters in the input layer, 10 neurons for the hidden layer 1, 10 neurons for the hidden input layer 2, and 2 neurons for output layer for the *in-situ* hybrids. The same was applicable to the *ex-situ* hybrids except that there are 20 neurons in the input hidden layer 2. The corresponding plot of correlation coefficient for the training, testing, validation and all data sets for the two pathways are illustrated in Figures 6.3 and 6.4. The high values of R in the figures indicates good correlation between the actual and the predicted values. The high R values for the validation and testing sets implies good predicting potentials of the developed ANN models. The ANN prediction of the cetane numbers and calorific values for the *in-situ* and *ex-situ* hybrids are presented in Appendix A; Tables 1.1 and 1.2.

Table 6.2: Network comparison with different transfer functions of Levenberg-Marquardt back propagation with varied number of neurons in the input-hidden layer 2

Hybrid type	ANN structure Input: Neuron: Neuron Output	Transfer function Input hidden 1	 Input hidden 2	 Output hidden	R	R^2	MSE	RMSE	Best iteration
In-situ hybrids	5-10-10-2	Tansig	Tansig	Tansig	0.9987	0.9975	0.2021	0.4495	8
		Tansig	Losig	Tansig	0.9910	0.9821	1.7985	1.3411	3
		Tansig	Purelin	Tansig	0.9714	0.9436	13.090	3.6180	1
	5-10-20-2	Tansig	Tansig	Tansig	0.9974	0.9949	1.4949	1.2226	5
		Tansig	Losig	Tansig	0.9923	0.9848	2.3033	1.5176	6
		Tansig	Purelin	Tansig	0.9868	0.9737	2.0187	1.4208	6
Ex-situ hybrids	5-10-10-2	Tansig	Tansig	Tansig	0.9893	0.9787	6.300	2.5099	18
		Tansig	Losig	Tansig	0.9968	0.9937	0.2762	0.5255	7
		Tansig	Purelin	Tansig	0.9981	0.9962	1.5365	1.2395	31
	5-10-20-2	Tansig	Tansig	Tansig	0.9978	0.9956	1.4694	1.2121	5
		Tansig	Losig	Tansig	0.9974	0.9947	0.8393	0.9161	7
		Tansig	Purelin	Tansig	0.9989	0.9979	0.2799	0.5290	6

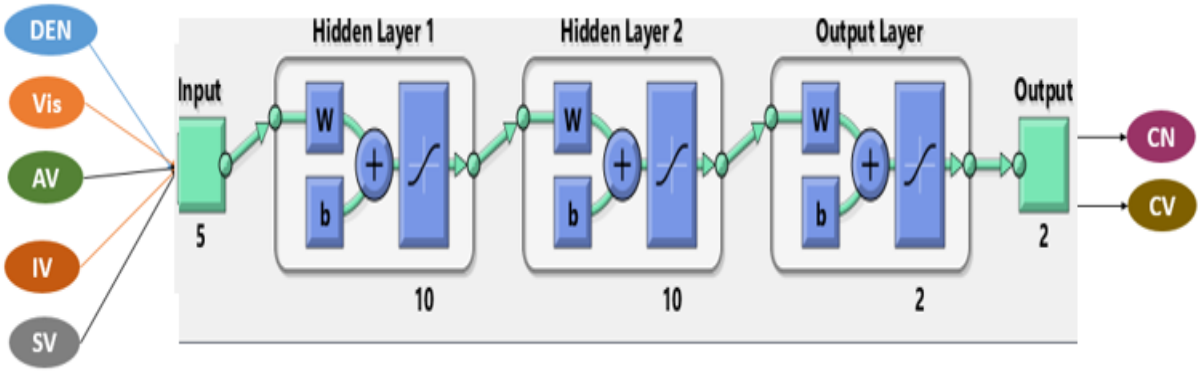

Figure 6.1: *In-situ* hybrids optimal network topography for the prediction of CN and CV

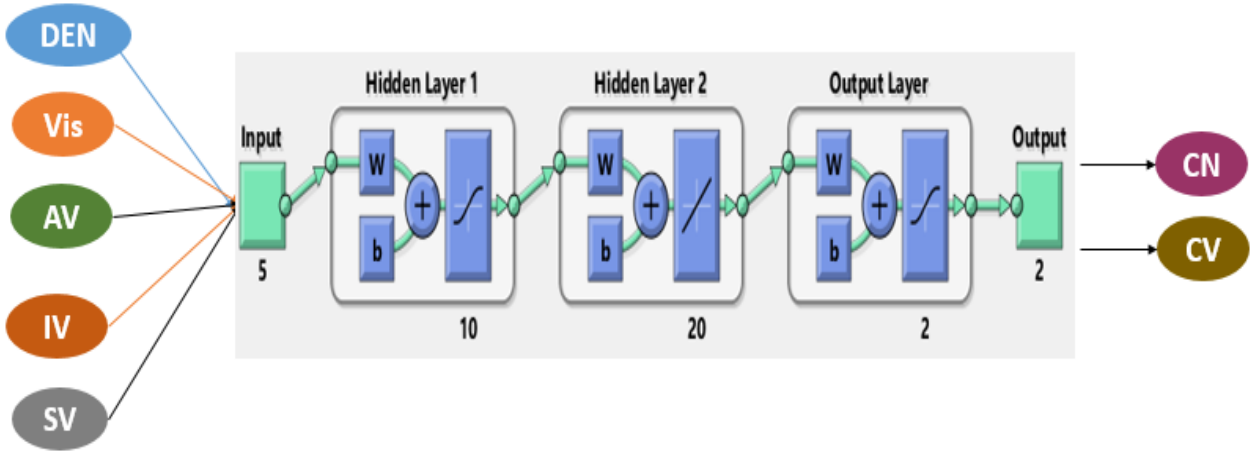

Figure 6.2: *Ex-situ* hybrids optimal network topography for the prediction of CN and CV

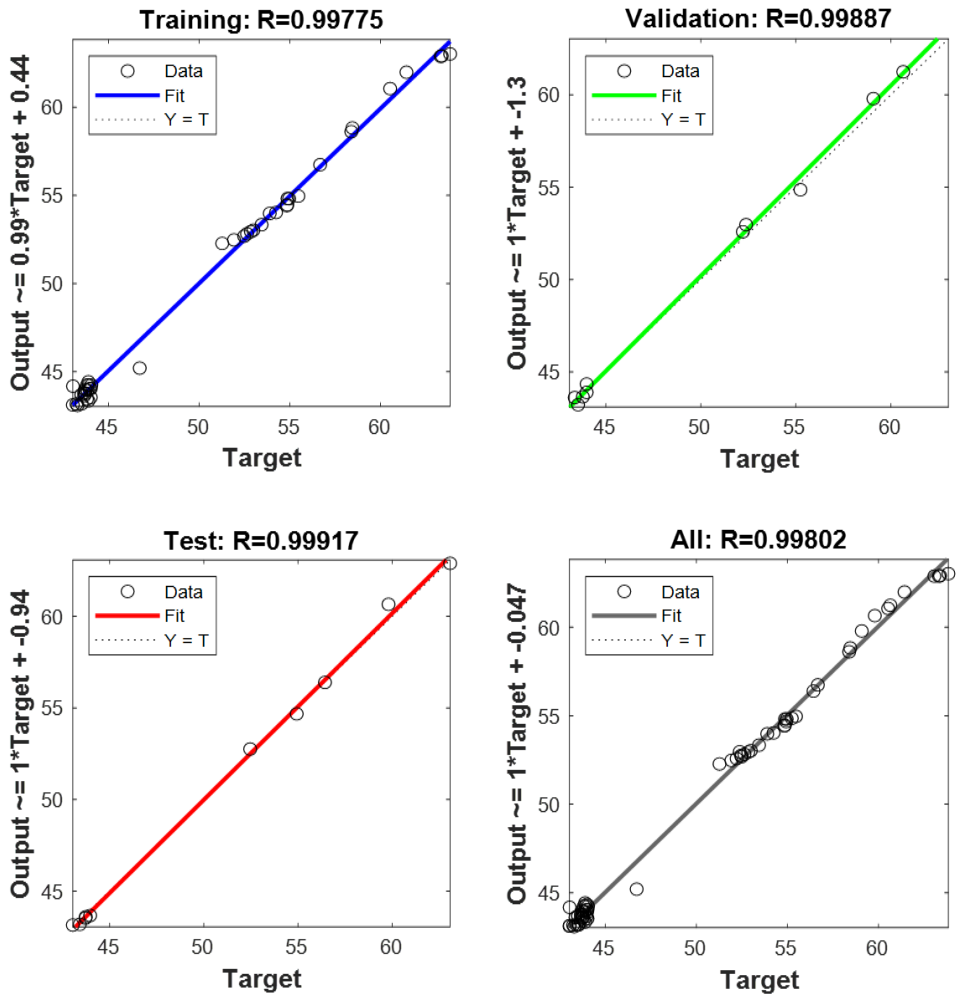

Figure 6.3: Regression plot for training, testing, validation and all data set for ANN model for the *in-situ* hybrids

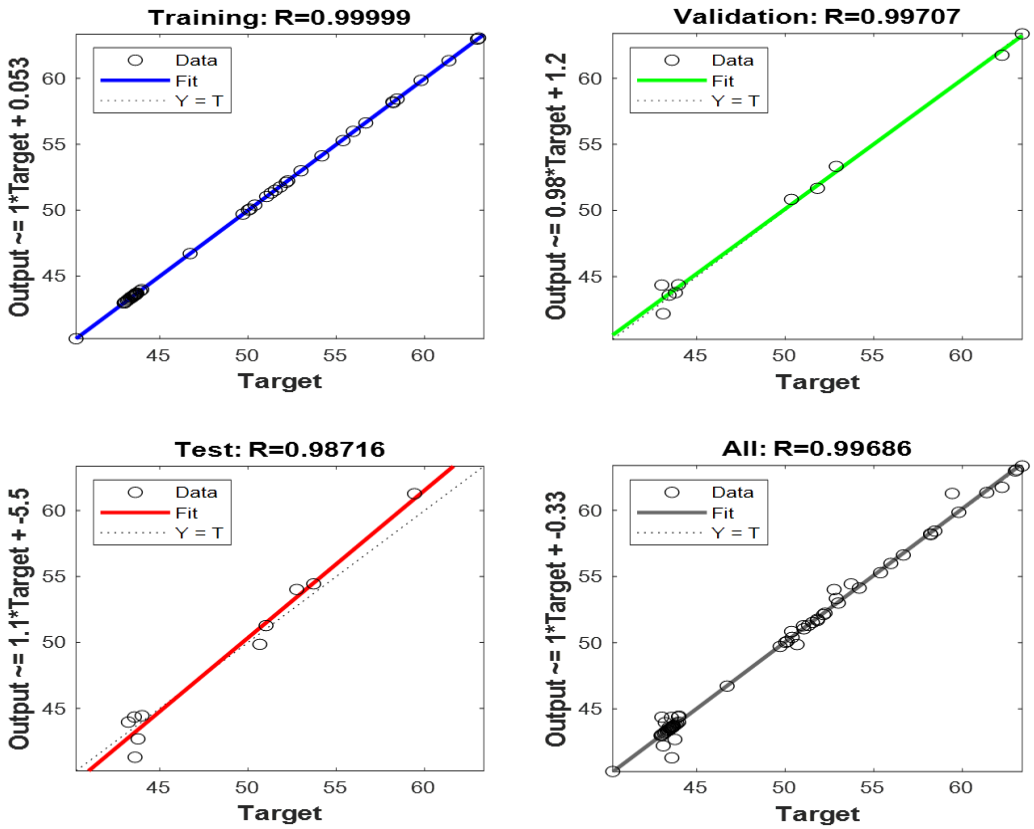

Figure 6.4: Regression plot for training, testing, validation and all data set for ANN model for the *ex-situ* hybrids

6.4.2 Comparison of the ANN predicting potential on *in-situ* and *ex-situ* hybrids properties

ANN predicting capabilities on the *in-situ* and *ex-situ* hybrid biodiesel fuel properties were appraised and compared based on some statistical indices which include: R, R^2, RMSE, SEP, MAE and AAD. It can be seen that both hybrid pathways are very effective. According to the prediction, *ex-situ* hybrids have the highest R (0.9989) and R^2 (0.9979) values compared to the *in-situ* with R (0.99877) and R^2 (0.9975). The lower values from the error analysis performed using RMSE, SEP, MAE and AAD parameters signifies good performance of the model. The level of accuracy and precision of the models was evaluated based on the statistical indices given in Eq. (6.4 - 6.11). The error values obtained by ANN for *in-situ* hybrids are lower than those of the *ex-situ* hybrids. The result generated for all the statistical indicators are presented in Table 6.3. They also indicate that both hybrid pathways are effective, but ANN model performed better in terms of error accuracy in the *in-situ* hybrids than in the *ex-situ*. Figures 6.5(a,b) and 6.6 (a,b), illustrate the close alignment of the experimental and predicted values of the cetane numbers and calorific values for the two pathway hybrids respectively. The plots are also in congruent of the statistical results. The plot alignment for the *ex-situ* hybrids were well

fitted with high R values for the CN (0.990) and the CV (0.975) in Figures 6.4 (a,b) than the *in-situ* with R values for the CN (0.985) and the CV (0.934) (Figures 6.3 (a,b)) respectively. The efficacy of ANN model application in predicting complex processes similar to the ones in this study of biodiesel production were also reported in literature (Aminian and ZareNezhad, 2018; Giakoumis and Sarakatsanis, 2018; Karmakar *et al*., 2018).

Table 6.3: Assessment of ANN model potential on the *in-situ* and *ex-situ* hybrids properties

Statistical factors	***In-situ* Hybrids**	***Ex-situ* hybrids**
R	0.99877	0.9989
R^2	0.9975	0.9979
Adjusted R^2	0.9970	0.9975
MSE	0.2021	0.2799
RMSE	0.4495	0.5290
MAE	0.3700	0.4020
SEP	0.0135	0.0158
AAD	0.0120	0.0469

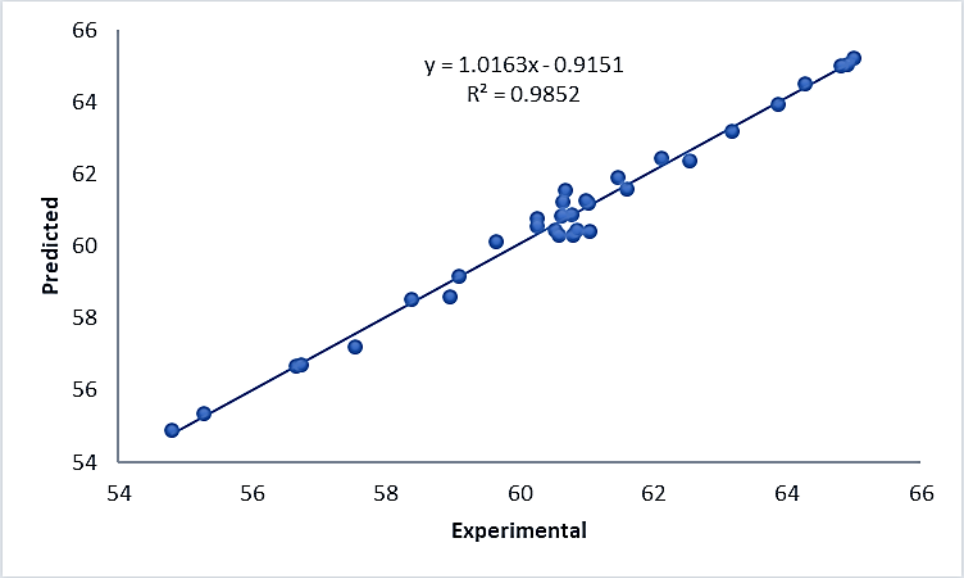

(a)

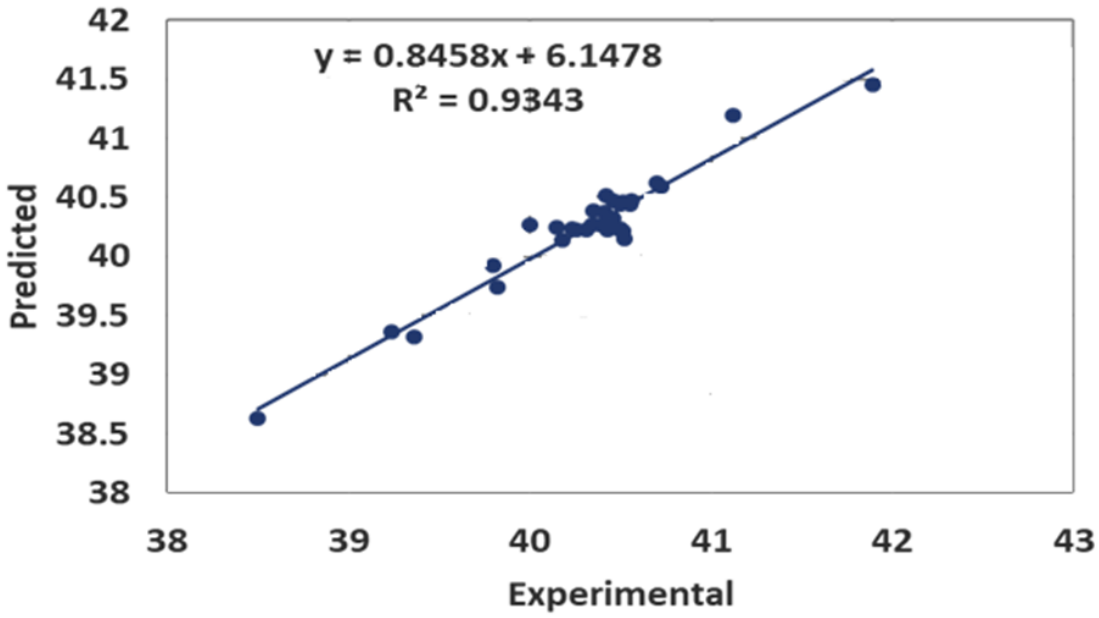

(b)

Figure 6.5 (a,b): Experimental vs Predicted values for In-situ Hybrid FAME: (a) CN and (b) CV

(a)

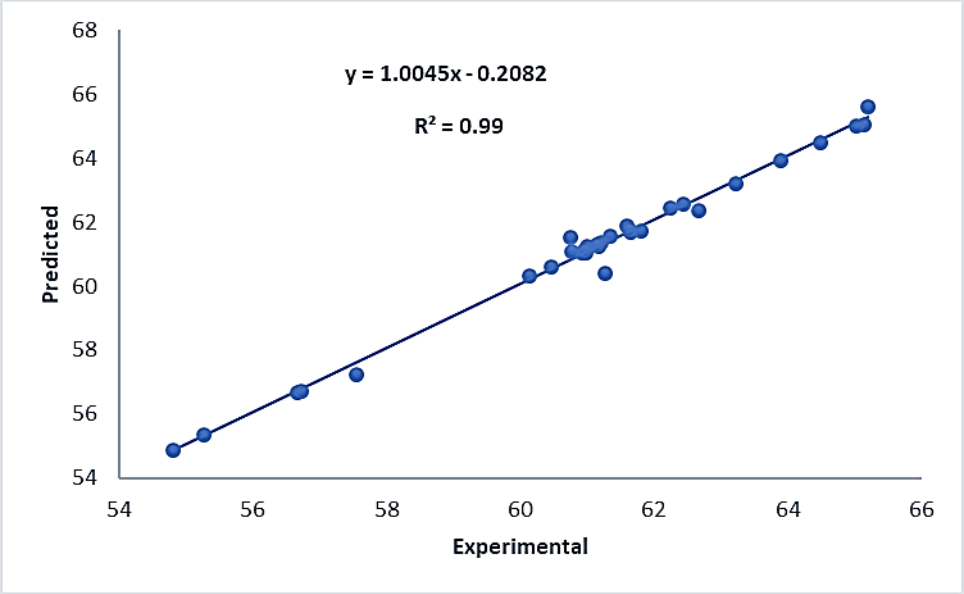

(a)

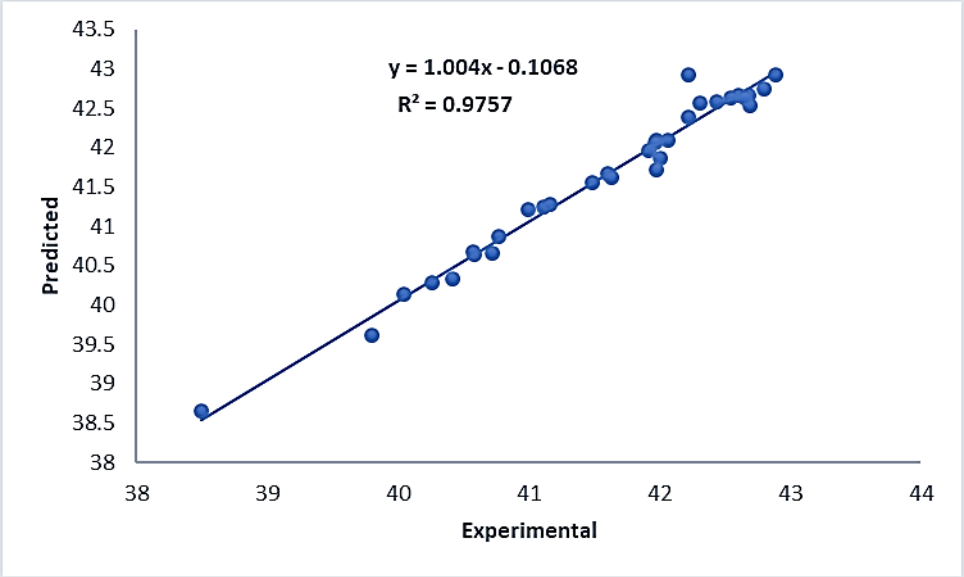

(b)

Figure 6.6 (a,b): The Plot of experimental vs Predicted for Ex-situ Hybrids for (a) CN and (b) CV

6.5 Conclusion

ANN predictive model was successfully used in modelling the biodiesel properties of the *in-situ* and *ex-situ* hybrid fuels. The model comprises three layers with five input parameters (density, viscosity, acid value, saponification and iodine value) and two output parameters (cetane number and calorific value), all obtained from the experimental analysis. The best topological network for the two processes were 5-10-10-2 with tansis-tansig-tansig transfer function for the *in-situ* hybrids and 5-10-20-2 with tansig-purelin-tansig for the *ex-situ* hybrids. The measures of the predictive ability of the models were based on the high value of R^2, and the least value of RMSE which were 0.9975, 0.4495 for the *in-situ* and 0.9979, 0.5490 for the *ex-situ* respectively. The statistical evaluation of the two hybridization pathways showed effective prediction due to the high values of R and R^2, and the low values of RMSE, SEP, MAE and AAD. This implies that the empirical model derived from ANN can adequately be used to describe the input variables for CN and CV predictive relationships. In comparison, *ex-situ* Rs were higher than the *in-situ* while the predictive errors in the *in-situ* were lower than the *ex-situ*. The two hybrid processes are indeed effective to be explored and adopted at the commercialisation scale-up or at the industrial level application.

7 CHAPTER SEVEN: Biodiesel fuels blend with petro-diesel and characterization

7.1 Introduction

Overdependence on non-renewable fossil fuel resources has placed the environment in much-aggravated condition(s) because of constant toxic emission arising from their combustion. The renewable and alternative fuels hold potential assurance for sustainable development with the security of energy supply alongside acceptable environmental implications. To ensure adequate supply of energy for transportation and industrial utilization, the mix of both alternative and conventional fuels is of socio-economic and sustainable essence. The advantages of blending biodiesel with mineral diesel cannot be overemphasized. Apart from resulting in meeting stringent automotive emission norms, other important benefits include: reparation of loss of fuel lubricity in diesel, reduction of greenhouse and other harmful gas pollutants, improvement in storage and handling capability of mineral diesel due to high flash points of biodiesel, and also the promotion of the compatibility of biodiesel with the existing infrastructure for safe fuel delivery and distribution. Moreover, it can also strengthen the rural industries and create employment since biodiesel can be produced from locally available biomass materials (Agarwal and Dhar, 2015). To ensure constant supply, the current rate of biodiesel production from different generations do not meet the worldwide demand of liquid fuels. Therefore, this leads to the deployment of various blending fuel options from other sources like biodiesel-petrodiesel blends (Elkelawy *et al*., 2020; Ghanbari *et al*., 2017; Hariharan *et al*., 2020; Şahin and Öğüt, 2018), biodiesel-alcohol blends (Alptekin *et al*., 2015; Sanli *et al*., 2015; Wei *et al*., 2018) and biodiesel-biodiesel blends (Elkelawy *et al*., 2020; Falowo and Betiku, 2022; Falowo *et al*., 2020). Biodiesel fuels characteristics can change due to some reasons. The major ones behind these are the lower energy content and high oxygen level, hydrogen and carbon amounts (Atabani *et al*., 2014). Compared with petro-diesel, biodiesel has higher fuel density, cetane number and viscosity but lesser amount of heat of combustion. Blending therefore compensate each fuel source with the deficient properties for better performance in the engine. Standard specifications have been established to accommodate various biodiesel characteristics from various feedstock sources. ASTM D6751 and EN 14214 standards have been developed for pure biodiesel fuel (B100), and ASTM D7467 for biodiesel blends from B6 to B20 with petro-diesel (which implies 6 % to 20 % biodiesel blend with 94 to 80 % petro-diesel). ASTM D975 standards permits B5 and lower blends, while EN 590 accommodates blends up to B5 and B7 (Singh *et al.*, 2019). Recently, EN 16709 was introduced to cover for B20 and B30 blends for

application by captive fleets. Biodiesel and diesel blend studies have severally been investigated in literature; the effect of blending of linseed oil biodiesel with mineral diesel was investigated by Şahin and Öğüt, (2018), soybeans biodiesel and diesel blends was conducted by Lapuerta et al. (2013), Coconut and palm oil biodiesel fuels were respectively blended with conventional diesel in a study carried out by Habibullah *et al*. (2014) and many others. The novel part of this study is the comparison of single and hybrid biodiesel fuel blends with petrodiesel, which has limited information in literature.

In this study, various biodiesel fuels including single, bi- and poly-hybrid fuels produced from four different plant oil sources (used sunflower, linseed, baobab and marula seed oils) were investigated with petro-diesel blends from B10 to B50. Their effects on some important fuel properties such as density viscosity, cetane number and heating value were investigated and compared with petro-diesel, international and local specifications (ASTM D6751, EN 14214 and SANS 833).

7.2 Experimental

7.2.1 Biodiesel-diesel blending

The blending of petro-diesel with biodiesel produced from used sunflower oil, linseed, baobab and marula and their various hybrids was investigated in this chapter. A total number of 31 various biodiesel (including single and hybrid) samples were used at various blends with mineral diesel ranging from 0-50 % by volume (B0 – B50). Each blend sample; B0 (0 % biodiesel, 100 % diesel); B10 (denote 10 % biodiesel, 90 % diesel); B20 (20 % biodiesel to 80 % diesel); B30 (30 % biodiesel, 70 % diesel); B40 (60 % biodiesel, 60 % diesel); B50 (50 % biodiesel, 50 % diesel) were measured and homogenised by placing on a magnetic stirrer at 400 rpm for 10 min before being subjected to characterization for fuel properties which were densities, viscosities, cetane numbers and heating values. The properties were determined according to the standard methods outlined in chapter 5.

7.3 Results and discussion

7.4 Physicochemical properties of single and hybrid biodiesel blend with petro-diesel

The physico-chemical properties of the blend samples were determined in accordance with the standards. Table 7.1 shows the physico-chemical properties of the single biodiesel blends in

comparison with the petro-diesel, international and South African standards. The results obtained for both the single and poly-hybrid biodiesel fuel blends with petro-diesel for all the properties investigated are displayed in Appendix B. Figures 7.1 – 7.4 show the graphical illustration of each property investigated.

Table 7.1: Physiochemical properties of single FAME blend with diesel

	Property	**B0**	**B10**	**B20**	**B30**	**B40**	**B50**
USOME	Density at 15 ^{o}C	829	836.5	840.3	844.9	849.6	852.4
blend with	Viscosity at 40 ^{o}C	2.18	2.38	2.98	3.18	3.25	3.32
diesel	Cetane Number	52	52.82	53.69	54.76	55.18	56.29
	Heating value	45.6	44.65	43.73	43.12	42.98	42.54
LOME blend	Density	829	835.2	841.2	846.5	850.3	854.5
with diesel	Viscosity at 40 ^{o}C	2.18	2.27	3.28	3.34	3.38	3.45
	Cetane Number	52	52.16	53.62	54.19	55.65	56.21
	Heating value	45.6	44.90	44.29	43.52	42.66	41.78
BOME blend	Density	829	832.4	842.4	849.8	855.2	858.5
with diesel	Viscosity at 40 ^{o}C	2.18	2.26	2.56	3.16	3.23	3.39
	Cetane Number	52	52.84	53.54	54.24	55.24	56.16
	Heating value	45.6	44.56	43.70	42.94	42.17	41.07
MOME blend	Density at 15 ^{o}C	829	834.7	841.7	849.9	850.4	858.1
with diesel	Viscosity at 40 ^{o}C	2.18	2.25	2.63	3.27	3.35	3.41
	Cetane Number	52	52.99	53.77	55.25	55.76	56.89
	Heating value	45.6	44.80	43.84	43.00	42.21	41.43

7.4.1 Biodiesel fuel blends: density

Figure 7.1. shows the graphical illustration of the effect of single and hybrids biodiesel blends with petro-diesel on densities. The plot shows that the density increases with the percentage increase of biodiesel in the blend (B10 – B50). There are also improvements on the hybrid biodiesel blends with petro-diesel. The density of the single biodiesel fuel blends with petro-diesel blends were higher than the hybrids. The petro-diesel density used in the blend was 829.12 kg/m^3 and the stipulated range of density for biodiesel by EN 14214 at 15 ^{o}C is from 860 – 900 kg/m^3. The values of the B10 and B20 blends obtained were observed to be closer to those of the petro-diesel used. The values obtained for B10, B20, B30 are all lower than the EN standard limits. B40, B50 single, and some hybrid biodiesel blends are well situated within ASTM D6751 standard of 850 kg/m^3 and EN14214 of 860 – 900 kg/m^3.

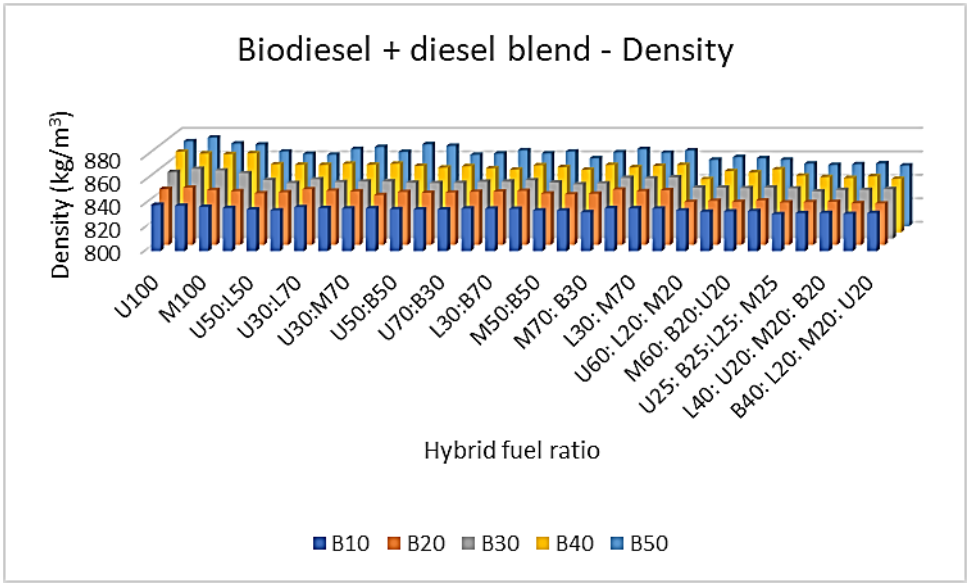

Figure 7.1: The effect of single and hybrid biodiesel blend with diesel on density

7.4.2 Biodiesel blends: Viscosity

The acceptable limits for a kinematic viscosity at 40 °C are 1.9 − 6.0 and 3.5 − 5.0 mm^2/s based on the American and European SANS standards respectively. The plot showed that the percentage increase in biodiesel increases the viscosity of the samples. The viscosity of the single biodiesel blend were found to be higher than the hybrid biodiesel blend. The kinematic viscosity at 40 ^{o}C of the petro-diesel used was 2.18 mm^2/s. The values obtained for 10 % and 20 % biodiesel blend (B10 and B20) were observed to be almost similar to the viscosity of the petro-diesel used. The viscosity of B10, B20 and B30 conformed to the ASTM 6751 standard

especially the lower limit but lower than the EN 14214 standards. The viscosities of all the blend samples were within the international and SANS standard limits.

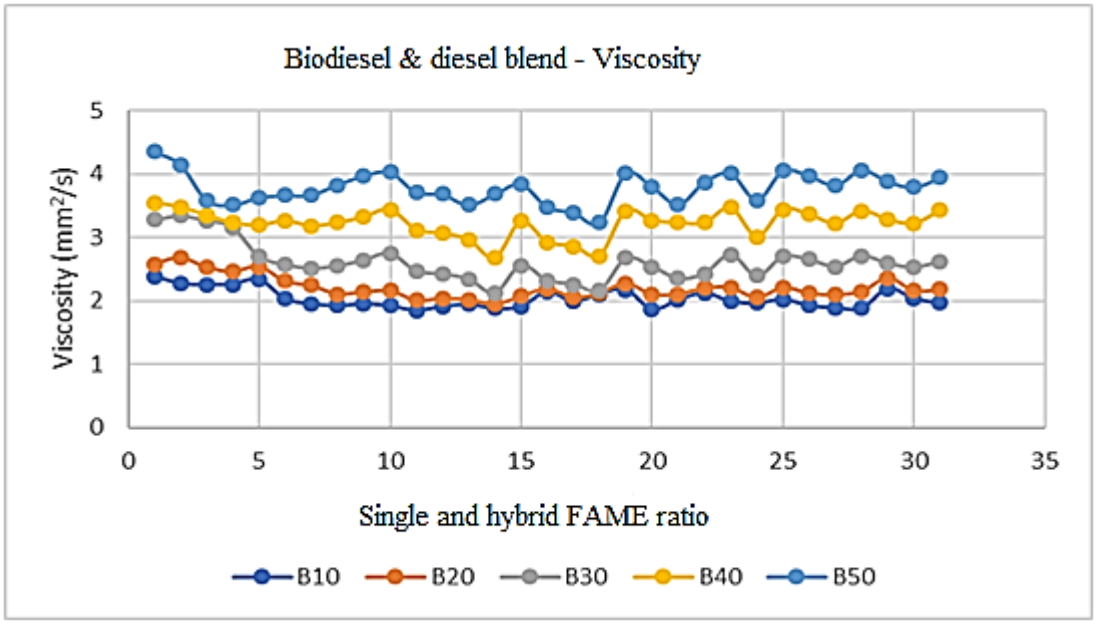

Figure 7.2: The effect of single and hybrid biodiesel blend with diesel on viscosity

7.4.3 Biodiesel blends: Cetane number

Figure 7.3 shows the plot of biodiesel blends of 31 samples. The value of the cetane number of the reference petro-diesel used for the blending was 52. The cetane number was found to increase with increasing percentage of biodiesel in the blends. Thus, higher cetane number allows for a smooth and noiseless running of the engine. The cetane numbers of the hybrid biodiesel blends were found higher than the single blends. A remarkable improvement of the blend trend was observed to occur in ternary and quaternary – biodiesel hybrid ratios. The minimum CN number for biodiesel prescribed by ASTM D675 and EN 14214 and SANS standards are 47 and 51 respectively. The cetane number of all the blend samples were above the minimum specification standards. This indicates that all the blend samples show shorter ignition delay and can run smoothly when run in a diesel engine.

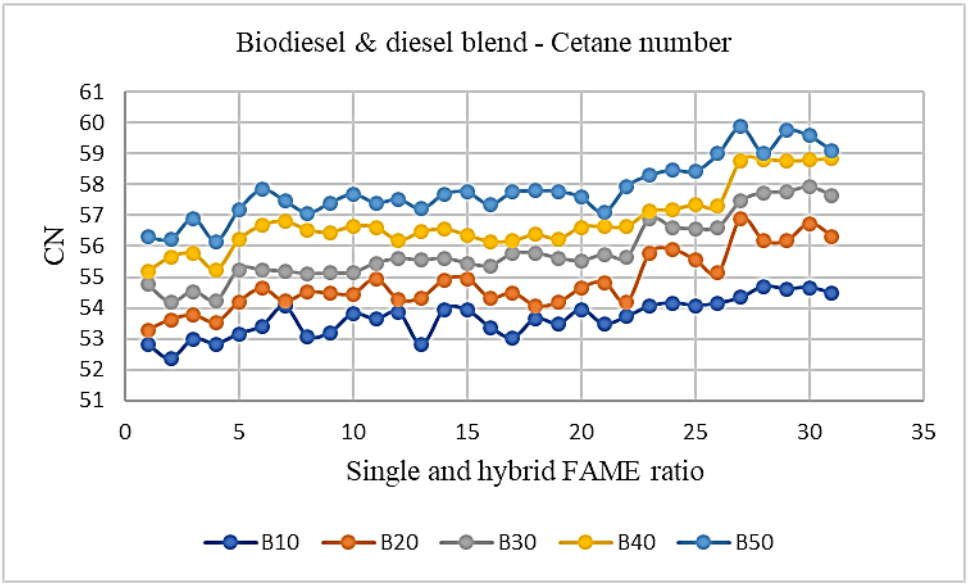

Figure 7.3: The effect of single and hybrid biodiesel blend with diesel on cetane number

7.4.4 Biodiesel blends: Heating value

Calorific values determine the power output of the engine during combustion. Figure 7.4 shows the heating value of various biodiesel blends with petro-diesel. The heating value of the petro-diesel used was 46 MJ/kg. The heating values of all the blend samples were found to decrease with the percentage increase of biodiesel in the blends in the order of B10 > B20 > B30 > B40 > B50. Hybrid biodiesel-diesel blends showed higher heating values than the single biodiesel-diesel blends. The improvement was also observed to occur based on the increase ratio of the hybrid biodiesel. The higher the ratio of hybrid biodiesel, the higher the HV of the blend samples, and the higher the biodiesel percentage blend, the lower the HV of the samples. The trend was observed in the improving order of Bi- < ternary - < quaternary hybrids. The B10 and B20 of hybrid biodiesel blends HV values were very close to those of the petro-diesel used in blending. The HV of all the samples were higher than the minimum limit of 35 MJ/kg specified by EN 14214 standard.

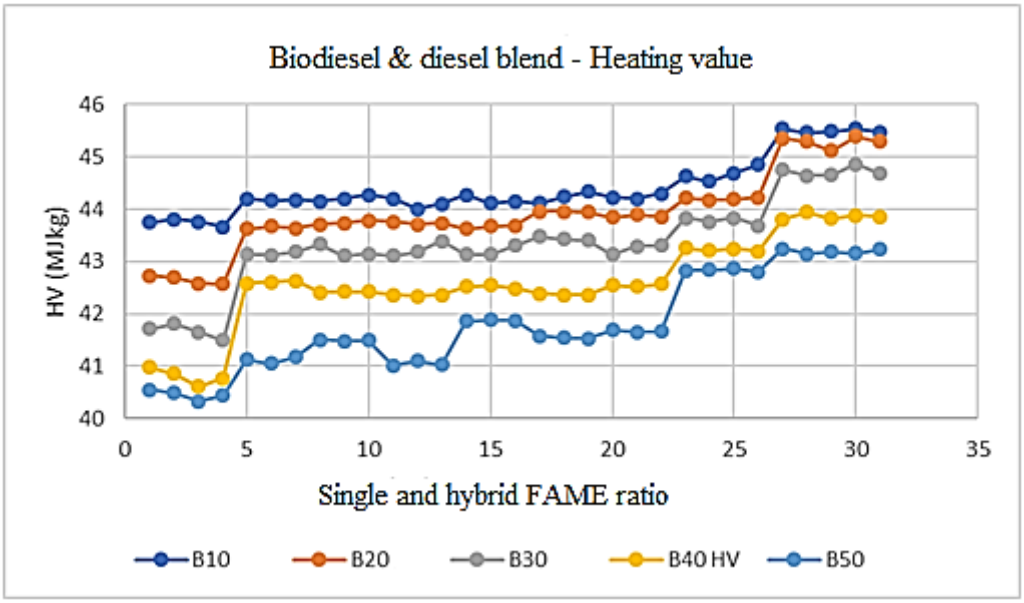

Figure 7.4: The effect of single and hybrid biodiesel blend with diesel on heating values

7.5 Conclusion

This chapter presents the physical and chemical properties of biodiesel produced from used sunflower (U100), linseed (L100), baobab (B100) and marula (M100) with their various hybrids fuel blend with petro-diesel (B10 – B50). These properties include densities, kinematic viscosities, cetane numbers and heating values. The analysis shows that blending of diesel fuel with biodiesel indicates improvement in the physical and thermal properties investigated. The result further indicated that diesel fuel blended with biodiesel up to B50 could be used in diesel engine without any modification. Blending of diesel with hybrid biodiesel fuel showed much improvement in fuel properties than the single biodiesel fuel blends. Thus, the result obtained in this study can be used as a template for any hybrid biodiesel blend(s) with diesel and also in the development of any biodiesel fuel engine system(s).

8 GENERAL CONCLUSION

Research exploration into the advanced biodiesel production from hybridized feedstock was successfully carried out in this study. The study shows that simple process synthesis of highly active heterogeneous catalysts from low cost, waste and renewable materials can offer a solution to the associated problem encountered in homogenous catalysts. Biomass waste resources such banana, pawpaw peels and eggshells are viable feedstock for effective bio-alkaline heterogeneous catalyst synthesis and they can be hybridized to achieve a synergetic function of the active properties present in them for effective transesterification process.

The prospect of biodiesel production from the underutilized oils of marula, baobab and *Trichilia emetica* was effective, indicating that they can be harnessed into the system as viable feedstock. The transesterification process conducted on the single and hybrid oils appears to be impartial to the number of hybrid ratios of the oils and their compositions. The percentage yields of biodiesel obtained using the local catalysts in the optimised transesterification protocol are quite satisfactory.

The two-pathway hybridization process (*in-situ* and *ex-situ* hybridization) was successfully analysed and evaluated. The process has actually given rise to new products with efficient qualities. The result showed that both processes are effective in biodiesel development. In terms of some improved properties such as viscosity, density, acid value, and cetane number, the *ex-situ* hybrids were found to be a bit improved than the *in-situ* hybrids. On the other hand, calorific values in *in-situ* hybrids shows a little improvement than the *ex-situ*.

The two-pathway hybridization process were viable approaches to be adopted for feedstock supplementation and optimization of fuel composition and properties. Application of ANN in predicting the thermal properties (CN and CV) of the biodiesel fuels was effective and recommendable. The result of this study showed that a three-layer feedforward neural network could be used to achieve a desirable mapping between the input and outputs of the problem to be solved. The statistical appraisal of the two hybridization pathways showed effective prediction of high values of R and R^2, and the low values of RMSE, SEP, MAE and AAD. This indicates that the derived ANN empirical model can adequately be used to define the input variables relationships for effective predictive of CN and CV.

Blending of biodiesel and petro-diesel shows good improvement on biodiesel properties. Blending of biodiesel up to B50 can result in the use of the blend in CI engines without requiring

any modification. Blending of diesel with hybrid biodiesel fuels showed much improvement in fuel properties than the single biodiesel fuel blends with diesel. The chemo-physical and thermal properties all fell within the ASTM, EN and SANS specification standards. This showed that all the biodiesel fuels produced are environmentally friendly and are suitable to power any CI engines for transportation, machineries or any other use.

In the general evaluation of the whole process, *in-situ* hybrids process seems to be more economical in terms of time and resources conservation than *ex-situ*. The study highlights the possible application of oil hybrids in biodiesel synthesis to ensure sustainability. The biodiesel obtained could be used as an alternative to petrol-diesel either directly or partly blended with diesel fuel without modification of the diesel engines. Therefore, following the protocols of this study, full adoption of biodiesel fuels into the global renewable energy infrastructure can no longer be overlooked as far as the persisting need of shifting from fossil fuel remain an imperative

9 RECOMMENDATIONS

Biodiesel developed from renewable and domestic sources holds a huge prospect in providing energy for transportation and other industrial purposes. However, limited feedstock appears the biggest challenge to reaching these goals. The fact that feedstock quality has significant effect on the biodiesel properties therefore requires that the biological structure of feedstock has critical roles to play in biodiesel development. Application of biosynthesis technology in increasing and improving feedstock for bioenergy production is a new and on-going process that need to be standardized at industrial levels. Several viable ways of developing oils feedstock for biodiesel production have been proposed via genetic and biochemical engineering technologies, including suggested approaches of producing oils from vegetative tissues instead of seeds. These aim towards achieving high-yielding energy crops with increase oils for suitable and sustainable biodiesel production. Based on this evolving technological approach, similar strategy was adopted in this study by means of feedstock hybridization, which enhance the engineering of the fatty acid profiles of oil to optimize biodiesel characteristics. Although, this was effectively evaluated using a two-pathway hybrid process in this study. However, other important areas need to be further investigated based on the findings of this study. This can also be recommended for the future studies following this protocol. These include:

i. The detailed investigation into the effect of fatty acid alteration of oils that constitute the hybrids, as well as prediction of the fuel properties based on fatty acid combinations.

ii. Investigation on environmental gaseous assessment of the hybrid feedstock biodiesel production.

iii. Elucidation on hybrid bio-alkaline catalysed reaction kinetics

iv. Exploration of more waste materials for heterogeneous catalyst production and bio-alcohol solvents should be encouraged to make biodiesel production a complete green process

v. Cost analysis of feedstock hybridization application in biodiesel process.

vi. Life cycle analysis of biodiesel production using hybrid biomass catalysis at scale up production facility.

Hybrid of other oil and waste materials should be further explored for more feedstock for biodiesel synthesis in order to meet the huge global demand.

10 REFERENCES

Acharya, N., Nanda, P., Panda, S., Acharya, S., 2017. Engineering Science and Technology , an International Journal Analysis of properties and estimation of optimum blending ratio of blended mahua biodiesel. Eng. Sci. Technol. an Int. J. 20, 511–517.

Adedayo, E., Oluwatumininu, O., Betiku, E., 2020. Cocoa pod husk-plantain peel blend as a novel green heterogeneous catalyst for renewable and sustainable honne oil biodiesel synthesis : A case of biowastes-to-wealth. Renew. Energy 166, 163–175.

Adinew, B., 2014. Biodiesel production from Trichilia emetica seeds using in-situ transesterification. Bulg. Chem. Commun. 46, 334–338.

Agarwal, A.K., Dhar, A., 2015. Biofuels and the hybrid fuel sector. Proc. Indian Natl. Sci. Acad. 81, 775–785.

Agarwal, A.K., Gupta, J.G., Dhar, A., 2017a. Potential and challenges for large-scale application of biodiesel in automotive sector. Prog. Energy Combust. Sci.

Agarwal, A.K., Gupta, J.G., Dhar, A., 2017b. Potential and challenges for large-scale application of biodiesel in automotive sector. Prog. Energy Combust. Sci. 61, 113–149.

Agarwal, M., Arya, I., Chaurasia, S.P., Singh, K., George, S., Arya, I., Chaurasia, S.P., Singh, K., George, S., Agarwal, M., Arya, I., Chaurasia, S.P., Singh, K., George, S., 2010. Synthesis and Characterisation of Biodiesel 4506.

Aghbashlo, M., Peng, W., Tabatabaei, M., Kalogirou, S.A., Soltanian, S., Hosseinzadeh-Bandbafha, H., Mahian, O., Lam, S.S., 2021. Machine learning technology in biodiesel research: A review. Prog. Energy Combust. Sci. 85, 100904.

Ahmad, T., Danish, M., Kale, P., Geremew, B., Adeloju, S.B., Nizami, M., Ayoub, M., 2019. Optimization of process variables for biodiesel production by transesterification of flaxseed oil and produced biodiesel characterizations. Renew. Energy 139, 1272–1280.

Al-Shanableh, F., Evcil, A., Savaş, M.A., 2016. Prediction of Cold Flow Properties of Biodiesel Fuel Using Artificial Neural Network. Procedia Comput. Sci. 102, 273–280.

Alam, F., Mobin, S., Chowdhury, H., 2015. Third generation biofuel from Algae. Procedia Eng. 105, 763–768.

Aleman-Ramirez, J.L., Moreira, J., Torres-Arellano, S., Longoria, A., Okoye, P.U., Sebastian, P.J., 2021. Preparation of a heterogeneous catalyst from moringa leaves as a sustainable precursor for biodiesel production. Fuel 284, 118983.

Almeida, V.F., García-Moreno, P.J., Guadix, A., Guadix, E.M., 2015. Biodiesel production from mixtures of waste fish oil, palm oil and waste frying oil: Optimization of fuel properties. Fuel Process. Technol. 133, 152–160.

Alptekin, E., Canakci, M., Necati, A., Turkcan, A., Sanli, H., 2015. Using waste animal fat based biodiesels – bioethanol – diesel fuel blends in a DI diesel engine. Fuel 157, 245–254.

Ambat, I., Srivastava, V., Sillanpää, M., 2018. Recent advancement in biodiesel production methodologies using various feedstock: A review. Renew. Sustain. Energy Rev. 90, 356–369.

Aminian, A., ZareNezhad, B., 2018. Accurate predicting the viscosity of biodiesels and blends using soft computing models. Renew. Energy 120, 488–500.

Ashraful, A.M., Masjuki, H.H., Kalam, M.A., Rizwanul Fattah, I.M., Imtenan, S., Shahir, S.A., Mobarak, H.M., 2014. Production and comparison of fuel properties, engine performance, and emission characteristics of biodiesel from various non-edible vegetable oils: A review. Energy Convers. Manag. 80, 202–228.

Atabani, A.E., Mofijur, M., Masjuki, H.H., Badruddin, I.A., Kalam, M.A., Chong, W.T., 2014. Effect of Croton megalocarpus, Calophyllum inophyllum, Moringa oleifera, palm and coconut biodiesel-diesel blending on their physico-chemical properties. Ind. Crops Prod. 60, 130–137.

Atabani, A.E., Silitonga, A.S., Ong, H.C., Mahlia, T.M.I., Masjuki, H.H., Badruddin, I.A., Fayaz, H., 2013. Non-edible vegetable oils : A critical evaluation of oil extraction, fatty acid compositions, biodiesel production, characteristics, engine performance and emissions production. Renew. Sustain. Energy Rev. 18, 211–245.

Atadashi, I.M., 2015. Purification of crude biodiesel using dry washing and membrane technologies. Alexandria Eng. J. 54, 1265–1272.

Atadashi, I.M., Aroua, M.K., Abdul Aziz, A.R., Sulaiman, N.M.N., 2011. Membrane biodiesel production and refining technology: A critical review. Renew. Sustain. Energy Rev. 15,

5051–5062. https://doi.org/10.1016/j.rser.2011.07.051

Atadashi, I.M., Aroua, M.K., Aziz, A.R.A., Sulaiman, N.M.N., 2013. The effects of catalysts in biodiesel production : A review. J. Ind. Eng. Chem. 19, 14–26.

Avhad, M.R., Marchetti, J.M., 2015. A review on recent advancement in catalytic materials for biodiesel production. Renew. Sustain. Energy Rev. 50, 696–718.

Baghban, A., Navid, M., Mohammadi, A.H., 2018. Improved estimation of Cetane number of fatty acid methyl esters (FAMEs) based biodiesels using TLBO-NN and PSO-NN models. Fuel 232, 620–631.

Balabin, R.M., Lomakina, E.I., Safieva, R.Z., 2011. Neural network (ANN) approach to biodiesel analysis: Analysis of biodiesel density, kinematic viscosity, methanol and water contents using near infrared (NIR) spectroscopy. Fuel 90, 2007–2015.

Balajii, M., Niju, S., 2020. Banana peduncle – A green and renewable heterogeneous base catalyst for biodiesel production from Ceiba pentandra oil. Renew. Energy 146, 2255–2269.

Balajii, M., Niju, S., 2019. A novel biobased heterogeneous catalyst derived from Musa acuminata peduncle for biodiesel production – Process optimization using central composite design. Energy Convers. Manag. 189, 118–131.

Balasubramanian, S., Allen, J.D., Kanitkar, A., Boldor, D., 2011. Oil extraction from Scenedesmus obliquus using a continuous microwave system - design, optimization, and quality characterization. Bioresour. Technol. 102, 3396–3403.

Barabas, I., Todoru, I.-A., 2012. Biodiesel Quality, Standards and Properties. Biodiesel- Qual. Emiss. By-Products.

Basumatary, S., Nath, B., Das, B., Kalita, P., Basumatary, B., 2021. Utilization of renewable and sustainable basic heterogeneous catalyst from Heteropanax fragrans (Kesseru) for effective synthesis of biodiesel from Jatropha curcas oil. Fuel 286, 119357.

Betiku, E., Akintunde, A.M., Ojumu, T.V., 2016a. Banana peels as a biobase catalyst for fatty acid methyl esters production using Napoleon's plume (Bauhinia monandra) seed oil: A process parameters optimization study. Energy 103, 797–806.

Betiku, E., Etim, A.O., Pereao, O., Ojumu, T.V., 2017. Two-Step Conversion of Neem (Azadirachta indica) Seed Oil into Fatty Methyl Esters Using a Heterogeneous Biomass-Based Catalyst: An Example of Cocoa Pod Husk. Energy & Fuels 31, 6182–6193.

Betiku, E., Ishola, N.B., 2020. Optimization of sorrel oil biodiesel production by base heterogeneous catalyst from kola nut pod husk : Neural intelligence-genetic algorithm versus neuro-fuzzy-genetic algorithm. Environ. Process Sustain. Energy.

Betiku, E., Odude, V.O., Ishola, N.B., Bamimore, A., Osunleke, A.S., Okeleye, A.A., 2016b. Predictive capability evaluation of RSM, ANFIS and ANN: A case of reduction of high free fatty acid of palm kernel oil via esterification process. Energy Convers. Manag. 124, 219–230.

Betiku, E., Okeleye, A.A., Ishola, N.B., Osunleke, A.S., Ojumu, T. V., 2019. Development of a Novel Mesoporous Biocatalyst Derived from Kola Nut Pod Husk for Conversion of Kariya Seed Oil to Methyl Esters: A Case of Synthesis, Modeling and Optimization Studies. Catal. Letters 149, 1772–1787.

Bhuiya, M.M.K., Rasul, M.G., Khan, M.M.K., Ashwath, N., Azad, A.K., Hazrat, M.A., 2014. Second generation biodiesel: Potential alternative to-edible oil-derived biodiesel. Energy Procedia 61, 1969–1972.

Birnin-Yauri, U., Garba, S., 2011. Comparative Studies on Some Physicochemical Properties of Baobab, Vegetable, Peanut and Palm Oils. Niger. J. Basic Appl. Sci. 19, 64–67.

Bokhari, A., Chuah, L.F., Yusup, S., Klemeš, J.J., Kamil, R.N.M., 2016. Optimisation on pretreatment of rubber seed (Hevea brasiliensis) oil via esterification reaction in a hydrodynamic cavitation reactor. Bioresour. Technol. 199, 414–422.

Bora, A.P., Dhawane, S.H., Anupam, K., Halder, G., 2018. Biodiesel synthesis from Mesua ferrea oil using waste shell derived carbon catalyst. Renew. Energy 121, 195–204.

Bora, P., Boro, J., Konwar, L.J., Deka, D., 2016. Formulation of microemulsion based hybrid biofuel from waste cooking oil - A comparative study with biodiesel. J. Energy Inst. 89, 560–568.

Caldeira, C., Freire, F., Olivetti, E.A., Kirchain, R., 2017. Fatty acid based prediction models for biodiesel properties incorporating compositional uncertainty. Fuel 196, 13–20.

Changmai, B., Sudarsanam, P., Rokhum, L., 2020. Biodiesel production using a renewable mesoporous solid catalyst. Ind. Crops Prod. 145, 111911.

Chattopadhyay, S., Sen, R., 2013. Fuel properties, Engine performance and environmental benefits of biodiesel produced by a green process. Appl. Energy 105, 319–326.

Chen, G.Y., Shan, R., Shi, J.F., Yan, B.B., 2015. Transesterification of palm oil to biodiesel using rice husk ash-based catalysts. Fuel Process. Technol. 133, 8–13.

Choedkiatsakul, I., Ngaosuwan, K., Assabumrungrat, S., Mantegna, S., Cravotto, G., 2015. Biodiesel production in a novel continuous flow microwave reactor. Renew. Energy 83, 25–29.

Chuah, L.F., Klemeš, J.J., Yusup, S., Bokhari, A., Akbar, M.M., Chong, Z.K., 2017. Kinetic studies on waste cooking oil into biodiesel via hydrodynamic cavitation. J. Clean. Prod. 146, 47–56.

Chuah, L.F., Yusup, S., Aziz, A.R.A., Klemeš, J.J., Bokhari, A., Abdullah, M.Z., 2016. Influence of fatty acids content in non-edible oil for biodiesel properties. Clean Technol. Environ. Policy 18, 473–482.

Chueluecha, N., Kaewchada, A., Jaree, A., 2017. Biodiesel synthesis using heterogeneous catalyst in a packed-microchannel. Energy Convers. Manag. 141, 145–154.

Corro, G., Sánchez, N., Pal, U., Bañuelos, F., 2016. Biodiesel production from waste frying oil using waste animal bone and solar heat. Waste Manag. 47, 105–113.

Corro, G., Sánchez, N., Pal, U., Cebada, S., Fierro, J.L.G., 2017. Solar-irradiation driven biodiesel production using Cr/SiO2 photocatalyst exploiting cooperative interaction between Cr6+ and Cr3+ moieties. Appl. Catal. B Environ. 203, 43–52.

Deh Kiani, M.K., Ghobadian, B., Tavakoli, T., Nikbakht, A.M., Najafi, G., 2009. Application of artificial neural networks for the prediction of performance and exhaust emissions in SI engine using ethanol- gasoline blends. Energy 35, 65–69.

Demirbas, A., 2007. Importance of biodiesel as transportation fuel. Energy Policy 35, 4661–4670.

Dharma, S., Masjuki, H.H., Ong, H.C., Sebayang, A.H., Silitonga, A.S., Kusumo, F., Mahlia,

T.M.I., 2016. Optimization of biodiesel production process for mixed Jatropha curcas-Ceiba pentandra biodiesel using response surface methodology. Energy Convers. Manag. 115, 178–190.

Dhawane, S.H., Karmakar, B., Ghosh, S., Halder, G., 2018. Parametric optimisation of biodiesel synthesis from waste cooking oil via Taguchi approach. J. Environ. Chem. Eng. 6, 3971–3980.

Dhawane, S.H., Kumar, T., Halder, G., 2016a. Parametric effects and optimization on synthesis of iron (II) doped carbonaceous catalyst for the production of biodiesel. Energy Convers. Manag. 122, 310–320.

Dhawane, S.H., Kumar, T., Halder, G., 2016b. Biodiesel synthesis from Hevea brasiliensis oil employing carbon supported heterogeneous catalyst: Optimization by Taguchi method. Renew. Energy 89, 506–514.

Domínguez-Sáez, A., Rattá, G.A., Barrios, C.C., 2018. Prediction of exhaust emission in transient conditions of a diesel engine fueled with animal fat using Artificial Neural Network and Symbolic Regression. Energy 149, 675–683.

Durrett, T.P., Benning, C., Ohlrogge, J., 2008. Plant triacylglycerols as feedstocks for the production of biofuels. Plant J. 54, 593–607.

Ehiri, R.C., Ikelle, I.I., Ozoaku, O.F., 2014. Acid-Catalyzed Transesterification Reaction of Beef Tallow For Biodiesel Production By Factor Variation. Am. J. Eng. Res. 19–20.

Ejilah, R., Lukman, A., Bello, A., 2012. Review of Sclerocarya birrea seed oil extracted as a bioenergy resource for compression ignition engines. Int. J. Agric Biol Eng 5, 1–9.

Elkelawy, M., Bastawissi, H.A.E., Esmaeil, K.K., Radwan, A.M., Panchal, H., Sadasivuni, K.K., Suresh, M., Israr, M., 2020. Maximization of biodiesel production from sunflower and soybean oils and prediction of diesel engine performance and emission characteristics through response surface methodology. Fuel 266, 117072.

Eloka-eboka, A.C., Inambao, F.L., 2016. Hybridization of feedstocks — A new approach in biodiesel development : A case of Moringa and Jatropha seed oils. Energy Resour. 38, 1495–1502.

Etim, A., Betiku, E., Ajala, S., Olaniyi, P., Ojumu, T., 2018. Potential of Ripe Plantain Fruit

Peels as an Ecofriendly Catalyst for Biodiesel Synthesis: Optimization by Artificial Neural Network Integrated with Genetic Algorithm. Sustainability 10, 707.

Etim, A.O., Eloka-Eboka, A.C., Musonge, P., 2021. Potential of Carica papaya peels as effective biocatalyst in the optimized parametric transesterification of used vegetable oil. Environ. Eng. Res. 26, 200–299.

Etim, Anietie Okon, Musonge, P., Eloka-eboka, A.C., 2021. Transesterification via Parametric Modelling and Optimization of Marula (Sclerocarya birrea) Seed Oil Methyl Ester Synthesis. J. Oleo Sci. 93, 77–93.

Etim, A.O., Musonge, P., Eloka-Eboka, A.C., 2021. An effective green and renewable from the fusion of bi-component transesterification of linseed oil methyl ester. Biofuels, Bioprod. Biorefining 1–12.

Etim, A.O., Musonge, P., Eloka-Eboka, A.C., 2020. Effectiveness of biogenic waste-derived heterogeneous catalysts and feedstock hybridization techniques in biodiesel production. Biofuels, Bioprod. Biorefining 14, 620–649.

Fadhil, A.B., Al-tikrity, E.T.B., Albadree, M.A., 2015. Transesterification of a novel feedstock , Cyprinus carpio fish oil : Influence of co-solvent and characterization of biodiesel. FUEL 162, 215–223.

Falowo, A.O., Betiku, E., 2022. A novel heterogeneous catalyst synthesis from agrowastes mixture and application in transesterification of yellow oleander-rubber oil : Optimization by Taguchi approach. Fuel 312, 122999.

Falowo, O.A., Ojumu, T. V., Pereao, O., Betiku, E., 2020. Sustainable biodiesel synthesis from honne-rubber-neem oil blend with a novel mesoporous base catalyst synthesized from a mixture of three agrowastes. Catalysts 10, 1–24.

Farooq, M., Ramli, A., Naeem, A., 2015. Biodiesel production from low FFA waste cooking oil using heterogeneous catalyst derived from chicken bones. Renew. Energy 76, 362–368.

Freire, L.M.S., Filho, J.R.C., Moura, C.V.R., Soledade, L.E.B., Stragevitch, L., Cordeiro, Â.M.T.M., Santos, I.M.G., Souza, A.G., 2012. Evaluation of the oxidative stability and flow properties of quaternary mixtures of vegetable oils for biodiesel production. Fuel 95, 126–130.

Gardy, J., Hassanpour, A., Lai, X., Ahmed, M.H., Rehan, M., 2017. Biodiesel production from used cooking oil using a novel surface functionalised TiO2 nano-catalyst. Appl. Catal. B Environ. 207, 297–310.

Ghanbari, M., Najafi, G., Ghobadian, B., Yusaf, T., Carlucci, A.P., Kiani Deh Kiani, M., 2017. Performance and emission characteristics of a CI engine using nano particles additives in biodiesel-diesel blends and modeling with GP approach. Fuel 202, 699–716.

Giakoumis, E.G., Sarakatsanis, C.K., 2018. Estimation of biodiesel cetane number, density, kinematic viscosity and heating values from its fatty acid weight composition. Fuel 222, 574–585.

Girdhar, J., Pandey, J.K., Rana, S., Rawat, D.S., 2017. Challenges and opportunities for the application of biofuel. Renew. Sustain. Energy Rev. 79, 850–866.

Giwa, S., Adekomaya, O., Nwaokocha, C., 2016. Potential hybrid feedstock for biodiesel production in the tropics. Front. Energy 10, 329–336.

Gohain, M., Devi, A., Deka, D., 2017. Musa balbisiana Colla peel as highly effective renewable heterogeneous base catalyst for biodiesel production. Ind. Crops Prod. 109, 8–18.

Gohain, M., Laskar, K., Paul, A.K., Daimary, N., Maharana, M., Goswami, I.K., Hazarika, A., Bora, U., Deka, D., 2020a. Carica papaya stem: A source of versatile heterogeneous catalyst for biodiesel production and C–C bond formation. Renew. Energy 147, 541–555.

Gohain, M., Laskar, K., Phukon, H., Bora, U., Kalita, D., Deka, D., 2020b. Towards sustainable biodiesel and chemical production: Multifunctional use of heterogeneous catalyst from littered Tectona grandis leaves. Waste Manag. 102, 212–221.

Gupta, A.R., Rathod, V.K., 2018. Waste cooking oil and waste chicken eggshells derived solid base catalyst for the biodiesel production: Optimization and kinetics. Waste Manag.

Gupta, J., Agarwal, M., Dalai, A.K., 2016. Optimization of biodiesel production from mixture of edible and nonedible vegetable oils. Biocatal. Agric. Biotechnol.

Habibullah, M., Masjuki, H.H., Kalam, M.A., Rizwanul Fattah, I.M., Ashraful, A.M., Mobarak, H.M., 2014. Biodiesel production and performance evaluation of coconut, palm and their combined blend with diesel in a single-cylinder diesel engine. Energy Convers. Manag. 87, 250–257.

Hamze, H., Akia, M., Yazdani, F., 2014. Optimization of biodiesel production from the waste cooking oil using response surface. Process Saf. Environ. Prot. 94, 1–10.

Hanis, S., Sayid, Y., Hanis, N., Hanapi, M., Azid, A., 2017. A review of biomass-derived heterogeneous catalyst for a sustainable biodiesel production. Renew. Sustain. Energy Rev. 70, 1040–1051.

Hariharan, N., Senthil, V., Krishnamoorthi, M., Karthic, S. V., 2020. Application of artificial neural network and response surface methodology for predicting and optimizing dual-fuel CI engine characteristics using hydrogen and bio fuel with water injection. Fuel 270, 117576.

Harsha Hebbar, H.R., Math, M.C., Yatish, K. V., 2018. Optimization and kinetic study of CaO nano-particles catalyzed biodiesel production from Bombax ceiba oil. Energy 143, 25–34.

Hegde, K., Chandra, N., Sarma, S.J., Brar, S.K., Veeranki, V.D., 2015. Genetic Engineering Strategies for Enhanced Biodiesel Production. Mol. Biotechnol. 57, 606–624.

Hoekman, S.K., Broch, A., Robbins, C., Ceniceros, E., Natarajan, M., 2012a. Review of biodiesel composition, properties, and specifications. Renew. Sustain. Energy Rev. 16, 143–169.

Hoekman, S.K., Broch, A., Robbins, C., Ceniceros, E., Natarajan, M., 2012b. Review of biodiesel composition, properties, and specifications. Renew. Sustain. Energy Rev. 16, 143–169.

Hosseinpour, S., Aghbashlo, M., Tabatabaei, M., Khalife, E., 2016. Exact estimation of biodiesel cetane number (CN) from its fatty acid methyl esters (FAMEs) profile using partial least square (PLS) adapted by artificial neural network (ANN). Energy Convers. Manag. 124, 389–398.

Imdadul, H.K., Masjuki, H.H., Kalam, M.A., Zulkifli, N.W.M., Alabdulkarem, A., Rashed, M.M., Ashraful, A.M., 2016. Influences of ignition improver additive on ternary (diesel-biodiesel-higher alcohol) blends thermal stability and diesel engine performance. Energy Convers. Manag. 123, 252–264.

Islam, M.A., Brown, R.J., Brooks, P.R., Jahirul, M.I., Bockhorn, H., Heimann, K., 2015. Investigation of the effects of the fatty acid profile on fuel properties using a multi-criteria decision analysis. Energy Convers. Manag. 98, 340–347.

Jahirul, M.I., Brown, R.J., Senadeera, W., O'Hara, I.M., Ristovski, Z.D., 2013. The use of artificial neural networks for identifying sustainable biodiesel feedstocks. Energies.

Jain, T., Singh, G., Dwivedi, G., Nandan, G., 2018. Study of emission parameter of biodiesel from non edible oil sources. Mater. Today Proc. 5, 3581–3586.

Jazie, A.A., Pramanik, H., Sinha, A.S.K., 2012. Egg Shell Waste-Catalyzed Transesterification of Mustard Oil : Optimization Using Response Surface Methodology (RSM) 56, 52–57.

Joshi, S., Gogate, P.R., Moreira, P.F., Giudici, R., 2017. Intensification of biodiesel production from soybean oil and waste cooking oil in the presence of heterogeneous catalyst using high speed homogenizer. Ultrason. Sonochem. 39, 645–653.

Joshi, S.M., Gogate, P.R., Suresh Kumar, S., 2018. Intensification of esterification of karanja oil for production of biodiesel using ultrasound assisted approach with optimization using response surface methodology. Chem. Eng. Process. - Process Intensif. 124, 186–198.

Karmakar, R., Kundu, K., Rajor, A., 2018. Fuel properties and emission characteristics of biodiesel produced from unused algae grown in India. Pet. Sci. 15, 385–395.

Knothe, G., 2014. A comprehensive evaluation of the cetane numbers of fatty acid methyl esters. FUEL 119, 6–13.

Knothe, G., Razon, L.F., 2017. Biodiesel fuels. Prog. Energy Combust. Sci. 58, 36–59.

Knothe, G., Sharp, C. a, Ryan, T.W., 2006. Exhaust Emissions of Biodiesel , Petrodiesel , Neat Methyl Esters , and Alkanes in a New Technology Engine Exhaust Emissions of Biodiesel , Petrodiesel , Neat Methyl Esters , and Alkanes in a New Technology Engine. Energy & Fuels 20, 403–408.

Kumar, R., Sureshkumar, K., Velraj, R., 2015. Optimization of biodiesel production from Manilkara zapota (L.) seed oil using Taguchi method. Fuel 140, 90–96.

Lapuerta, M., Rodríguez-Fernández, J., Agudelo, J.R., Boehman, A.L., 2013. Blending scenarios for soybean oil derived biofuels with conventional diesel. Biomass and Bioenergy 49, 74–85.

Lathiya, D.R., Bhatt, D. V, Maheria, K.C., 2018. Bioresource Technology Reports Synthesis of sulfonated carbon catalyst from waste orange peel for cost effective biodiesel production.

Bioresour. Technol. Reports 2, 69–76.

Ma, Y., Gao, Z., Wang, Q., Liu, Y., 2018. Biodiesels from microbial oils: Opportunity and challenges. Bioresour. Technol. 263, 631–641.

Mahmudul, H.M., Hagos, F.Y., Mamat, R., Adam, A.A., Ishak, W.F.W., Alenezi, R., 2017. Production, characterization and performance of biodiesel as an alternative fuel in diesel engines – A review. Renew. Sustain. Energy Rev. 72, 497–509.

Manaf, I.S.A., Embong, N.H., Khazaai, S.N.M., Rahim, M.H.A., Yusoff, M.M., Lee, K.T., Maniam, G.P., 2019a. A review for key challenges of the development of biodiesel industry. Energy Convers. Manag. 185, 508–517.

Manaf, I.S.A., Embong, N.H., Khazaai, S.N.M., Rahim, M.H.A., Yusoff, M.M., Lee, K.T., Maniam, G.P., 2019b. A review for key challenges of the development of biodiesel industry. Energy Convers. Manag. 185, 508–517.

Mansir, N., Teo, S.H., Rashid, U., Saiman, M.I., Tan, Y.P., Alsultan, G.A., Taufiq-Yap, Y.H., 2018a. Modified waste egg shell derived bifunctional catalyst for biodiesel production from high FFA waste cooking oil. A review. Renew. Sustain. Energy Rev.

Mansir, N., Teo, S.H., Rashid, U., Saiman, M.I., Tan, Y.P., Alsultan, G.A., Taufiq-Yap, Y.H., 2018b. Modified waste egg shell derived bifunctional catalyst for biodiesel production from high FFA waste cooking oil. A review. Renew. Sustain. Energy Rev. 82, 3645–3655.

Mardhiah, H.H., Ong, H.C., Masjuki, H.H., Lim, S., Lee, H. V., 2017. A review on latest developments and future prospects of heterogeneous catalyst in biodiesel production from non-edible oils. Renew. Sustain. Energy Rev. 67, 1225–1236.

Marwaha, A., Rosha, P., Mohapatra, S.K., Mahla, S.K., Dhir, A., 2018. Waste materials as potential catalysts for biodiesel production: Current state and future scope. Fuel Process. Technol.

Mendonça, I.M., Paes, O.A.R.L., Maia, P.J.S., Souza, M.P., Almeida, R.A., Silva, C.C., Duvoisin, S., de Freitas, F.A., 2019. New heterogeneous catalyst for biodiesel production from waste tucumã peels (Astrocaryum aculeatum Meyer): Parameters optimization study. Renew. Energy 130, 103–110.

Meng, X., Jia, M., Wang, T., 2014. Neural network prediction of biodiesel kinematic viscosity

at 313 K. Fuel 121, 133–140.

Milano, J., Ong, H.C., Masjuki, H.H., Silitonga, A.S., Chen, W.H., Kusumo, F., Dharma, S., Sebayang, A.H., 2018. Optimization of biodiesel production by microwave irradiation-assisted transesterification for waste cooking oil-Calophyllum inophyllum oil via response surface methodology. Energy Convers. Manag. 158, 400–415.

Mofijur, M., Masjuki, H.H., Kalam, M.A., Atabani, A.E., 2013. Evaluation of biodiesel blending, engine performance and emissions characteristics of Jatropha curcas methyl ester: Malaysian perspective. Energy 55, 879–887.

Mofijur, M., Masjuki, H.H., Kalam, M.A., Atabani, A.E., Fattah, I.M.R., Mobarak, H.M., 2014. Comparative evaluation of performance and emission characteristics of Moringa oleifera and Palm oil based biodiesel in a diesel engine. Ind. Crops Prod. 53, 78–84.

Mohadesi, M., Aghel, B., Khademi, M.H., Sahraei, S., 2017. Optimization of biodiesel production process in a continuous microchannel using response surface methodology. Korean J. Chem. Eng. 34, 1013–1020.

Mohammed, N.I., Kabbashi, N.A., Alade, A.O., Sulaiman, S., 2018. Advancement in the Utilization of Biomass-Derived Heterogeneous Catalysts in Biodiesel Production. Green Sustain. Chem. 08, 74–91.

Mohd Noor, C.W., Noor, M.M., Mamat, R., 2018. Biodiesel as alternative fuel for marine diesel engine applications: A review. Renew. Sustain. Energy Rev. 94, 127–142.

Mohod, A. V., Gogate, P.R., Viel, G., Firmino, P., Giudici, R., 2017. Intensification of biodiesel production using hydrodynamic cavitation based on high speed homogenizer. Chem. Eng. J. 316, 751–757.

Muhammad, C., Usman, Z., Agada, F., 2018. Biodiesel Production from Ceiba pentandra Seed Oil Using CaO Derived from Snail Shell as Catalyst. Pet. Sci. Eng. 2, 7–16.

Najafi, B., Fakhr, M.A., Jamali, S., 2011. Prediction of Heating Value of Vegetable Oil-Based Ethyl Esters Biodiesel Using Artificial Neural Network. Tarım Makinaları Bilim. Derg. 7, 361–366.

Nayebzadeh, H., Saghatoleslami, N., Tabasizadeh, M., 2016. Optimization of the activity of KOH/calcium aluminate nanocatalyst for biodiesel production using response surface

methodology. J. Taiwan Inst. Chem. Eng. 68, 379–386.

Nisar, J., Razaq, R., Farooq, M., Iqbal, M., Khan, R.A., Sayed, M., Shah, A., Rahman, I. ur, 2017. Enhanced biodiesel production from Jatropha oil using calcined waste animal bones as catalyst. Renew. Energy 101, 111–119.

Nizah, M.F.R., Taufiq-yap, Y.H., Rashid, U., Hwa, S., Nur, Z.A.S., 2014. Production of biodiesel from non-edible Jatropha curcas oil via transesterification using Bi2O3 – La2O3 catalyst. Energy Convers. Manag. 88, 1257–1262.

Nndwammbi, M., Ligavha-mbelengwa, M.H., Anokwuru, C.P., Ramaite, I.D.I., 2018. The effects of seasonal debarking on physical structure , polyphenolic content and antibacterial and antioxidant activities of Sclerocarya birrea in the Nylsvley nature reserve. South African J. Bot. 118, 138–143.

Noriega, M.A., Narváez, P.C., Habert, A.C., 2018. Simulation and validation of biodiesel production in Liquid-Liquid Film Reactors integrated with PES hollow fibers membranes. Fuel 227, 367–378.

Nyoka, B.I., Chanyenga, T., Mng, S.A., Akinnifesi, F.K., Sagona, W., 2015. Variation in growth and fruit yield of populations of Sclerocarya birrea (A . Rich .) Hochst . Agrofor. Syst. 397–407.

Odude, V.O., Adesina, A.J., Oyetunde, O.O., Adeyemi, O.O., Ishola, N.B., Etim, A.., Betiku, E., 2019. Application of Agricultural Waste-Based Catalysts to Transesterification of Esterified Palm Kernel Oil into Biodiesel : A Case of Banana Fruit Peel Versus Cocoa Pod Husk. Waste and Biomass Valorization 10, 877–888.

Ogbu, I.M., Ajiwe, V.I.E., Okoli, C.P., 2018. Performance Evaluation of Carbon-based Heterogeneous Acid Catalyst Derived From Hura crepitans Seed Pod for Esterification of High FFA Vegetable Oil. Bioenergy Res. 11, 772–783.

Okpalaeke, K.E., Ibrahim, T.H., Latinwo, L.M., Betiku, E., 2020. Mathematical Modeling and Optimization Studies by Arti fi cial Neural Network , Genetic Algorithm and Response Surface Methodology : A Case of Ferric Sulfate – Catalyzed Esteri fi cation of Neem (Azadirachta indica) Seed Oil 8, 1–14.

Oladipo, B., Ojumu, T. V, Latinwo, L.M., Betiku, E., 2020. Pawpaw (Carica papaya) Peel Waste as a Novel Green Heterogeneous Catalyst for Moringa Oil Methyl Esters Synthesis :

Process Optimization and 1–25.

Ozcanli, M., Gungor, C., Aydin, K., 2013. Biodiesel fuel specifications: A review. Energy Sources, Part A Recover. Util. Environ. Eff. 35, 635–647.

Papargyriou, D., Broumidis, E., de Vere-Tucker, M., Gavrielides, S., Hilditch, P., Irvine, J.T.S., Bonaccorso, A.D., 2019. Investigation of solid base catalysts for biodiesel production from fish oil. Renew. Energy 139, 661–669.

Pathak, G., Das, D., Rajkumari, K., Rokhum, L., 2018. Exploiting waste: Towards a sustainable production of biodiesel using: Musa acuminata peel ash as a heterogeneous catalyst. Green Chem. 20, 2365–2373.

Perdomo, F.A., Millán, B.M., Aragón, J.L., 2014. Predicting the physical-chemical properties of biodiesel fuels assessing the molecular structure with the SAFT-γ group contribution approach. Energy 72, 274–290.

Rafati, A., Tahvildari, K., Nozari, M., 2019. Production of biodiesel by electrolysis method from waste cooking oil using heterogeneous MgO-NaOH nano catalyst. Energy Sources, Part A Recover. Util. Environ. Eff. 41, 1062–1074.

Rahman, W.U., Fatima, A., Anwer, A.H., Athar, M., Khan, M.Z., Khan, N.A., Halder, G., 2019. Biodiesel synthesis from eucalyptus oil by utilizing waste egg shell derived calcium based metal oxide catalyst. Process Saf. Environ. Prot. 122, 313–319.

Rajkumari, K., Rokhum, L., 2020. A sustainable protocol for production of biodiesel by transesterification of soybean oil using banana trunk ash as a heterogeneous catalyst. Biomass Convers. Biorefinery.

Ramos, M.J., Fernández, C.M., Casas, A., Rodríguez, L., Pérez, Á., 2009. Bioresource Technology Influence of fatty acid composition of raw materials on biodiesel properties 100, 261–268.

Rashid, U., Anwar, F., 2008. Production of biodiesel through base-catalyzed transesterification of safflower oil using an optimized protocol. Energy and Fuels 22, 1306–1312.

Risso, R., Ferraz, P., Meireles, S., Fonseca, I., Vital, J., 2018. Highly active Cao catalysts from waste shells of egg, oyster and clam for biodiesel production. Appl. Catal. A Gen. 567, 56–64.

Rocabruno-Valdés, C.I., Ramírez-Verduzco, L.F., Hernández, J.A., 2015. Artificial neural network models to predict density, dynamic viscosity, and cetane number of biodiesel. Fuel 147, 9–17.

Şahin, S., Öğüt, H., 2018. Investigation of the Effects of Linseed Oil Biodiesel and Diesel Fuel Blends on Engine Performance and Exhaust Emissions. Int. J. Automot. Eng. Technol. 7, 149–157.

Salinas, D., Sepúlveda, C., Escalona, N., GFierro, J.L., Pecchi, G., 2018. Sol–gel La2O3–ZrO2 mixed oxide catalysts for biodiesel production. J. Energy Chem. 27, 565–572.

Sanli, H., Canakci, M., Alptekin, E., Turkcan, A., Ozsezen, A.N., 2015. Effects of waste frying oil based methyl and ethyl ester biodiesel fuels on the performance , combustion and emission characteristics of a DI diesel engine. Fuel 159, 179–187.

Santacesaria, E., Vicente, G.M., Di Serio, M., Tesser, R., 2012. Main technologies in biodiesel production: State of the art and future challenges. Catal. Today 195, 2–13.

Saxena, P., Jawale, S., Joshipura, M.H., 2013. A review on prediction of properties of biodiesel and blends of biodiesel. Procedia Eng. 51, 395–402.

Selvan, T., Nagarajan, G., 2013. Combustion and emission characteristics of a diesel engine fuelled with biodiesel having varying saturated fatty acid composition. Int. J. Green Energy 10, 952–965.

Selvaraj, R., Moorthy, I.G., Kumar, R.V., Sivasubramanian, V., 2019. Microwave mediated production of FAME from waste cooking oil: Modelling and optimization of process parameters by RSM and ANN approach. Fuel 237, 40–49.

Serqueira, D.S., Fernandes, D.M., Cunha, R.R., Squissato, A.L., Santos, D.Q., Richter, E.M., Munoz, R.A.A., 2014. Influence of blending soybean, sunflower, colza, corn, cottonseed, and residual cooking oil methyl biodiesels on the oxidation stability. Fuel 118, 16–20.

Shahir, V.K., Jawahar, C.P., Suresh, P.R., Vinod, V., 2017. Experimental Investigation on Performance and Emission Characteristics of a Common Rail Direct Injection Engine Using Animal Fat Biodiesel Blends. Energy Procedia 117, 283–290.

Sharma, A., Kodgire, P., Kachhwaha, S.S., 2020. Investigation of ultrasound-assisted KOH and CaO catalyzed transesterification for biodiesel production from waste cotton-seed cooking

oil: Process optimization and conversion rate evaluation. J. Clean. Prod. 259.

Silitonga, A.S., Shamsuddin, A.H., Mahlia, T.M.I., Milano, J., Kusumo, F., Siswantoro, J., Dharma, S., Sebayang, A.H., Masjuki, H.H., Ong, H.C., 2020. Biodiesel synthesis from Ceiba pentandra oil by microwave irradiation-assisted transesterification: ELM modeling and optimization. Renew. Energy 146, 1278–1291.

Singh, D., Sharma, D., Soni, S.L., Sharma, S., Kumari, D., 2019. Chemical compositions, properties, and standards for different generation biodiesels: A review. Fuel 253, 60–71.

Singh, R., Liu, H., Shanklin, J., Singh, V., 2021. Hydrothermal pretreatment for valorization of genetically engineered bioenergy crop for lipid and cellulosic sugar recovery. Bioresour. Technol. 341, 125817.

Stamenković, O.S., Rajković, K., Veličković, A. V., Milić, P.S., Veljković, V.B., 2013. Optimization of base-catalyzed ethanolysis of sunflower oil by regression and artificial neural network models. Fuel Process. Technol. 114, 101–108.

Sundus, F., Fazal, M.A., Masjuki, H.H., 2017. Tribology with biodiesel: A study on enhancing biodiesel stability and its fuel properties. Renew. Sustain. Energy Rev. 70, 399–412.

Syazwani, O.N., Rashid, U., Mastuli, M.S., Taufiq-Yap, Y.H., 2019. Esterification of palm fatty acid distillate (PFAD) to biodiesel using Bi-functional catalyst synthesized from waste angel wing shell (Cyrtopleura costata). Renew. Energy 131, 187–196.

Tabatabaei, M., Aghbashlo, M., Dehhaghi, M., Panahi, H.K.S., Mollahosseini, A., Hosseini, M., Soufiyan, M.M., 2019. Reactor technologies for biodiesel production and processing: A review. Prog. Energy Combust. Sci.

Tan, Y.H., Abdullah, M.O., Kansedo, J., Mubarak, N.M., Chan, Y.S., Nolasco-Hipolito, C., 2019a. Biodiesel production from used cooking oil using green solid catalyst derived from calcined fusion waste chicken and fish bones. Renew. Energy 139, 696–706.

Tan, Y.H., Abdullah, M.O., Kansedo, J., Mubarak, N.M., Chan, Y.S., Nolasco-Hipolito, C., 2019b. Biodiesel production from used cooking oil using green solid catalyst derived from calcined fusion waste chicken and fish bones. Renew. Energy 139, 696–706.

Tanawannapong, Y., Kaewchada, A., Jaree, A., 2013. Biodiesel production from waste cooking oil in a microtube reactor. J. Ind. Eng. Chem. 19, 37–41.

Thoai, D.N., Tongurai, C., Prasertsit, K., Kumar, A., 2019. Review on biodiesel production by two-step catalytic conversion. Biocatal. Agric. Biotechnol. 18, 101023.

Tin, G., Nee, S., Tat, K., Teong, K., Rahman, A., 2015. Optimization and kinetic studies of sea mango (Cerbera odollam) oil for biodiesel production via supercritical reaction. Energy Convers. Manag. 99, 242–251.

Tosun, E., Aydin, K., Bilgili, M., 2016. Comparison of linear regression and artificial neural network model of a diesel engine fueled with biodiesel-alcohol mixtures. Alexandria Eng. J.

Tran, T.T.V., Kaiprommarat, S., Kongparakul, S., Reubroycharoen, P., Guan, G., Nguyen, M.H., Samart, C., 2016. Green biodiesel production from waste cooking oil using an environmentally benign acid catalyst. Waste Manag. 52, 367–374.

Tshizanga, N., Aransiola, E.F., Oyekola, O., 2017. Optimisation of biodiesel production from waste vegetable oil and eggshell ash. South African J. Chem. Eng. 23, 145–156.

Ullah, Z., Khan, A.S., Muhammad, N., Ullah, R., Alqahtani, A.S., Shah, S.N., Ghanem, O. Ben, Bustam, M.A., Man, Z., 2018. A review on ionic liquids as perspective catalysts in transesterification of different feedstock oil into biodiesel. J. Mol. Liq. 266, 673–686.

Vargas, E.M., Neves, M.C., Tarelho, L.A.C., Nunes, M.I., 2019. Solid catalysts obtained from wastes for FAME production using mixtures of refined palm oil and waste cooking oils. Renew. Energy 136, 873–883.

Veljković, V.B., Banković-Ilić, I.B., Stamenković, O.S., 2015. Purification of crude biodiesel obtained by heterogeneously-catalyzed transesterification. Renew. Sustain. Energy Rev. 49, 500–516.

Verma, P., Sharma, M.P., 2016. Review of process parameters for biodiesel production from different feedstocks. Renew. Sustain. Energy Rev. 62, 1063–1071.

Verma, P., Sharma, M.P., Dwivedi, G., 2016. Impact of alcohol on biodiesel production and properties 56, 319–333.

Vermaak, I., Kamatou, G.P.P., Komane-Mofokeng, B., Viljoen, A.M., Beckett, K., 2011. African seed oils of commercial importance - Cosmetic applications. South African J. Bot. 77, 920–933.

Wei, L., Cheung, C.S., Ning, Z., 2018. Effects of biodiesel-ethanol and biodiesel-butanol blends on the combustion, performance and emissions of a diesel engine. Energy 155, 957–970.

Wen, Z., Yu, X., Tu, S.T., Yan, J., Dahlquist, E., 2009. Intensification of biodiesel synthesis using zigzag micro-channel reactors. Bioresour. Technol. 100, 3054–3060.

Wong, Y.C., Tan, Y.P., Taufiq-Yap, Y.H., Ramli, I., Tee, H.S., 2015. Biodiesel production via transesterification of palm oil by using CaO-CeO2 mixed oxide catalysts. Fuel 162, 288–293.

Yadav, A.K., Khan, M.E., Pal, A., Dubey, A.M., 2016. Biodiesel production from Nerium oleander (Thevetia peruviana) oil through conventional and ultrasonic irradiation methods. Energy Sources, Part A Recover. Util. Environ. Eff. 38, 3447–3452.

Yesilyurt, M.K., Cesur, C., Aslan, V., Yilbasi, Z., 2020. The production of biodiesel from safflower (Carthamus tinctorius L.) oil as a potential feedstock and its usage in compression ignition engine: A comprehensive review. Renew. Sustain. Energy Rev. 119, 109574.

Yusuff, A.S., Adeniyi, O.D., Olutoye, M.A., Akpan, U.G., 2017. A Review on Application of Heterogeneous Catalyst in the Production of Biodiesel from Vegetable Oils. J. Appl. Sci. Process Eng. 4, 142–157.

Yusup, S., Bokhari, A., Chuah, L.F., Akbar, M.M., 2017. Influence of fatty acids in waste cooking oil for cleaner biodiesel. Clean Techn Env. Policy 859–868.

Zamberi, M.M., Ani, F.N., Fadzli, M., Abdollah, B., 2016. Heterogeneous transesterification of heterogeneous transesterification of rubber seed oil biodiesel production. J. Teknol. 8–14.

APPENDICES

Appendix A

Table 1.1: In-situ hybrid FAME properties with ANN predicted values

Single & Hybrid FAME	Den	Vis	AV	SV	IV	CN Actual	CN Pred.	HV Actual	HV Pred.
U100	0.887	4.18	0.47	175.31	100.05	54.81	54.88	38.50	38.63
T100	0.886	4.13	0.48	178.12	90.10	56.67	56.66	40.12	40.39
L100	0.889	3.67	0.46	178.12	96.27	55.28	55.35	39.80	39.92
M100	0.872	3.08	0.44	175.31	88.35	57.55	57.22	40.00	40.52
B100	0.875	3.51	0.38	178.12	89.78	56.74	56.72	40.05	40.25
U50:L50	0.876	4.57	0.45	178.12	70.56	61.06	60.41	40.38	40.40
U70:L30	0.873	3.56	0.42	175.31	74.58	60.65	61.24	40.36	39.22
U30:L70	0.873	3.02	0.38	172.51	77.34	60.54	60.44	40.52	40.15
U50:M50	0.875	3.07	0.35	172.51	76.64	60.69	61.55	40.51	40.21
U30:M70	0.872	2.87	0.40	176.72	70.00	61.47	61.89	40.23	40.24
U70:M30	0.877	3.24	0.36	173.91	72.65	59.09	59.16	40.39	40.27
U50:B50	0.870	3.22	0.38	172.51	75.86	60.79	60.86	40.50	40.24
U30:B70	0.874	3.06	0.42	173.91	74.00	61.03	61.18	40.41	40.28
U70:B30	0.870	3.37	0.43	172.51	76.12	60.81	60.32	40.50	40.24
L50:B50	0.860	3.29	0.36	173.04	74.83	61.00	61.27	40.46	40.32
L30:B70	0.861	3.01	0.40	176.72	75.17	60.27	60.75	40.31	40.22
L70: B30	0.868	2.77	0.38	175.31	73.61	60.87	60.44	40.35	40.39
M50:B50	0.871	2.95	0.45	173.91	83.20	58.96	58.59	40.55	40.24
M30: B70	0.870	2.70	0.42	174.00	80.05	59.65	60.14	40.50	40.23
M70: B30	0.879	2.87	0.40	175.31	84.62	58.39	58.52	40.51	40.46
L50:M50	0.864	3.69	0.42	175.31	79.27	60.59	60.32	40.43	40.22
L30: M70	0.869	3.01	0.41	173.91	77.43	60.26	60.57	40.46	40.17
L70: M30	0.879	2.78	0.39	173.91	75.75	60.64	60.83	40.44	40.27
U60: L20: M20	0.867	3.11	0.36	176.72	64.76	61.61	61.57	40.96	40.87
L60: M20: B20	0.865	2.73	0.34	175.31	68.01	62.13	62.45	41.26	41.22
M60: B20:U20	0.862	2.39	0.31	172.51	65.56	63.19	63.20	41.34	41.27
B60: U20: L20	0.868	3.50	0.35	175.31	66.31	62.54	62.36	41.24	41.36
U25: B25:L25: M25	0.859	3.11	0.28	172.51	57.49	65.00	65.23	42.82	42.49
U40: L20: M20: B20	0.858	3.18	0.31	173.91	56.73	64.90	65.03	42.89	42.45
L40: U20: M20: B20	0.865	3.29	0.23	175.31	60.20	63.88	63.92	42.70	42.62
M40: L20: U20: B20	0.859	3.21	0.26	173.91	59.54	64.82	64.50	42.82	42.34
B40: L20: M20: U20	0.856	2.95	0.27	176.72	55.00	64.81	65.01	42.25	42.27

Table 1.2: Ex-situ hybrid FAME properties with ANN predicted values

Single & Hybrid FAME	Den	Vis	AV	SV	IV	CN Actual	CN Pred.	HV Actual	HV Pred.
U100	0.886	4.48	0.47	175.31	100.0	54.81	54.88	38.50	38.65
T100	0.887	4.13	0.48	178.12	90.10	56.67	56.66	40.72	40.66
L100	0.889	3.67	0.46	178.12	96.27	55.28	55.35	39.80	39.61
M100	0.872	3.08	0.44	175.31	88.35	57.55	56.22	40.42	40.34
B100	0.875	3.51	0.38	178.12	89.78	56.74	56.72	40.05	40.13
U50:L50	0.883	3.01	0.40	179.52	68.52	61.28	59.41	41.98	42.09
U70:L30	0.878	2.74	0.41	179.52	73.50	61.17	61.24	42.22	42.93
U30:L70	0.875	2.56	0.37	185.13	66.00	60.93	61.04	42.01	41.87
U50:M50	0.867	3.07	0.34	178.12	69.25	61.36	61.55	41.11	41.24
U30:M70	0.865	2.72	0.40	178.12	68.16	61.60	61.89	41.16	41.28
U70:M30	0.867	3.01	0.38	176.72	72.00	60.98	61.66	40.26	40.29
U50:B50	0.878	2.92	0.43	184.80	65.00	61.21	61.36	41.22	42.39
U30:B70	0.866	2.85	0.34	176.72	69.00	61.66	61.68	41.97	42.06
U70:B30	0.878	2.83	0.35	178.12	70.02	61.18	61.32	41.89	42.92
L50:B50	0.876	2.65	0.33	182.33	67.11	61.14	61.27	41.60	42.66
L30:B70	0.867	2.91	0.41	175.31	70.15	61.64	61.75	41.00	41.22
L70: B30	0.869	2.69	0.40	183.00	67.20	61.00	61.44	41.68	42.66
M50:B50	0.867	2.65	0.33	182.33	70.10	60.46	60.59	41.69	42.53
M30: B70	0.865	2.50	0.37	177.60	72.08	61.81	61.74	40.77	40.87
M70: B30	0.850	2.41	0.39	179.52	70.90	60.75	61.52	41.60	41.67
L50:M50	0.858	3.09	0.35	183.73	70.50	60.14	60.30	41.92	41.96
L30: M70	0.862	2.51	0.34	179.52	70.75	60.78	61.07	42.65	42.63
L70: M30	0.869	2.49	0.30	178.12	71.05	60.96	61.33	42.80	42.74
U60: L20: M20	0.874	2.61	0.32	183.73	60.23	62.45	62.57	42.44	42.59
L60: M20: B20	0.872	2.23	0.29	182.33	62.10	62.26	62.45	41.31	42.57
M60: B20:U20	0.867	2.92	0.31	182.33	57.80	63.23	63.20	42.55	42.64
B60: U20: L20	0.876	2.98	0.30	183.73	59.20	62.68	62.36	41.49	41.55
U25: B25:L25: M25	0.873	2.52	0.25	183.73	48.00	65.20	63.63	42.63	42.62
U40: L20: M20: B20	0.876	3.09	0.24	180.92	50.30	65.15	65.03	42.77	42.1
L40: U20: M20: B20	0.879	2.86	0.22	175.31	60.10	63.91	63.92	42.98	42.72
M40: L20: U20: B20	0.878	2.92	0.20	182.33	52.20	64.49	64.50	42.58	42.65
B40: L20: M20: U20	0.876	2.87	0.21	184.12	48.50	65.03	65.01	42.57	42.67

Appendix B

All the properties of biodiesel fuels blend discussed in chapter 7

B10

Single & Hybrid FAME	DEN	VIS	AV	SV	IV	CN	HV
U100	836.5	2.14	0.181	168.3	80.58	52.82	43.65
T100	833.1	1.98	0.18	168.3	84.071	52.97	43.5
L100	838.2	1.92	0.175	168.3	96.127	52.16	43.1
M100	834.7	1.91	0.181	173.51	96.762	52.99	43.6
B100	832.4	1.96	0.167	166.89	96.762	52.84	43.96
U50:L50	836.5	2.33	0.124	168.3	91.34	53.17	44.2
U70:L30	834.8	2.03	0.165	169.7	92.954	53.41	44.16
U30:L70	837.5	1.95	0.139	166.89	91.369	55.05	44.18
U50:M50	836.2	1.92	0.153	166.89	93.589	53.09	44.15
U30:M70	835.6	1.95	0.181	168.3	95.809	53.21	44.2
U70:M30	832.5	1.92	0.167	169.7	90.099	53.81	44.28
U50:B50	835.1	1.85	0.11	168.3	95.809	53.64	44.2
U30:B70	834.4	1.91	0.166	169.7	96.762	53.86	44.8
U70:B30	834.6	1.94	0.182	168.3	96.127	52.81	44.1
L50:B50	835.3	1.88	0.112	169.7	90.099	53.96	44.28
L30:B70	835.5	1.91	0.124	168.3	93.589	53.93	44.11
L70: B30	836	2.14	0.153	172.51	94.309	53.38	44.15
M50:B50	833.8	1.99	0.124	168.3	93.589	53.04	44.11
M30: B70	834.1	2.11	0.197	168.3	90.416	53.65	44.24
M70: B30	833.6	2.17	0.166	169.7	88.513	53.49	44.34
L50:M50	837.2	1.87	0.181	168.3	90.734	53.95	44.23
L30: M70	835.8	2.01	0.167	168.3	91.485	53.48	44.2
L70: M30	836.6	2.12	0.152	169.7	91.039	53.73	44.83
U60: L20: M20	836.6	1.99	0.181	164.7	89.465	54.06	45.63
L60: M20: B20	837.6	1.96	0.124	169.7	88.83	54.17	45.53
M60: B20:U20	834.6	2.02	0.146	165.49	88.196	54.08	45.49
B60: U20: L20	835.9	1.92	0.11	168.3	87.727	54.16	45.35
U25: B25:L25: M25	836.2	1.86	0.125	166.89	85.023	54.34	46.44
U40: L20: M20: B20	836.5	1.83	0.181	168.3	87.56	54.7	46.36
L40: U20: M20: B20	836.7	2.29	0.138	168.3	84.389	54.62	46.49
M40: L20: U20: B20	835.5	2.03	0.181	168.3	85.958	54.67	46.43
B40: L20: M20: U20	835.3	1.96	0.167	168.3	87.244	54.48	46.37

B20

Single & Hybrid FAME	DEN	VIS	AV	SV	IV	CN	HV
U100	842.3	2.21	0.21	169	95.17	53.29	42.73
T100	837.6	2.24	0.21	169.91	98.94	53.77	42.62
L100	843.2	1.95	0.2	169	106.44	53.62	42.29
M100	841.7	2.13	0.24	171.61	99.39	53.77	42.48
B100	842.4	2.1	0.24	167.59	100.57	53.54	42.07
U50:L50	846.5	2.54	0.183	169	95.37	54.2	43.63
U70:L30	834.8	2.31	0.19	170.41	96.13	54.63	43.48
U30:L70	837.5	2.24	0.18	169.5	96.39	54.22	43.43
U50:M50	836.2	2.11	0.22	168.29	98.69	54.51	43.11
U30:M70	835.6	2.14	0.24	169.71	97.84	54.47	43.14
U70:M30	832.5	2.16	0.23	170.41	96.36	54.46	43.18
U50:B50	835.1	2.01	0.17	169	102.15	54.94	43.03
U30:B70	834.4	2.04	0.18	171.81	101.68	54.27	43.91
U70:B30	834.6	2.02	0.24	169.71	97.72	54.33	43.94
L50:B50	835.3	1.95	0.16	169.7	97.39	54.91	43.93
L30:B70	835.5	2.07	0.17	169	98.82	54.96	43.98
L70: B30	836	2.19	0.18	171.11	98.46	54.33	43.89
M50:B50	833.8	2.06	0.18	169	97.23	54.49	43.96
M30: B70	834.1	2.12	0.24	169.71	95.02	54.07	43.89
M70: B30	833.6	2.28	0.2	169.7	98.82	54.18	43.95
L50:M50	837.2	2.1	0.24	169	96.76	54.64	43.95
L30: M70	835.8	2.11	0.19	169.71	95.23	54.83	43.9
L70: M30	836.6	2.2	0.17	170.95	95.96	54.18	43.86
U60: L20: M20	836.6	2.21	0.21	167.91	96.33	55.76	43.89
L60: M20: B20	837.6	2.05	0.15	183.2	97.39	55.89	44.68
M60: B20:U20	834.6	2.21	0.19	166.89	94.03	55.55	44.59
B60: U20: L20	835.9	2.12	0.18	169	94.62	55.13	44.82
U25: B25:L25: M25	836.2	2.1	0.17	167.59	96.44	56.89	45.85
U40: L20: M20: B20	836.5	2.15	0.21	167.59	95.49	56.18	45.79
L40: U20: M20: B20	836.7	2.36	0.15	169	94.86	56.17	45.92
M40: L20: U20: B20	835.5	2.16	0.24	169	92.47	56.73	45.89
B40: L20: M20: U20	835.3	2.18	0.21	169.71	95.97	56.33	45.69

B30

Single & Hybrid FAME	DEN	VIS	AV	SV	IV	CN	HV
U100	846.9	2.29	0.28	169.7	109.76	54.76	41.12
T100	842.2	2.42	0.25	171.51	95.81	54.57	41.83
L100	849.5	2.04	0.25	169.7	116.75	54.19	41.22
M100	845.1	2.28	0.29	169.7	101.84	54.54	41.00
B100	849.8	2.26	0.28	168.3	104.38	54.24	41.49
U50:L50	849.9	2.7	0.22	169.7	98.73	55.25	42.54
U70:L30	837.4	2.57	0.23	171.11	99.31	55.23	42.52
U30:L70	844.6	2.51	0.27	172.11	101.42	55.19	42.29
U50:M50	845.2	2.55	0.25	169.7	103.79	55.11	42.33
U30:M70	842.7	2.64	0.28	171.11	99.87	55.13	42.41
U70:M30	843.8	2.75	0.26	171.11	102.61	55.15	42.65
U50:B50	840.7	2.47	0.23	169.7	108.49	55.45	42.51
U30:B70	837.4	2.42	0.24	173.91	106.59	55.6	42.49
U70:B30	840.5	2.34	0.29	171.11	99.31	55.55	42.69
L50:B50	840.5	2.12	0.22	169.7	104.69	55.61	42.54
L30:B70	838.6	2.56	0.23	169.7	104.06	55.45	42.03
L70: B30	841.8	2.32	0.25	169.7	102.61	55.37	42.01
M50:B50	837.8	2.26	0.22	169.7	100.88	55.76	42.08
M30: B70	838.3	2.16	0.27	171.11	99.62	55.78	42.13
M70: B30	840.1	2.67	0.25	169.7	109.13	55.61	42.11
L50:M50	841.8	2.54	0.29	169.7	102.79	55.53	42.01
L30: M70	841.4	2.35	0.27	171.11	98.98	55.73	42.59
L70: M30	842.2	2.43	0.24	172.51	100.89	55.64	42.61
U60: L20: M20	843.4	2.73	0.25	171.11	103.2	56.88	43.63
L60: M20: B20	843.4	2.39	0.23	167.7	105.96	56.62	43.56
M60: B20:U20	839.1	2.7	0.29	168.3	99.87	56.56	43.43
B60: U20: L20	839.6	2.65	0.25	169.7	101.52	56.62	43.69
U25: B25:L25: M25	843.8	2.54	0.28	168.3	107.87	57.46	44.15
U40: L20: M20: B20	844.3	2.71	0.24	166.89	103.42	57.73	44.14
L40: U20: M20: B20	845.5	2.59	0.26	169.7	105.33	57.76	44.55
M40: L20: U20: B20	838.6	2.53	0.28	169.7	98.98	57.92	44.36
B40: L20: M20: U20	839.2	2.62	0.29	171.11	104.69	57.64	44.38

B40

Single & Hybrid FAME	DEN	VIS	AV	SV	IV	CN	HV
U100	854.6	2.45	0.34	171.46	105.97	55.18	40.98
T100	848.5	2.95	0.36	172.36	98.66	55.18	40.84
L100	854.3	2.19	0.33	171.61	117.70	55.65	40.26
M100	851.8	2.51	0.35	170.41	104.70	55.76	40.21
B100	855.2	2.45	0.32	170.91	109.77	55.24	40.17
U50:L50	858.1	3.19	0.37	171.51	106.31	56.21	41.59
U70:L30	847.6	3.26	0.35	172.51	108.03	56.67	41.58
U30:L70	847.5	3.18	0.32	172.31	105.59	56.81	41.60
U50:M50	848.5	3.23	0.33	171.11	107.09	56.53	41.11
U30:M70	847.6	3.32	0.31	171.11	105.45	56.45	41.10
U70:M30	848.5	3.44	0.31	171.81	109.36	56.65	41.13
U50:B50	846.7	3.12	0.32	171.81	111.67	56.61	41.06
U30:B70	845.2	3.06	0.34	172.51	109.61	56.19	41.00
U70:B30	846.4	2.96	0.35	171.81	105.49	56.47	41.57
L50:B50	844.6	2.67	0.35	173.91	110.08	56.55	41.53
L30:B70	843.5	3.25	0.34	174.61	109.29	56.36	41.55
L70: B30	847.2	2.92	0.36	172.51	109.36	56.15	41.49
M50:B50	845.6	2.86	0.34	171.11	105.33	56.17	41.39
M30: B70	843.4	2.71	0.36	171.11	102.79	56.38	41.36
M70: B30	847.5	3.42	0.33	173.21	109.45	56.23	41.47
L50:M50	845.4	3.27	0.34	171.1	109.13	56.62	41.55
L30: M70	846.7	3.03	0.34	173.21	106.59	56.63	41.53
L70: M30	847.5	3.23	0.32	173.21	109.45	56.64	41.57
U60: L20: M20	845.4	3.47	0.36	173.92	110.77	57.13	42.66
L60: M20: B20	848.2	3.01	0.31	171.11	112.47	57.18	42.61
M60: B20:U20	846.1	3.44	0.34	171.81	104.5	57.34	42.45
B60: U20: L20	843.8	3.36	0.32	172.51	105.8	57.31	42.40
U25: B25:L25: M25	848.4	3.22	0.33	171.11	112.47	58.77	43.10
U40: L20: M20: B20	849.1	3.42	0.35	171.81	110.56	58.81	43.04
L40: U20: M20: B20	846.3	3.28	0.32	170.41	111.83	58.75	43.12
M40: L20: U20: B20	847.8	3.22	0.33	171.81	108.18	58.78	43.08
B40: L20: M20: U20	844.6	3.43	0.34	173.21	108.82	58.83	43.16

B50

Single & Hybrid FAME	DEN	VIS	AV	IV	CN	HV
U100	862.4	2.52	0.39	102.169	56.29	39.85
T100	859.3	3.18	0.42	101.52	56.35	39.84
L100	859.5	2.25	0.37	118.652	56.21	39.09
M100	850.4	2.61	0.40	107.548	56.89	39.03
B100	858.5	2.79	0.36	115.162	56.16	39.04
U50:L50	863.7	3.63	0.42	113.893	57.18	40.03
U70:L30	851.6	3.86	0.41	116.748	57.83	40.05
U30:L70	850.8	3.77	0.39	109.768	57.48	40.88
U50:M50	855.8	3.83	0.37	110.403	57.07	40.01
U30:M70	857.4	3.97	0.36	111.043	57.40	40.08
U70:M30	853.2	4.13	0.38	116.113	57.69	40.09
U50:B50	849.8	3.71	0.37	114.845	57.40	40.02
U30:B70	848.4	3.68	0.39	112.624	57.52	40.10
U70:B30	850.7	3.51	0.42	111.672	57.21	40.03
L50:B50	851.8	3.18	0.40	115.479	57.69	40.86
L30:B70	854.7	3.84	0.39	114.527	57.75	40.79
L70: B30	851.9	3.48	0.41	116.114	57.35	40.98
M50:B50	858.6	3.39	0.42	109.769	57.75	40.88
M30: B70	847.8	3.23	0.38	105.962	57.79	40.80
M70: B30	852.9	4.01	0.42	109.768	57.78	40.83
L50:M50	849.6	3.8	0.37	115.479	57.58	40.09
L30: M70	852.6	3.52	0.37	114.21	57.09	40.05
L70: M30	854.5	3.87	0.36	118.017	57.94	40.07
U60: L20: M20	853.5	4.09	0.38	118.334	58.30	41.86
L60: M20: B20	855.4	3.59	0.37	118.969	58.47	41.84
M60: B20:U20	852.8	4.05	0.39	109.134	58.43	41.87
B60: U20: L20	852.6	3.97	0.38	110.086	58.99	41.80
U25: B25:L25: M25	854.3	3.82	0.37	117.065	59.87	42.55
U40: L20: M20: B20	856.1	4.06	0.39	117.7	59.02	42.45
L40: U20: M20: B20	852.8	3.88	0.38	118.335	59.74	42.49
M40: L20: U20: B20	855.4	3.79	0.37	117.383	59.58	42.46
B40: L20: M20: U20	851.7	3.94	0.37	112.941	59.10	42.54

Appendix C

Original Article

Biofpr Biofuels, Bioproducts & Biorefining

An effective green and renewable heterogeneous catalyst derived from the fusion of bi-component biowaste materials for the optimized transesterification of linseed oil methyl ester

Anietie O. Etim, Institute of Systems Science, Durban University of Technology, Durban, South Africa
Paul Musonge, Institute of Systems Science, Durban University of Technology, Durban, South Africa; Faculty of Engineering, Mangosuthu University of Technology, Durban, South Africa
Andrew C. Eloka-Eboka, School of Chemical and Minerals Engineering, North West University, Potchefstroom, South Africa

Received April 07 2021; Revised May 15 2021; Accepted May 17 2021;
View online at Wiley Online Library (wileyonlinelibrary.com);
DOI: 10.1002/bbb.2252; *Biofuels, Bioprod. Bioref*. (2021)

Abstract: Biological waste materials are rich sources of important minerals such as calcium and potassium, which are required in the preparation of effective biocatalysts for biodiesel production. Their adoption into green catalyst production is becoming important due to the ease of process synthesis and the availability of waste animal shells and agricultural materials. In this study, the potential of a bi-component, heterogeneous catalyst of fused chicken eggshells and pawpaw peels was tested in the transesterification reaction of linseed oil. The waste materials, separately, were dried and calcined at 900 °C or at 700 °C for 3 h to obtain their calcined ashes (calcined eggshells (CES) and calcined pawpaw peels (CPP)). The CES and CPP were then bonded by the wet impregnation method (by dissolving each ash at weight concentration of 7:3 CES/CPP in 100 mL warm distilled water and further calcining them at 600 °C for 2 h). The catalyst that was developed was characterized using Scanning Electron Microscopy - Energy Dispersive X-Ray Spectroscopy (SEM–EDX), X-ray diffraction (XRD) and Fourier transform infrared spectroscopy (FTIR). The Box–Behnken design was applied to generate 15 experimental runs, which were used to investigate the effect of the operational parameters such as methanol-to-oil molar ratio, catalyst loading, and reaction time. The characterization results show that the ash is very rich in Ca and K ions. The best reaction condition for the transesterification process was found to be a methanol / oil molar ratio of 14.9:1, catalyst loading of 3.78 wt%, process reaction time of 80 min at constant reaction temperature of 65 °C with a biodiesel

Correspondence to: Andrew C. Eloka-Eboka, School of Chemical and Minerals Engineering, North West University, Potchefstroom, South Africa. E-mail: fatherfounder@yahoo.com

Appendix D

Environ. Eng. Res. 2021; 26(4): 200299
https://doi.org/10.4491/eer.2020.299

pISSN 1226-1025
eISSN 2005-968X

Research

Potential of *Carica papaya* peels as effective biocatalyst in the optimized parametric transesterification of used vegetable oil

A.O. Etim[1], Andrew C. Eloka-Eboka[2†*], P. Musonge[3*]

[1]*Department of Chemical Engineering, Durban University of Technology, Durban, South Africa*
[2]*School of Chemical and Minerals Engineering, North West University, Potchefstroom, South Africa*
[3]*Institute of Systems Science, Durban University of Technology, Durban, South Africa*
[*]*These authors contributed equally to this work*

ABSTRACT

This study investigates the effectiveness of a base heterogenous catalyst derived from waste *Carica papaya* peels in the transesterification of used vegetable oil (UVO). The calcined *Carica papaya* peels (CCPP) were characterised using scanning electron microscope-energy dispersive X-ray (SEM-EDX), X-ray diffraction (XRD) and Fourier transform infrared spectroscopy (FT-IR). The EDX result indicated that the ash contains various minerals with potassium (K) as the main active element in remove for the charge of the high catalytic activity. Response surface methodology (RSM) based on the Box Behnken design (BBD) was used to optimise and investigate the effect of the critical process parameters which include: the reaction time (50 – 70 min), catalyst loading (2.5 – 4.5 wt%) and methanol-to-oil molar ratio (9:1 – 15:1). The optimal reaction condition for the transesterification process was found to be catalyst loading of 3.5 wt%, methanol/oil molar ratio of 12:1, process reaction time of 60 min at constant reaction temperature of 65 °C which resulted in the maximum biodiesel yield of 97.5 wt%. The quality of the produced biodiesel was in agreement with ASTM standards. The catalyst was reused up to three times with minimal decrease in the catalytic activity in the biodiesel conversion. The study demonstrates the potential of waste biomass feedstocks in the production of sustainable biodiesel fuel.

Keywords: Biodiesel, *Carica papaya* peels, Heterogeneous catalysts, Optimization, Used vegetable oil

Appendix E

Journal of Oleo Science
Copyright ©2021 by Japan Oil Chemists' Society
doi : 10.5650/jos.ess20258
J. Oleo Sci. **70**, *(1) 77-93 (2021)*

JOURNAL OF OLEO SCIENCE
Jos

Transesterification *via* Parametric Modelling and Optimization of Marula (*Sclerocarya birrea*) Seed Oil Methyl Ester Synthesis

Anietie Okon Etim[1], Paul Musonge[2], and Andrew C. Eloka-Eboka[3]*

[1] *Department of Chemical Engineering, Durban University of Technology, Durban, SOUTH AFRICA*
[2] *Institute of Systems Science, Durban University of Technology, Durban, SOUTH AFRICA*
[3] *School of Chemical and Minerals Engineering, North West University, Potchefstroom, SOUTH AFRICA*

Abstract: This study investigates Marula (*Sclerocarya birrea*) seed oil (SBSO) as a novel feedstock for biodiesel production through the transesterification process catalysed by heterogeneous bio-alkali derived from banana (*Musa acuminata*) peels. Response surface methodology (RSM) and artificial neural network (ANN) tools were used for the modelling and optimization of the process variables. The reaction process parameters considered were methanol/SBSO molar ratio, catalyst loading levels, reaction time and temperature. Central composite design (CCD) was espoused to generate 30 experimental conditions which were deployed in investigating the individual and synergetic effect of the process input variables on *Sclerocarya birrea* oil methyl ester (SBOME) yield. Appropriate statistical indices were adopted to investigate the predictive aptitude of the two models. Analysis shows that ANN model obtained for the transesterification process has a higher coefficient of determination (R^2) of 0.9846 and lower absolute average deviation (AAD) of 0.07% compared to RSM model with R^2 of 0.9482 and AAD of 0.12%. The process modelling outcome also confirmed ANN performance to be more precise than RSM. At methanol/SBSO ratio of 6:1, catalyst loading level of 2 wt%, process reaction time of 50 min and temperature of 55℃, the experimental maximum SBOME yield was observed to be 96.45 wt % following the ANN predicted yield of 96.45 wt % and RSM predicted yield of 96.65 wt % respectively. The analysed fuel properties of SBOME was found satisfactory within the biodiesel stipulated standard limit(s). The study establishes that SBSO is a good source for biodiesel production and its biodiesel methyl ester is a potential substitute for petroleum diesel and a bioenergy fuel.

Key words: biodiesel production, *Sclerocarya birrea* seed oil, heterogenous catalyst, modelling, optimization